Lawrence Berkeley National Laboratory
Recent Work

Title

TRIBOLOGY OF CYLINDER WALL/PISTON RING PAIRS IN ADIABATIC DIESEL ENGINE SERVICE ENVIRONMENTS: FINAL REPORT

Permalink

https://escholarship.org/uc/item/1cx4r4hx

Authors

Levy, A.V.
Oee, N.

Publication Date

1987

eScholarship.org Powered by the California Digital Library
University of California

LBL-24880
c.2

Lawrence Berkeley Laboratory
UNIVERSITY OF CALIFORNIA

Materials & Chemical Sciences Division

RECEIVED
LAWRENCE
BERKELEY LABORATORY
MAY 3 4 1988
LIBRARY AND
DOCUMENTS SECTION

Tribology of Cylinder Wall/Piston Ring Pairs in Adiabatic Diesel Engine Service Environments: Final Report

A.V. Levy and N. Jee

January 1987

TWO-WEEK LOAN COPY

This is a Library Circulating Copy which may be borrowed for two weeks.

Prepared for the U.S. Department of Energy under Contract DE-AC03-76SF00098

LBL-24880
c.2

DISCLAIMER

This document was prepared as an account of work sponsored by the United States Government. While this document is believed to contain correct information, neither the United States Government nor any agency thereof, nor the Regents of the University of California, nor any of their employees, makes any warranty, express or implied, or assumes any legal responsibility for the accuracy, completeness, or usefulness of any information, apparatus, product, or process disclosed, or represents that its use would not infringe privately owned rights. Reference herein to any specific commercial product, process, or service by its trade name, trademark, manufacturer, or otherwise, does not necessarily constitute or imply its endorsement, recommendation, or favoring by the United States Government or any agency thereof, or the Regents of the University of California. The views and opinions of authors expressed herein do not necessarily state or reflect those of the United States Government or any agency thereof or the Regents of the University of California.

TRIBOLOGY OF CYLINDER WALL/PISTON RING PAIRS IN ADIABATIC DIESEL ENGINE SERVICE ENVIRONMENTS

by

Alan V. Levy and Nancy Jee*
Lawrence Berkeley Laboratory
University of California
Berkeley, California 94720

FINAL REPORT OF
CONTRACT 41X-70342V

*Currently at Smith International Inc.
Irvine, California

Research sponsored by the Office of Energy Utilization Research, Energy Conversion and Utilization Technologies (ECUT)Program, U. S. Department of Energy, under contract DE-AC05-840R21400 with Martin Marietta Systems Inc.

Researchers operating under DOE Contract No. DE-AC03-76SF00098.

ABSTRACT

An investigation was conducted to determine the sliding wear behavior of candidate coatings for cylinder walls and piston rings in adiabatic diesel engines. Plasma sprayed carbides and oxide compositions on flat washers were tested against a slurry applied and impregnated multi-oxide on a flat disc. The tests were performed at temperatures of 25°, 425° and 730°C at a range of pressures from 0.17 to 14 MPa for tests periods up to 10 hours.

It was determined that the pairs reached a steady wear rate after 1 - 2 hours of testing at 25°C. At elevated temperatures some of the materials wore through the coating within two minutes while others lasted for the test duration. No material pair that was tested performed markedly better than the others. The wear rates were related to changes in the surface microstructure. The molybdenum matrix in the carbide materials on the washers smeared over the wear surface of both the washer and disc at elevated temperatures and dominated their wear behavior. The wear surface microstructures were primarily related to the test temperature and less related to contact pressures. In some cases nearly the same wear rates occurred over a 10 fold increase in contact pressure with the surface morphology remaining the same.

INTRODUCTION

The use of insulating ceramic layers on the inside surfaces of the cylinder walls of advanced diesel engines introduces a new sliding wear regime to diesel engine design. The purpose of the project reported herein was to gain some insight into the nature of the elevated temperature sliding wear behavior of ceramic and hard material

pairs that are candidates for cylinder wall liner-piston ring service in adiabatic diesel engines.

The materials to be tested and the initial test conditions were selected by the Cummins Engine Company which is developing an advanced diesel engine that could use ceramic coatings on the cylinder wall to insulate the structural metal from the combustion gas temperatures. The higher surface temperatures that result prevent the use of the normal organic lubricants used in engines to reduce friction between the cylinder wall and the piston rings. Several materials that maintain their hardness and wear resistance at elevated temperatures that can be applied to the wear surfaces of piston rings are candidates to be paired with the ceramic insulating materials in unlubricated sliding wear environments.

There is relatively little information available in the literature on how ceramic and hard material pairs behave in unlubricated sliding wear at elevated temperatures. The DOE-ECUT program has carried out exploratory research in this area.[1,2] The work reported herein is part of the DOE-ECUT program. The selection of the materials pairs to be tested and the test conditions were not based on already obtained wear data. Rather they were selected because of their performance on components tested at the Cummins Engine Company in experimental engines. In this regard it was decided to test only the single, most promising ceramic material on the disc, the simulated cylinder wall. Against the ceramic, a group of six different materials were selected for the washer, all of which could be applied to the relatively narrow, sharp edged wear surface of a piston ring.

The test specimen configuration and the test conditions were selected to simulate the flat surface, reversing, sliding movement of a piston ring on a cylinder wall. Thus, the tests did not duplicate any previous sliding wear tests which primarily have been pin-on-disc tests in a single direction. The test temperatures and pressures were initially selected to simulate anticipated worst conditions in an engine. However, it was determined early in the testing program that a more mild portion of the conditions in a diesel engine were required as the initially selected conditions resulted in wear-through of the materials pairs in 1 - 2 minutes of testing.

The test data obtained provide an insight into the sliding wear behavior of the types of materials pairs tested. The wear rates measured and the morphology and composition changes that occurred in the material pairs tested provide a valuable base for the further effort that will be required before acceptable levels of performance can be achieved under unlubricated wear conditions. The results of the tests reported herein should not be interpreted as the complete failure of the most promising materials currently available to perform successfully in the very demanding environment of the insulated cylinder wall-piston ring combination in an advanced diesel engine.

MATERIALS

The cylinder wall coating selected was a proprietary, slurry applied silica-chromia-alumina, porous ceramic impregnated with chromia, designated SCA that is applied by Kaman Sciences, Inc. The final coating thickness was 0.07 mm (0.003 inches). The hard coatings

selected for the piston ring sliding surfaces were proprietary, plasma sprayed materials of varying thicknesses applied by the Koppers Co. (see Table 1) The presence of the principal carbides and oxides in the coatings applied by the Koppers Co were verified by x-ray diffraction. The coatings on the washers were applied on a 1018 mild steel base, and honed after spraying to typical finishes for piston rings, which were not measured. The coatings on the washer were also beveled on each side of the rim after spraying to remove edge build-up. Both of the suppliers companies considered their coatings to be so proprietary that they refused to supply any details regarding them. In one case the composition was reported by the company incorrectly and the actual rough composition was not known until x-ray diffraction analysis was performed. For the exploratory nature of the sliding wear behavior of these materials, the rough compositions are adequate. However, further research on the wear behavior of these materials would require a more detailed description of the materials.

EQUIPMENT

A Falex-6 tester described in ASTM standard D-3702-78 was selected to carry out the room and elevated temperature tests, Figure 1. This tester rotates a washer against a stationary disc horizontally in a continuous or reversing motion at various speeds, contact pressures and temperatures. It consists of a lower, stationary column to hold the disc through which the load is applied, and an upper rotary spindle to hold and to rotate the washer. The stationary column transfers load applied by a bail rod of weight through its attachment to a lever arm. The length of the lever arm is adjusted to apply a vertical 2 to 1

ratio of load on the bail rod to the washer interface. The rotary spindle is driven by a variable speed dc motor which has a maximum speed of 4000 rpm for rotary motion and 200 cpm for osillatory motion.

Figure 2 is a close-up of the specimen fixture area of the machine along with a typical disc (left side) and washer (right side) which are detailed in Figure 3. Elevated test temperatures were achieved by adding a clam shell type furnace that encapsulated the region containing the upper and lower specimen holders. The furnace consists of eight heating cartridges held in two Inconel 600 shells that are surrounded by insulation in a steel case. The temperature is monitored at the specimen disc and the Inconel 600 shell. For tests with temperatures below 425°C an Inconel 600 specimen holder was sufficient. However, for tests above 425°C a ceramic cap over the holder was required to reduce heat loss to the upper and lower bearings, and to maintain a higher specimen temperature. Additional cooling of the upper bearings were achieved with heat fin attachments and a small fan directed at the bearings.

A pin on disc type of tester commonly used for sliding wear testing was not used because it did not sufficiently simulate the action of a cylindrical, flat or near flat piston ring surface sliding up and down a cylindrical cylinder wall. The change in the geometry of the pin, the varying contact surface with the disc as the pin wears and the resulting change in contact pressure in a pin on disc test were all concerns that precluded its use. Rather, a flat washer shaped specimen was used instead of a pin to wear on a flat, wider surface disc. While neither the pin or the washer on the disc simulates the action of the

piston ring on the cylinder wall liner of the diesel engine, the constant wear condition of the flat washer made interpretation of the behavior of the coatings easier than would a coating on a pin.

TEST CONDITIONS

The specimens were oscillated with no lubrication at 200 cpm with the sliding direction reversed each 90° of rotation. They were tested at 25°, 425° and 730°C under contact pressures from 0.17 MPa to 14MPa for times from 15 minutes up to 8 hours or until the coating failed, with interruptions to weigh the specimen. The minimum test time for each increment was 1 minute. A coating was determined to be worn through when iron was detected on the surface by observation of a brown wear track and by x-ray diffraction analysis. Also, no weight measurements were made for 730°C tests because the 1018 steel substrate oxidized and negated the weight loss data.

The contact area of each washer was measured and calculated to determine the contact pressure. The specimens were then ultrasonically cleaned in ethanol for 5 minutes and dried with hot forced air for 5 minutes before testing. After each test increment the specimens were cleaned with a dry brush and forced air before weighing. The cumulative wear loss was calculated by dividing the cumulative weight loss by the contact area. The incremental weight loss was calculated by dividing weight loss during each time increment by the contact area and the time increment. Upon completion of the tests the specimens were examined with a scanning electron microscope (SEM) and energy dispersive x-ray analyzer (EDX) to determine the wear mechanisms which

had occurred.

RESULTS

The test data consisted of incremental and steady state wear rates for each of the sliding couples tested, visual observations of the condition of the wear surfaces after each test and metallographic documentation of the morphology and composition of the sliding surfaces and their cross sections. This part of the report is organized into two primary sections. The first section presents the wear data and before and after surface appearance of each material in a manner that permits ready comparisons between coating materials to be made. The second section is an in-depth metallographic analysis of the behavior of each material pair tested.

Comparative Test Data

Table 2 lists the data obtained in all of the tests carried out in the project. The tests were carried out at a number of different combinations of contact pressures, temperatures and test durations. Tests were terminated in less than 15 minutes only when a visual appearance of wear-through of a coating occurred. Generally, as the contact pressure increased or the test temperature was raised, the wear became more severe. In those cases where wear-through occurred in the first one or two minutes of testing, no weight measurements were made.

At the lower contact pressures the wear tracks appeared to be polished beyond the honed condition of the materials prior to the test. At the lower contact pressures, up to 6.9 MPa in the case of the Cr_3C_2 washers, there was very little effect of increasing the contact

pressure on the amount of wear measured. This behavior and the accompanying fine polishing of the surfaces that occurred could be evidence of the wear debris acting as a super fine polishing agent or as a solid film lubricant.

In order to take advantage of the observed polishing action at low contact pressures, several tests were run where the surfaces were preworn for at least 10 minutes at 0.17 MPa and 25°C and subsequently tested at a higher temperature in the cases of the Cr_3C_2 and WC-Mo washers and a higher pressure in the case of the Al_2O_3-TiO_2 washer. It can be seen that the wear life was increased by the wearing-in process. Without the wear-in, only some of the pairs exceeded 1, 2 minutes of testing at elevated temperatures. In some tests, generally at higher contact pressures, the wear life did not exceed 1 minute even at 25°C (WC-Mo, Al_2O_3-TiO_2).

The relative performance of the several materials pairs tested, as measured by weight loss in tests that ran for at least 10 minutes, is shown in the bar graphs in Figure 4. It can be seen that a comparatively wide spread in performance had occurred. Only the results of the 25° and 425°C tests are included in the bar chart. The 730°C measured test results were invalid because the weight changes were obscurred by oxide scale that formed on the sides of the steel substrate.

Generally the washer materials wore less than the SCA disc material. However, when the SCA material was worn on itself, it lasted the required 15 minutes test duration at 425°C, albeit at a high wear rate, while the Cr_3C_2 and the Al_2O_3 washer materials wearing on the SCA

coated disc did not. At 25°C test temperature, contact pressure did not appear to relate directly to wear rate at the lower pressures. In the case of the Cr_3C_2 the wear rates of the washer were essentially the same at contact pressures of 0.69 and 6.9 MPa.

The wear rates at 425°C test temperature were higher than the rates at 25°C, generally more than two times greater. The comparatively low wear rates of the Cr_3C_2 at 25°C were not indicative of the material's elevated temperature performance as the material pair wore through at 425°C. Overall it is difficult to make any comparisons of the performance of one material pair with respect to the others in this test series because not enough duplicative tests were made. Rather, Figure 4 establishes the level of behavior of different pairs with respect to each other. The data is intended to be qualitative for comparison purposes.

Figure 5 gives some further insight into the behavior of the materials tested. The same SCA disc material tested under the same test conditions has a wear rate range from 0.10 to 0.46 $g/cm^2s \times 10^{-5}$ depending on the wear rate and nature of its washer material. More sense can be made of this behavior when the micrographs of the wear surfaces are analyzed later. The coefficients of friction of the various materials pairs tested were not determined in this initial test series. They should be determined in later tests to shed more light on the comparative behavior of the materials tested.

Wear Rates

The wear rates determined by incremental weight loss measurements are plotted in Figure 6 - 13. They indicate that various patterns of weight loss occurred as a function of the nature of the materials and the test conditions. In particular, the shape of the early part of the wear curve gave an indication of the sensitivity of the honed surfaces of the materials to sliding wear material loss.

The weight losses were plotted in two ways. The upper curves in Figure 6 show cumulative weight loss of the Cr_3C_2 washer on the SCA disc at 0.17 MPa at 25°C. The curves became straight lines, indicating that a steady state wear condition is reached after a reasonably short test time, one to two hours. The lower curves show the wear data from the same test plotted incrementally. Incremental plots are made by plotting the weight loss of a contact area for each second of testing over a several minute increment. Subsequent test periods have only the weight lost in each specific test increment divided by its number of seconds plotted on the ordinate. Thus, when the curves become horizontal, after about two hours of testing, they indicate that a steady state wear rate has been reached where each second of wear time removes the same weight of material as the preceding and succeeding second, on average, over the few minutes of test time of each test increment. This rate persists, as can be seen in the 8 hour test plotted in Figure 6, until near coating wear-through.

Cr_3C_2 Mo/SCA Pair

The wear of the Cr_3C_2 washer as a function of contact pressure at 25°C in Figure 7 shows an initially high wear rate that decreases

with increasing contact pressure until, at 14 MPa, the initial portion of the curve reverses itself and starts out at a lower rate than its peak rate. This indicates that the remaining protrusions from the pre-test lapping are being increasingly crushed into micro voids to decrease the initial weight loss as the contact pressure increases. At 14 MPa, the highest contact pressure used, the voids are filled with crushed protrusions in the first test increment to the degree that the resulting wear rate is lower than the peak rate.

At 0.69 and 6.9 MPa the Cr_3C_2 washer material reaches a lower incremental wear rate of 0.1×10^{-5} g/cm^{2}s as can be seen in Figure 7. This wear rate, being the same for both contact pressures of 0.69 and 6.9 MPa, indicates that the wear debris could be acting as a solid film lubricant.[3] At 14 MPa, the possible lubricating effect of the wear debris is overcome and the wear rate after 10 minutes of testing increases to 0.3×10^{-5} g/cm^{2}s but has not leveled out; see Figure 7.

The apparent straight line portions of the curves in Figure 7 are actually still sloping downward. As was seen in Figure 6 steady state wear rates did not occur until approximately two hours of testing had occurred. This was true for all of the materials tested. A longer test was not possible because the high pressure resulted in the wear-through of the thin coating of Cr_3C_2-Mo. In the washer on disc type of test, the wear debris remains on the sliding surface throughout the test while in a service configuration such as a piston ring on a cylinder wall this may not occur.

The SCA disc in the Cr_3C_2-Mo tests also had a higher initial incremental wear rate than the steady state rate. The steady state

rate remained around 0.2 x 10^{-5} g/cm^2s, nearly twice that of the Cr_3C_2-Mo washer, up through a contact pressure of 6.9 MPa. At the highest contact pressure, as seen in Figure 7, the final wear rate of the SCA disc had reached the same final wear rate as the washer.

WC-Mo/SCA Pair

The incremental and cumulative wear rates of WC-Mo and SCA tested at 25°C at 0.17 MPa and 0.69 MPa, shown in Figures 8 and 9 respectively, reached a low steady state rate which was maintained for at least 8 hours. The short term test results shown in Figure 8 and long term tests results in Figure 9 are from separate tests. The washers in both tests appeared to undergo a nucleation period after which a low level of material loss occurred at steady state. It is speculated that there were fewer vulnerable protrusions that were initially worn on WC-Mo than on Cr_3C_2 specimens. Also, at 425°C the SCA had a wear rate which fluctuated.

TiC/SCA Pair

High initial wear rates and subsequent lower steady state rates are shown in Figure 10 for TiC and SCA at 25°C and 425°C. The smaller differences between the peak and steady state wear rates for the SCA disc at 425°C than at 25°C may also be significant as the same pattern occurred for the WC-Mo-SCA pair. Note that the initial wear rate of the washer in the 425°C test is more than 10 times the initial wear rate measured at 25°C even though the contact pressure is lower. The change in the wear mechanism between 25°C and 425°C is more important than the contact pressure in determining the wear rates.

Al_2O_3-TiO_2/SCA Pair

The Al_2O_3-TiO_2 has low wear rates at 25°C at 0.69 MPa and 1.0 MPa as shown in Figure 11. When the washer and disc are preworn the coating on the washer can perform at a much higher pressure with a comparatively low wear rate, see Figure 11C. The longer duration test results from a separate test are plotted in Figure 12. The behavior of the surfaces near wear-through are shown in both types of curves where sharp increases in weight loss began to occur after a low steady state wear loss out to 5.5 hours.

SCA/SCA Pair

The steady state wear of SCA on itself at 25°C and 0.35 MPa for 1 hour, plotted in Figure 13a, further indicates that ceramic coatings reach a constant wear rate within a short time. Doubling the contact pressure, in Figure 13b, more than doubled the steady state wear rate. This indicates that the SCA wear debris does not act as a solid film lubricant when worn against itself.[3] As shown in Figure 13c, at 425°C the SCA has higher steady state wear rates than at 25°C and, as was also observed with WC-Mo, the disc had a fluctuating wear rate.

METALLOGRAPHIC ANALYSIS

The scanning electron microscope (SEM) was used exclusively to study the morphologies and compositions of the worn surfaces. Specimen surfaces were selected for analysis that were representative of the predominant surface characteristics of the various test materials rather than unusual occurrences. Magnifications were selected that showed overall appearances and detailed textures and phase

distributions. Prior to wear testing each type of test material was photographed in its as-received condition.

The report was organized to permit ready comparisons between wear rate data, Figures 4 through 13, for the different materials tested. The microstructures, starting with Figure 14, were therefore, placed after the wear rate bars and curves. This makes it more difficult to relate microstructures to wear rates. However, it is felt that this organization was better than distributing the wear rate curves among 54 micrographic figures. It is left to the reader to relate the surface morphologies to the wear rates. However, it is not that important to do so. The principal observation to make when analyzing the worn surfaces' microstructures is the significant change in morphology that occurs at the various test temperatures.

Wear Surfaces Before and After Testing

The surfaces of the washers of each material, in the honed condition (left hand side) and after testing for 15 minutes at 25°C (right hand side), are shown in Figures 14 and 15. The polishing lines on the honed, carbide cermets in Figure 14 are removed during the 15 minute wear test. The wear action also caused a minor redistribution of the phases of the materials, which will be identified in subsequent sections on each materials pair. The relative sizes of individual phase areas of the carbides before and after testing are similar. A slight refinement of these sizes occurred on the Cr_3C_2 and WC-Mo washers. In the case of the WC-Mo, the phase boundaries are sharper after the 15 minutes wear exposure. The areas of material pull outs

and voids are similar for both the honed and wear tested surfaces.

The oxide base coatings on the washers shown in Figure 15 behaved in a somewhat different manner than the carbide cermets. The top photos show the SCA coating which is primarily a mixture of silica and chromia with a small amount of alumina. The as-honed surface on the left appears to have a rather even distribution of phases and void areas. The tested surface in the right side photo has a considerably coarser structure with relatively large pullout areas with most of the visible voids located in the pullout areas. The wear process caused a considerable change in the overall texture of the surface, coarsening it.

On the other hand, the Al_2O_3-TiO_2 mixed oxide coating surface on the washer shown in the lower photos appeared to have its morphology refined by the wear action of the test. Also, the void structure of the as-deposited and lapped coating seen in the left photo was filled in during the wear test.

In overall appearance, the five washer coatings appeared to be polished by the wear process beyond their as-honed condition. The morphology of the surfaces was also affected by the sliding wear action for some of the materials. On some materials, i.e., Cr_3C_2-Mo, WC-Mo and Al_2O_3-TiO_2, the microstructure was refined. On the SCA coating, the microstructure was coarsened and on the TiC, the initial microstructure was essentially unaffected.

The next sections of the report contain an in-depth microstructural analysis of each pair of materials tested over the

range of contact pressures and temperatures used to determine their sliding wear behavior. All of the specimens analyzed in this section of the report were tested for 15 minutes.

Cr_3C_2-Mo/SCA Pair - The overall appearance of the washer and disc surfaces of the Cr_3C_2-Mo - SCA pair are shown in Figure 16. The washer surface in the upper left photo shows the bevels on both sides of the test surface. This machining caused the inside edge of the rim to be sharper than the outside edge as seen for all the washers except the SCA coated one. The lower two photos, at increasingly higher magnification, show the phase and void distribution of the as-tested surface of the Cr_3C_2-Mo cermet. Several of the voids appear to have very small particles of wear debris packed into them, while others appear empty. There are more voids along the sides of the test area than in the middle of it.

The width of the wear areas on the washers and the disc are approximately the same with the outside track more uneven than the inside one on the washer. The middle right photo indicates that several isolated areas on the SCA disc were worn to a dense, flat texture while others maintained their as-deposited and honed texture. A high magnification region of one of the latter areas shown in the lower right photo appears almost identical to the as-deposited and honed surface of the SCA coating shown in the upper left photo of Figure 15.

The composition distribution of the Cr_3C_2-Mo surface after the 25°C, 0.69 MPa contact pressure test is shown in Figure 17. The darker phase is the Cr_3C_2. There is also chromium present in the

areas where nickel occurs as a Ni-Cr alloy was used as a second binder. The black voids have Cr_3C_2 debris in them. This indicates that chunks of the brittle carbide fractured along cleavage planes below the wear surface and were removed. The primary binder used to hold the Cr_3C_2 particles was molybdenum, which is the light grey phase. Connected with some of the molybdenum is the nickel-chromium which appears as a medium grey phase. There is only a slight indication of smearing of the molybdemum over the Cr_3C_2, generally near the phase interfaces.

The composition of the SCA disc in Figure 18 indicates that the three oxides that constitute the material: SiO_2, Cr_2O_3 and Al_2O_3, are present on the worn surface along with a small amount of molybdenum that was transferred from the Cr_3C_2-Mo washer. There is no pattern of the location of the three oxides that conforms with the microstructure shown in the upper left photo. The few cracked areas shown in the micrograph may outline platelets of material that were about to be removed.

As the test contact pressure increased to 6.9 MPa the wear zone widened but the surface morphology on the washer changed relatively little as can be seen by comparing Figure 19 with Figure 16. More voids, especially in the center region, and more evidence of debris, both in the voids and on the surface, were observed.

The wear track width was considerably wider and the morphology of the wear surface of the SCA disc was coarser in the 6.9 MPa test compared to the 0.69 MPa test (compare Figures 16 and 19). The changes in the wear tracks between the 0.69 and 6.9 MPa tests only had a small

effect on the measured wear rates as seen in Figure 4.

The wear surface of the Cr_3C_2-Mo washer tested at 6.9 MPa in Figure 20 has an overall composition similar to that shown for the 0.69 MPa test in Figure 17. The SCA disc wear surface from the 6.9 MPa test shown in Figure 21 shows that the composition distribution is similar to that which occurred in the 0.69 MPa test. A small amount of molybdenum was transferred to the disc at both pressures. A decade increase in contact pressure had relatively little effect on the composition distribution of the SCA disc coating in the 25°C tests. The mix of the three oxides that constitute the SCA coating appear to be quite stable while undergoing wear forces and temperatures.

Increasing the test temperature from 25°C to 425°C caused the washer material to fail after 1 - 2 minutes of testing, see Table 2. The coating on the washer was totally removed while a little SCA coating remained on the disc. The SCA coating, within the two minutes of wear, fared well. Its composition was the same as that observed in the 25°C tests, with a little iron smeared on the surface as can be seen in the peak analysis in Figure 22. Comparing the surfaces of the SCA discs from the 25°C, 0.69 MPa test, Figure 16 and the 425°C, 0.17 MPa test, Figure 22, it can be seen that there is relatively little difference between the morphologies. Apparently the SCA materials' morphology was more sensitive to the contact pressure than to the test temperature.

Cross sections of the washers that were plasma spray coated with Cr_3C_2-Mo and tested at various conditions are shown in Figure 23 and 24 with the ideal configuration of the deposit shown in the 25°C, 6.9 MPa

photo. The washers were coated by making a groove in the top of the washer and filling the groove with plasma deposited Cr_3C_2-Mo. After the spraying operation the sides of the washer were beveled to remove edge effects. The beveling operation did not line up absolutely symmetrical with the original groove and one side of the groove was leveled off. This also occurred with the other washer coatings.

The morphology of the cross sections are essentially the same. The edge of the Cr_3C_2 tested at 25°C and 0.69 MPa is smoother than that at 6.9 MPa which has fragments removed. It can be seen at 425°C, 0.17 MPa the Cr_3C_2 was almost completely removed as were the mild steel sides of the groove into which the Cr_3C_2-Mo was sprayed. This accounts for the iron peak in Figure 22.

WC-Mo/SCA Pair - The WC-Mo washer's surface behaved in a similar manner to the Cr_3C_2 in the 25°C tests, Figure 25. At the 0.69 MPa contact pressure, the demarcation of phases on the surface was more pronounced than occurred on the Cr_3C_2. There is an intimate mixing of the several phases of the material. Figure 25 shows the surface at a high magnification in the lower left photo. The areas that appear to be shallow voids on the surface occur at random locations and are of varying sizes.

The SCA disc wear surface was 33% wider than that on the washer, indicating that the two surfaces were not absolutely symmetrical to one another. The surface morphology was quite constant with several void areas distributed randomly that contained wear debris. The microstructure of the SCA coating was somewhat different from that

seen in the Cr_3C_2 tests shown in Figure 16. There appeared to be more well defined flat areas and the debris containing voids were more numerous and better defined. The basic size of the microstructural elements in both materials, other than the voids, was roughly the same. The small differences between the surfaces of both washer and disc in the WC-Mo and Cr_3C_2 tests are indicated by the fact that their wear rates at 25°C, 0.69 MPa were also similar, see Figure 4.

The composition of the surface of the WC-Mo washer can be seen in Figure 26. The distribution of the elements, as indicated by x-ray maps, is similar to the distribution prior to testing. The amount of tungsten carbide that occurs on the wear surface (light grey phase) is small compared to the molybdenum (medium gray phase) and the additional binder alloy in the composite, Cr-Ni (dark gray phase). There is considerably less WC in the plasma spray coating than occurs in a typical pressed and sintered WC-Co monolithic material such as Kennemetal K701. This is evidenced by the difference in hardness. Kennemetal K701 has a microhardness of 1400 VHN while the plasma spray coating WC-Mo has a microhardness of 900 VHN. There are sharp boundaries between the phases. The chromium and nickel occur together and neither appears to occur in the molybdenum phase.

The SCA coating on the disc is shown in Figure 27. It has the same distribution of oxides as the SCA material in the Cr_3C_2 tests, but in the case of the WC-Mo washer, considerable molybdenum was transferred from the washer surface to the disc surface in the 0.69 MPa test (smooth areas) while a smaller amount was transferred from the Cr_3C_2 washer.

At 425°C test temperature, the WC-Mo washer surface was quite different from the 25°C test. Figure 28 shows that the washer surface no longer has the well defined phases shown in Figure 25. Fine wear lines appear in the high magnification photo. The outside edge of the washer still is rougher than the inside edge, as occurred in the 25°C test but only by a small amount. The marked voids that occurred in the 25°C test are not obvious in the 425°C tests. Smooth areas occur on the washer surface that may be the remaining surface of the locations from which molybdenum was transferred to the disc surface.

The SCA disc in Figure 28 has a fine grained, even surface texture with periodic occurrences of smooth areas that will be shown to be molybdenum transferred from the washer. The morphology of the disc surface from the 425°C test is different from that which occurred on the disc in the 25°C test, see Figure 25. It has the same appearance as the disc from the Cr_3C_2 test at 425°C, see Figure 22.

The composition of the washer surface shown in Figure 29 indicates that the molybdenum binder alloy has spread over the surface more, covering over the WC phase to various depths. The location of the various elements on the surface no longer can be readily related to the surface morphology shown in the upper left photo. The wear lines can be more easily seen in the micrograph of Figure 29 as can elongated regions that have been pulled out of the surface.

The SCA disc from the 425°C test shown in Figure 30 has large smears of molybdenum on its surface. The smears appear to be thin because the silica and chromia and even the small areas of alumina beneath it are seen in their x-ray maps.

The surface morphology of the WC-Mo washer changed again in the 730°C test, Figure 31. The presence of needle shaped crystals, probably of molybdenum oxide, over the surface of the washer indicates that a major modification of the surface had occurred. The surface of the SCA disc shows that a major transfer of smeared layers of molybdenum from the washer had occurred. Beneath the molybdenum smears, the SCA retained its uniform, small grain size morphology.

The WC-Mo specimen that was pre-worn at 25°C, 0.17 Mpa for 5 minutes before testing at 730°C, 0.17 MPa is shown in Figure 32. The washer has, essentially, the same type of needle morphology as the specimen that was not pre-worn, although the structure is somewhat modified with the needles not being as long or as sharp. The transfer of molybdenum to the disc surface in the pre-worn specimen does not appear to be as extensive as occurred in the specimen that was not pre-worn. There also appears to be more wear debris on the pre-worn surface.

The composition of the surfaces tested at 730°C are shown in Figures 33 - 36. The molybdenum has spread out over the washer test surface in the form of oxide needles and metal smears, covering over WC and Ni-Cr alloy areas, Figure 33. The WC particles are indistinguishable from the molybdenum in the micrograph. However, the Ni-Cr alloy can be identified between and beneath molybdenum oxide needles and metal smears. The presence of such large amounts of molybdenum binder on the surface of the WC-Mo material is unusual for a WC based hard material.

The composition of the pre-worn washer, Figure 34, shows even more molybdenum on the surface. However, the x-ray maps for W and Ni show that in many areas the molybdenum is very thin, allowing the W and Ni x-rays to be picked up from beneath the molybdenum smear.

The SCA disc surfaces shown in Figures 35 and 36 indicate the basic SCA material retains its morphology and composition distribution in the 730°C tests as it did at the lower test temperatures. The Mo map in Figure 36 shows that Mo smeared over much of the SCA surface, in some areas so thin that it is not readily observed in the micrograph. The peak analysis shows that some Ni has also been transferred to the disc surface at 730°C. Measureable amounts of Ni transfer was not observed at the lower test temperatures.

The WC-Mo washer cross sections for the three test temperatures are shown in Figure 37 at a low magnification. The bulk of the sprayed coatings do not appear to have been affected by the test temperature. As in the case of the Cr_3C_2-Mo, the bevelling of the coated surface's edges was not even. In the case of the 730°C specimen an edge of the 1018 steel base appears to have been a part of the wear surface. Looking carefully at the x-ray peaks in Figure 35, a slight indication of the presence of iron can be seen immediately to the right of the two Cr peaks. Higher magnification photos in Figure 38 of the 730°C test washers tested in the pre-worn and in the as received conditions show that the edges were slightly rougher than the washers tested at 25°C and 425°C. This roughness could be the needlelike structure seen on the surface.

TiC - Mo/SCA Pair - The surface morphologies and composition patterns of the TiC-Mo washers sliding on the SCA discs were similar in nature to those of Cr_3C_2-MO/SCA pairs, see Figure 39. The washer wear rates were also similar to those of the WC-Mo/SCA pair tested at 25°C and 425°C, see Figure 4. In the review of the micrographs for the TiC-Mo/SCA pair in Figures 39 - 45, only the EDX peak analysis and x-ray map differences from the WC-Mo/SCA micrographs will be discussed.

The phase distribution of the TiC-Mo on the washer at 25°C shown in Figure 40 is very similar to that of the WC-Mo. The TiC phase has significant iron in it, the effect of which is not known. This composition also appears to have a higher percentage of the TiC hard particles at the wear surface than the other carbides. The micrograph in Figure 40 also shows some rather deep and narrow wear grooves, which were not seen on WC-Mo washers tested at 25°C or on the Cr_3C_2-Mo washers. The grooves appear to pass indiscriminately through the various constituents on the surface. The wear surface of the SCA disc, Figure 41 looks very similar to the SCA disc tested with the WC-Mo and shown in Figure 27.

The surfaces and composition of the TiC-Mo washer in the 425°C test, Figures 42 and 43, appear almost the same as the WC-Mo test surfaces shown in Figure 28 except that the TiC-Mo (Fe) particles are more evident than were the WC-Mo particles (compare Figures 43 and 29). The morphology and composition of the SCA disc in the 425°C test of the TiC-Mo(Fe) washer was also very similar to the disc in the WC-Mo test (compare Figures 44 and 30). The cross sections of the washer in the two material tests were also similar (compare Figures 45 and 46 to 37

and 38).

The surface of the TiC (Fe) washer and the SCA disc after the 730°C test is shown in Figure 47. These surfaces were somewhat different from the WC-Mo/SCA pair tested at 730°C. The needle structure which occurred on the WC-Mo washer, Figure 39, was much more distinct than that which occurred on the TiC-Mo washer. Also, there was not as much transfer of distinct molybdemum smears to the disc surface.

The composition of the TiC-Mo washer surface in Figures 48 and 49 shows that, like the WC-Mo washer (Figures 33 and 34), molybdenum was the dominant element. In Figure 49 the peak analyses show that at certain areas on the surface TiC particles were covered with a thin layer of Mo. Also the other binder, Ni-Cr, in some places combined with the Mo on the surface. The cross section of the TiC-Mo coating seen in Figure 50 shows the distribution of the phases.

Primarily though, molybdenum dominates the wear surface as the test temperature increases for both TiC-Mo and WC-Mo. This molybdenum also transferred to the SCA disc surface from the TiC-Mo washer as can be seen in Figure 51. A small amount of Ti and Fe was also determined to be on the disc surface, probably in the form of small chips of wear debris from the washer.

Al_2O_3-TiO_2/SCA Pair - The oxide coatings on the washer surface did not contain metal binders and had different surface morphologies after wear testing than the carbide cermet washer coatings. Figure 52 shows that at room temperature the general morphologies of the Al_2O_3-TiO_2 and the SCA were similar. The Al_2O_3-TiO_2 had localized areas where the coating

appears to have failed catastrophically compared to the rest of the surface which appeared to be smooth and fine grained. As noted in Figure 15, the worn surface was considerably finer grained than the as-sprayed coating. The void areas on the surface of the oxide before testing may be localized pits on the worn surface. Some crushed wear debris appears in areas of each pit.

However, the major portion of the washer surface is smooth, which may account for its low wear rate, see Figure 4. The SCA disc also had a smooth surface but was still more coarse than the as-applied coating. Since both surfaces are oxides of the same or similar hardness, their surface appearance and wear rates are similar.

The composition of the surface of the Al_2O_3-TiO_2 contains much more Al_2O_3 than TiO_2, as shown in Figure 53. The surface composition of the SCA coating after testing at 25°C, Figure 54, is the same as was observed in the carbide washer tests except for a small amount of Ti which was transferred from the washer.

At 425°C the surface of the Al_2O_3-TiO_2 washer appeared more torn and had more wear debris than in the 25°C test, see Figure 55. There were no distinct pits but the coarseness of the morphology of the surface of the SCA coated disc increased markedly. These changes occurred on surfaces that failed in 2 minutes as the detection of iron indicates that the disc had worn through, see Table 2.

Debris from the failed SCA coating on the disc was deposited on the Al_2O_3-TiO_2 coating remaining on the washer as can be seen in the peak analysis of Figure 55. Specific identification of the chromia wear debris formed at 425°C in the micrograph in Figure 56 is not

possible, indicating that fine, crushed particles adhered to the washer surface. Even a small amount of iron from the disc substrate adhered to the washer.

The surfaces of both the Al_2O_3-TiO_2 washer and SCA disc at 730°C in Figure 57 have comparatively constant morphologies across the wear surface. Figures 58 and 59 show the distribution of the oxides on the washer and disc surfaces respectively.

The cross sections of the washer from the tests at the three temperatures in Figures 60 and 61 show two coatings: a bond coat and the wear resistant Al_2O_3-TiO_2 coat. The oxidation of the sides of the 1018 steel washer in the 730°C test (lower left photo of Figure 60) prevented meaningful weight loss data from being obtained.

SCA Washer/Disc Pair - When the SCA material was worn on itself, there were large, smooth areas on both the washer and the disc with more on the washer, see Figure 62. The composition of an untested SCA coating in Figure 63 is similar to a tested washer surface in Figure 64 although the morphologies of the two surfaces appear slightly different. The wear process seems to smooth out some areas of the surface. However, the composition of these areas cannot be specifically identified from the x-ray maps.

The surfaces of the washer and the disc after the 425°C test in Figure 65 appear similar. As in the analysis of the wear surface of the SCA coating in the rest of the test series, the coating wears evenly and maintains its composition distribution during the wear process, see Figure 66. The cross sections of the coating over the

whole washer surface in Figure 67 after the 25°C and 425°C tests show the even wear of the coating.

DISCUSSION

Comparative Wear Rates

The wear rates of the materials pairs tested, shown in Table 2 and Figure 4, do not indicate one pair of materials to be better than all of the others. Washer wear rates that were low at 25°C such as the Cr_3C_2-Mo and Al_2O_3-TiO_2 wore through in 1 - 2 minutes at 425°C while materials with higher wear rates at 25°C, such as the WC-Mo and SCA washers were durable enough to last through the test period at 425°C.

The best example of this behavior was the SCA washer at a contact pressure of 0.69 MPa. The absence of a distinct morphology change in the SCA washer material, as compared to all of the other materials which underwent considerable change from the 25°C to 425°C tests, is probably what accounted for its durability at 425°C.

The changes in wear rates at 25°C did not correlate directly with increased contact pressure. Generally, only small increases in wear rate occurred as the result of large increases in contact pressure. For example, the ten-fold increase in contact pressure from 0.69 MPa to 6.9 MPa for the Cr_3C_2-Mo only caused a .03g/cm^{2}s x 10^{-5} increase in wear rate. The same magnitude of change occurred for the Al_2O_3-TiO_2 specimens. In both cases, there was little change in the surface morphology of the materials over the pressure range. It therefore appears that the maintenance of the morphology has a direct

effect on keeping the wear rates for the washer materials low and nearly the same over a range of contact pressures. When the morphology of the washer wear surfaces changed dramatically in the 425°C tests, the wear rates had a major increase to the point that some of the coatings failed in 1 - 2 minutes.

The formation of a super polished surface as the result of carrying out low contact pressure wear tests for short periods of time at 25°C also indicated the strong role that surface morphology plays in the wear of these types of materials. The test duration to wear-through of the Cr_3C_2-Mo and WC-Mo at 730°C when the specimens were first pre-worn at 25°C significantly exceeded that of the same materials tested at 730°C without being pre-worn, see Table2.

The ability of the washer's behavior to influence the wear rate of the SCA coating on the disc, as shown in Figure 5 is an interesting phenomenon. All of the carbide cermet washer materials had the super polished surface with molybdenum predominant after testing while the oxide coated washers had their nearly constant, small grained morphology. The test conditions were the same. Yet the SCA complex oxide coating had a wear rate that differed by almost five times when tested against the different washer materials. The surface of the SCA discs in the five tests are shown in Figures 16, 26, 39, 52, and 65. Comparing them shows some variation in morphology for the first four but not in a manner that could account for their different wear rates.

Only the SCA disc that was worn by the SCA washer had a significant difference in its surface morphology from that of the other four tests. It appears that there was significant transfer of

material between the washer and the disc with large, smooth deposits on the surface of the disc that probably came from the washer. The tearing out of sections of each surface appears to cause the much higher wear rates in the SCA-SCA pair compared to the wear rate of the discs in the tests of the other four pairs of materials.

Incremental Wear Rate Curves

All of the materials tested reached a steady state wear rate that was much lower than their initial rates after the relatively short time of 1 - 2 hours of testing, see Figure 6 - 13. Once reached, this wear rate remained essentially constant indicating that it should be possible to extrapolate wear rates for these kinds of hard materials over a considerable time after only a short test as shown in Figure 6 for the Cr_3C_2-Mo/SCA pair for an eight hour test. This is important when these materials are considered for an application. It appears that a mils/yr type of wear number could be assigned to a pair as is done in corrosion testing. However, the rates experienced in the pairs tested in this unlubricated test series are much higher in mils/yr than would be tolerable in an application. Also, the wear debris, for the most part, was contained between the wear surfaces where it may have acted as a solid film lubricant. This would not necessarily occur in service.

The initial, higher incremental wear rates experienced by the materials is due to the removal of high asperities on their surfaces, even though they were all honed before testing. The super polished condition of the washers seen in Figure 14 after testing, compared to their untested condition, appears to indicate the removal of the high

spots at the beginning of the test. Profilometer tests were not run on the specimens as the available profilometer was inoperative.

The role of the wear debris acting as a solid film lubricant, as shown in Figures 6 and 7 for the Cr_3C_2-Mo washer, is possible because of the continuous contact between the surfaces of the washer and disc in the test. In service the piston ring is not in continuous contact with the same area of the cylinder wall and the ability of the wear debris to act as a solid film lubricant is questionable. However, the potential of wear debris to behave as a solid film lubricant was demonstrated in this test series and it could occur in service because of the manner in which at least some of the transferred material smears on the wear surface.

Carbide Surface Morphology as a Function of Test Temperature

The sharper demarcation of phases as the result of the wear action on the carbide washers at room temperature may be indicative of a temperature rise at the surface from frictional heating. The fact that this does not occur in the 425°C tests may be due to the marked increase in the plasticity of the binder metals which smear over the surface and reduce the frictional heating potential of the sliding mechanism. In the 730°C tests, needle-like growths occur on the washer surfaces. This could indicate the formation of a molybdenum oxide as the result of the temperatures that occur at the mating surfaces of the washer and disc. Thus it appears that each test temperature resulted in a different magnitude of surface temperature that caused a completely different morphology to occur on the washer surface. It is

interesting to observe that the SCA coatings on the disc maintained a comparatively constant morphology at all three test temperatures.

Coarseness of Oxide Microstructure

The two oxides that were used on washers, SCA and Al_2O_3-TiO_2 changed their degree of coarseness as the result of 25°C testing, but not their basic morphology. In Figure 23 it can be seen that SCA surface morphology was coarsened by the wear process while the Al_2O_3-TiO_2 morphology was refined. It is not known why this occurred. The coarseness of the surface morphology of the carbide cermet coated washers did not change as the result of the wear tests, as can be seen in Figure 14, nor did the SCA discs.

Width of Wear Areas

In Figure 28 for the WC-Mo/SCA pair tested at 425°C the wear path on the disc is some 60% wider than the width of the washer that wore on it. This is due either to wear of the beveled section on the washers or to minor misalignments between the washer and the disc. This did not appear to modify the behavior of the materials. However, in seeking reproducability in multiple tests of the same materials pairs, there may be a problem. Ideally a larger flat on the washer would prevent edge effects from occurring. Only one specimen pair was tested at each condition in this series because of the limited number of specimens.

Stability of SCA Disc Morphology and Transfer of Molybdenum

The surface morphology and composition of the SCA multiple oxide coating on the disc were markedly stable over the range of test

pressures and temperatures and types of washer coatings used in the test series. Comparing the surface micrographs of the discs that were tested with the Cr_3C_2-Mo washer coating at contact pressures of 0.17 to 6.9 MPa and temperatures 25°C and 425°C in Figures 16, 19 and 22 show essentially the same surface morphology. There was very little molybdenum transferred to the disc from the washer as can be seen in Figures 18 and 21 over a tenfold increase in contact pressure.

For other washer materials, a significant amount of molybdenum transferred from the washer to the disc. This transfer at 425°C and 730°C changed the surface morphology of the disc coating. The case of the WC-Mo/SCA pair is shown in Figures 25, 29 and 31. The flat areas are high in molybdenum that was probably transferred from the washer coating to the disc. The morphology of the underlying SCA material appears to be quite stable as the test temperature was increased. As more molybdenum spread on the surface of the disc the wear rate of the disc increased, as can be seen in Figure 5. The tendency for the various washer materials to transfer molybdenum to the disc during the tests varied significantly.

The molybdenum also tended to smear over the washer surface in the elevated temperatures tests. It covered over the other binder constituent, NiCr alloy, as well as the carbide particles. An example is shown in Figure 34. Comparing the micrographs with the x-ray maps it can be seen that the molybdenum smears ranged from thick to quite thin. The smear is thin enough in several places to have the WC show through. Thus, the molybdenum constituent in the carbide coating played a major role in establishing the nature of both of the wear

surfaces.

Performance Similarity of Carbides

The wear rates at 25°C and 425°C and the morphology and composition distribution at 25°C, 425°C and 730°C of the three carbide-Mo washer coatings were very similar. The wear rate bar graphs at 0.69 MPa for the three materials can be seen in Figure 4. Their surface morphologies and compositions can be seen in Figures 16, 26 and 40 for 25°C, Figures 30 and 43 for 425°C and Figures 34 and 48 for 730°C. The only difference in the 25°C test surfaces is that some of the honing grooves remained on the TiC-Mo while they were polished off the Cr_3C_2-Mo and WC-Mo surfaces by the wear action. The correlation between surface morpholgoy and composition distribution and wear rates appears to be quite strong in these three materials. The difference in the carbide particles appears to have relatively little effect on the wear rates. The hardness of the composites also does not relate to their wear. The Cr_3C_2-Mo has a hardness of 1300 VHN, the WC 3000 VHN, and the TiC 3200 VHN, using a 100g load.

The tendency for the molybdenum to smear over the entire wear surface in the elevated temperature tests appears to be a major factor in the similarity of performance. As the test temperature increased the occurrence of molybdenum smears increased on both the washer and disc surfaces. It covered over the carbide particles, effectively neutralizing their effect on the wear behavior of the composite. Molybdenum was the predominant phase on the washer surface, even in the 25°C tests.

Transfer of Disc Material to Washer

The presence of Si and Cr on the Al_2O_3-TiO_2 washer material from the 425°C tests, as shown in Figure 56, indicates that, at least in the case of oxide sliding on oxide, there is transfer from each of the surfaces to the other. The degree to which this mutual transfer of materials may occur when the molybdenum containing carbides are sliding on the SCA oxide composite is not discernible, but if it occurs at all, it does to a much lesser degree. This is thought to be due to the predominance of the molybdenum from the washer and the apparent ease with which it transfers to the SCA oxide.

Microstructural Stability of SCA Composite Oxide

The stability of the SCA coating in regards to its morphology and composition throughout the test series, whether it was on the disc or the washer, was quite evident and somewhat surprising. The material is applied using a slurry which is baked onto the substrate surface and subsequently impregnated with chromia. This method of application of a coating was not thought to result in as durable coating as a plasma spray material. While its wear rate at both 25°C and 425°C exceeded that of most of the other materials, see Figure 5, its microstructure was the most stable of all the materials tested.

Comparing the thickness of the SCA coating to the other coatings in Table 1 and the location of wear-through, i.e. washer or disc or both, in Table 2, it can be seen that at 25°C and 425°C the much thicker carbide coatings on the washer either wore through before the thin SCA coating or at the same time with a couple of exceptions,

especially at higher pressures. Thus the microstructural stability of the SCA coating related to its wear resistance.

CONCLUSIONS

1. No single material behaved in an overall superior manner to the others.

2. The surface composition and morphology of the washer coatings was modified by the wear process.

3. The coatings achieved a steady state wear rate after 1 - 2 hours of testing.

4. Most of the materials had a higher, initial, incremental wear rate than their steady state wear rate.

5. Higher bulk material temperatures markedly increased the wear rates.

6. The wear rates correlated more with the morphology and composition distribution similarities of the carbide cermet coatings than with the differences in the carbide particles, hardnesses or contact pressures.

7. Molybdenum in the carbide composites was the predominant material on the wear surfaces, smearing over the carbides on the washers and transferring to the SCA coated discs.

8. The sliding wear action super polished the carbide surfaces at 25^{o}C, removing most or all of the honing marks.

9. Contact pressures between 0.69 and 6.9 MPa resulted in approximately the same Cr_3C_2 washer material wear rate at 25°C.

10. An initial wear-in at a low contact pressure improved subsequent, higher contact pressure or temperature wear resistance.

11. The SCA coating's morphology and composition distribution remained markedly stable at all test conditions.

RECOMMENDED FUTURE TASKS

The investigation reported herein constituted an initial look at the behavior of material systems that are potential candidates for the piston ring-cylinder wall liner material pair of an advanced diesel engine. What was learned in carrying out the reported experiments suggested several follow-on avenues of investigation. Future tasks that would add important knowledge to the behavior of materials in this severe application are listed below.

1. Effect of composition, Morphology variations on wear.

2. Relation between process variables and wear.

3. Determination of sliding wear behavior of additional materials.

4. Effect of wear-in on mechanisms, rates of subsequent wear.

5. Optimization of porosity for sliding wear-thermal fatigue resistance.

6. Effect of combined corrosion-wear on material loss rates.

7. Effect of coating thickness on wear.

8. Long time wear tests to verify short time steady state rates.

9. High temperature wear of coatings on stainless steel.

10. Role of wear debris as solid film lubricant at elevated temperature.

11. Effect of lower cost processing of SCA coatings on wear.

12. Coefficient of friction of candidate materials pairs.

13. Modelling of observed wear behavior of coatings.

REFERENCES

1. Yust, C. S. and Carignan, F. J., "Observations on the Sliding Wear of Ceramics," ASLE Transactions, vol. 28, No. 2, pp. 245 - 252.

2. West, A. L., Syniuta, W. D., "Trobological Screening of Ceramic Materials for Use in Advanced Diesel Engines," EPRI RD - 2369 - SR, pp. 4-163-174, May 1982.

3. Levy, A., Boone, D., January, E., Davis, A., "Sliding Wear Behavior of Protective Coatings for Dlesel Engine Components," WEAR 101 no. 2, pp. 127 - 140, January 1985.

Table 1

COATING MATERIALS

MATERIAL	APPLICATION METHOD	THICKNESS IN mm	SURFACE FINISH	SUBSTRATE MATERIAL
WASHER*				
Cr_3C_2-Mo	Plasma spray	max 0.400	Ground	1018 steel
WC-Mo	Plasma spray	max 0.250	Ground	1018 steel
TiC-Mo	Plasma spray	max 0.175	Ground	1018 steel
Al_2O_3-TiO_2	Plasma spray	max 0.275	Ground	1018 steel
SiO_2, Cr_2O_3, Al_2O_3	Slurry plus impregnation	max 0.060	Ground	1018 steel
DISC				
SiO_2, Cr_2O_3, Al_2O_3	Slurry plus impregnation	0.05-0.075	Ground	1018 steel

*The presence of the prinicpal carbides and oxides listed were determined by x-ray diffraction. The detailed compositions and processing parameters were not reported by the coating suppliers because of the proprietary nature of the material systems.

Table 2

WASHER COMPOSITION	CONTACT PRESSURE MPa (psi)	TEMP °C	WEAR RATE $g/cm^2s \times 10^{-5}$ WASHER	DISC	EXPOSURE TIME Min	OBSERVATIONS
Cr_3C_2-Mo	0.17(25)	25	0.05	0.07	15	Washer and disc wear tracks polished
	0.17(25)	25	0.01	0.005	480	Washer and disc wear tracks polished
	0.69(100)	25	0.10	0.26	15	Washer and disc wear tracks polished
	6.9(1000)	25	0.13	0.18	15	Washer and disc wear tracks polished
	14 (2000)	25	0.27	0.31	10	Wore through washer and disc
	0.17(25)	425	-	-	2	Wore through washer
	0.17(25)	425	-	-	5	Wore through washer and disc
	0.69(100)	425	-	-	1	Wore through washer
	0.69(100)	425	-	-	2	Wore through washer and disc
	6.9(1000)	425	-	-	1	Wore through disc
	0.17(25)	730	-	-	9	Preworn at 25°C and 0.17MPa; wore through disc
WC-Mo	0.17(25)	25	0.07	0.07	15	Washer and disc wear tracks polished
	0.69(100)	25	0.14	0.26	15	Washer and disc wear tracks polished
	0.69(100)	25	0.005	0.045	480	Washer and disc wear tracks polished
	1.4 (200)	25	-	-	1	Wore through washer and disc
	0.17(25)	425	0.41	0.63	15	Washer and disc wear tracks compressed
	0.17(25)	730	-	-	2	Wore through disc
	0.17(25)	730	-	-	5	Preworn at 25°C and 0.17MPa; wore through washer and disc
TiC-Mo	0.69(100)	25	0.08	0.23	15	Washer and disc wear tracks polished
	0.17(25)	425	0.41	0.54	15	Disc wear tracks polished
	0.17(25)	730	-	-	1	Wore through washer and disc; a section of coating detacked from washer
Al_2O_3-TiO_2	0.69(100)	25	0.10	0.10	15	Washer and disc wear tracks polished
	0.69(100)	25	0.05	0.21	480	Washer and disc wear tracks rough
	1.0(150)	25	0.08	0.08	15	Washer and disc wear tracks polished
	6.9(1000)	25	0.15	0.28	10	Preworn and 25°C and 1.0MPa; washer and disc wear tracks polished
	6.9(1000)	25	-	-	1	Wore through washer and disc
	0.17(25)	425	-	-	2	Wore through disc
	0.17(25)	730	-	-	15	Washer and disc wear tracks compressed
SCA	0.35(50)	25	0.08	0.13	70	Washer and disc wear tracks rough
	0.69(100)	25	0.40	0.46	10	Wore through washer and disc
	0.17(25)	425	0.66	1.66	20	Disc wear tracks polished
	0.17(25)	730	-	-	1	Wore through washer and disc

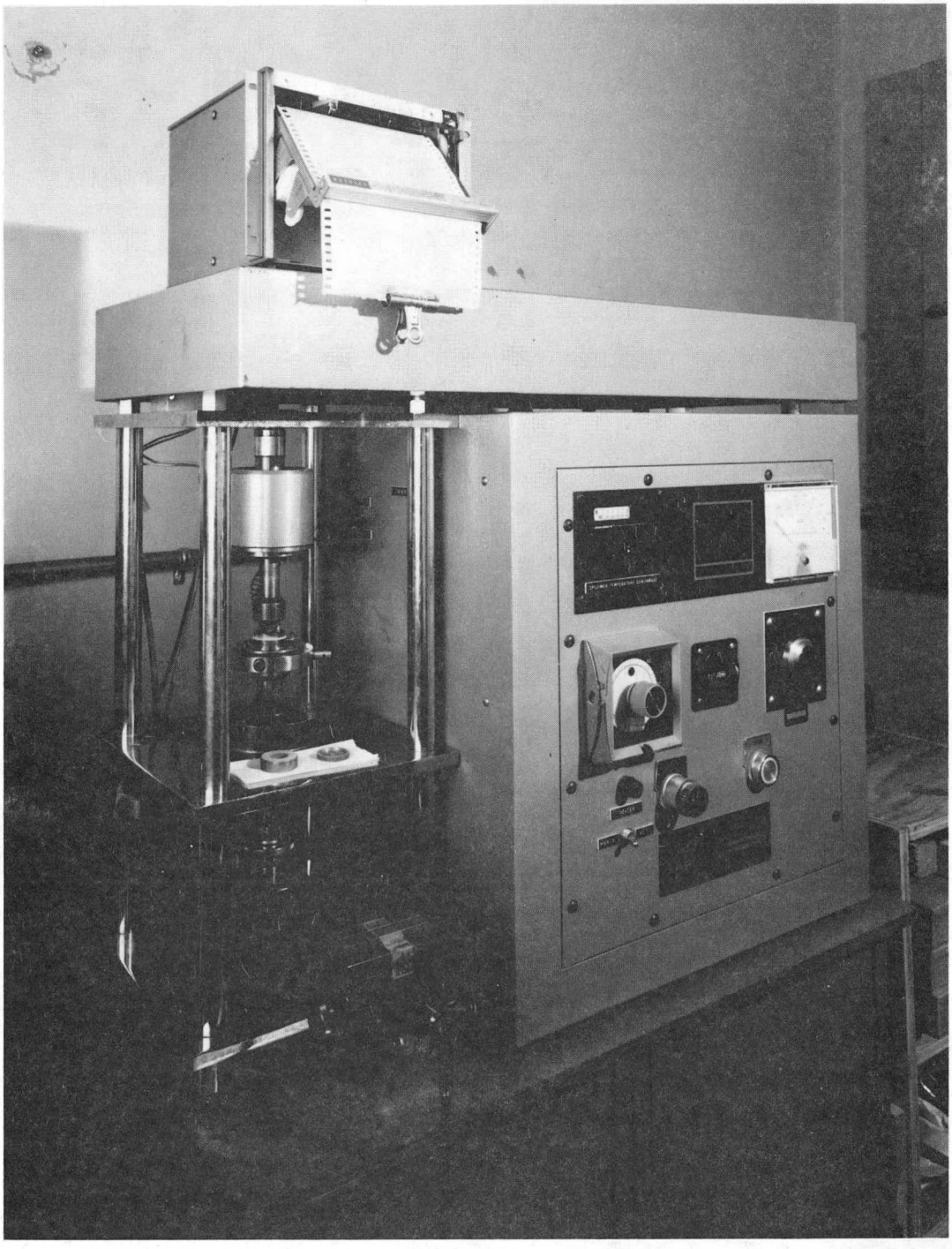

CBB 841-510

Figure 1. FALEX-6 washer on disc tester.

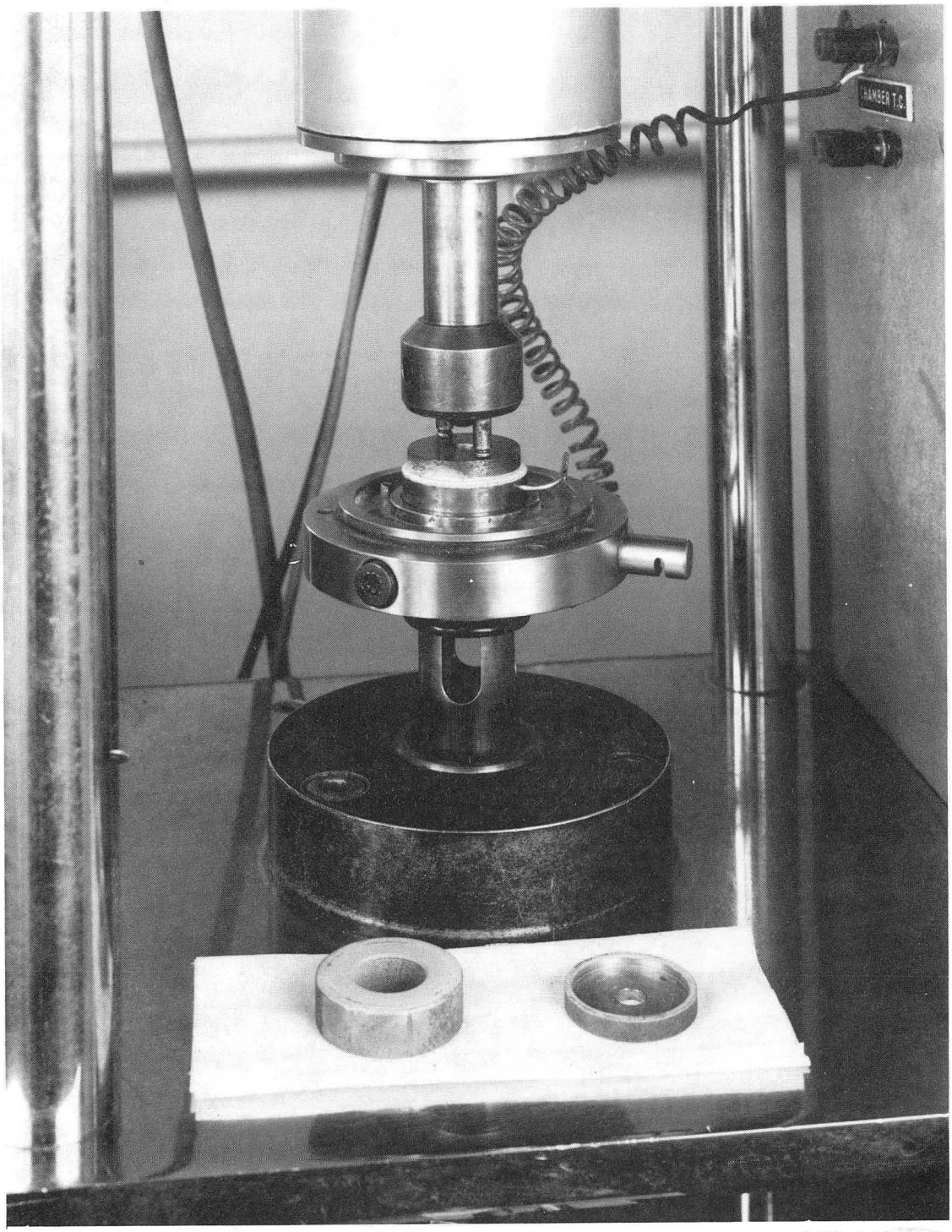

CBB 841-508

Figure 2. Washer, disc and specimen holder area of test machine.

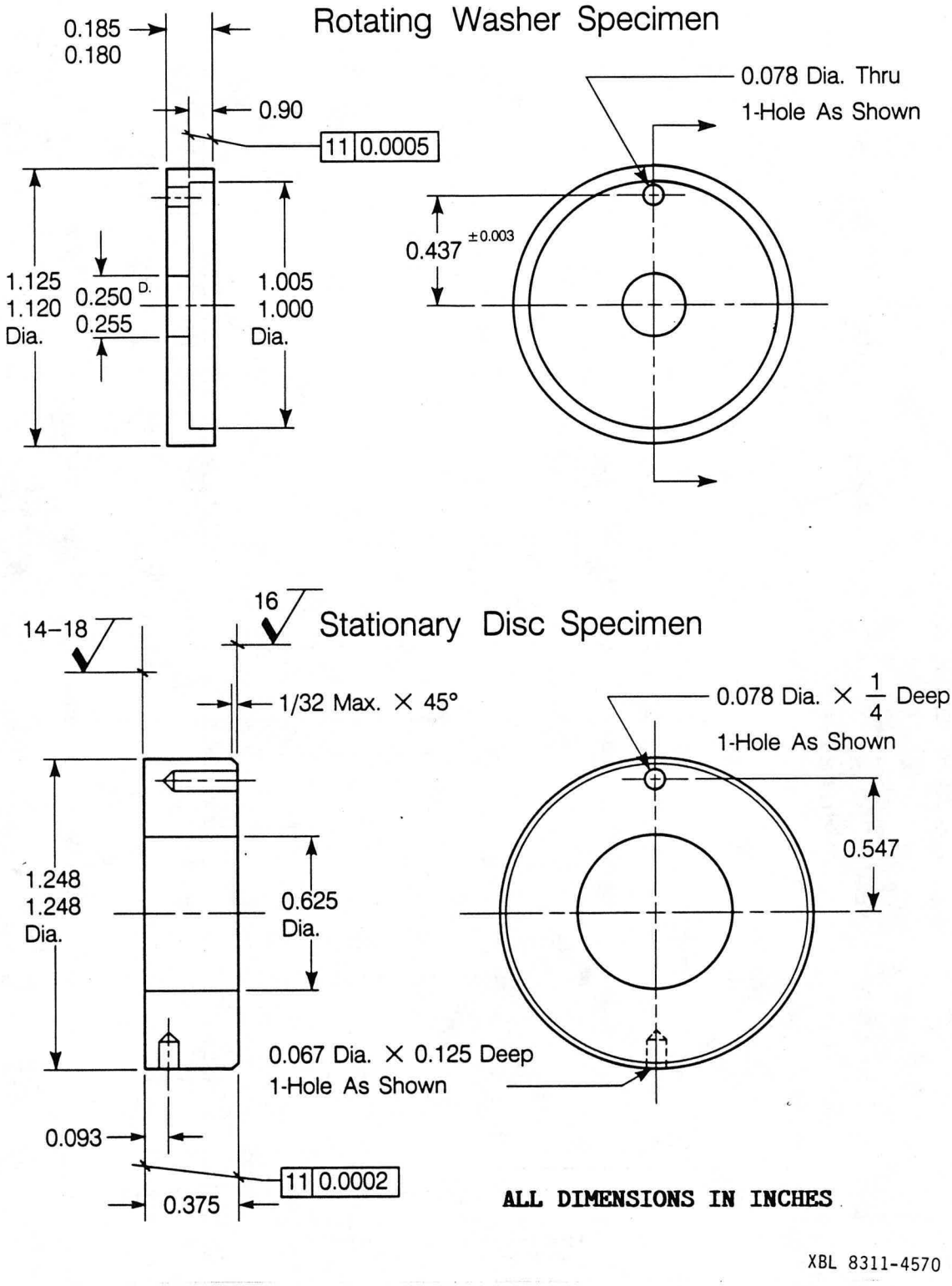

Figure 3. Dimensions of the rotating washer and stationary disc.

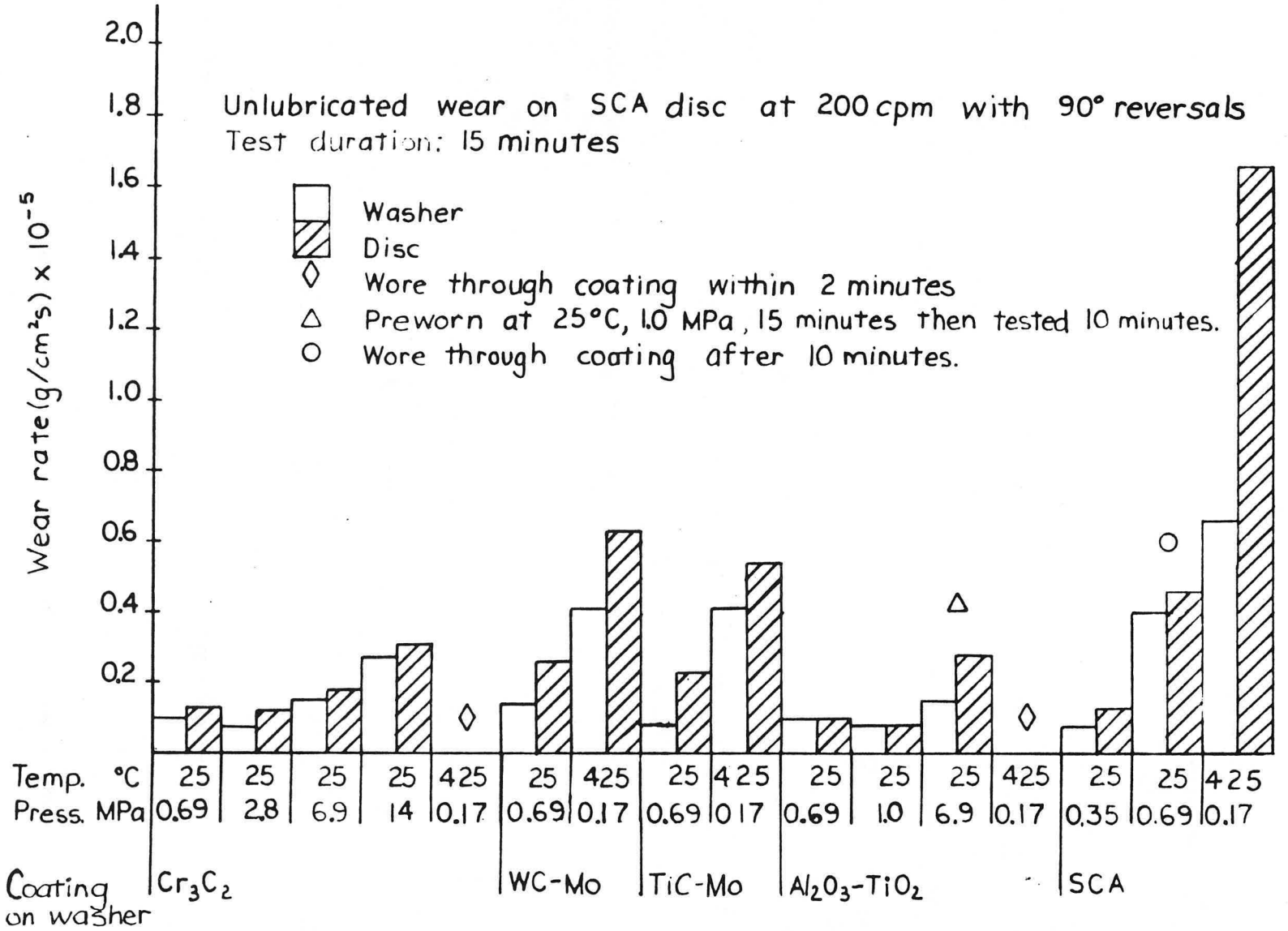

Figure 4. Wear rate of Cr_3C_2-Mo, WC-Mo, TiC-Mo, Al_2O_3-TiO_2, SCA washer on SCA disc.

XBL 8510-4163

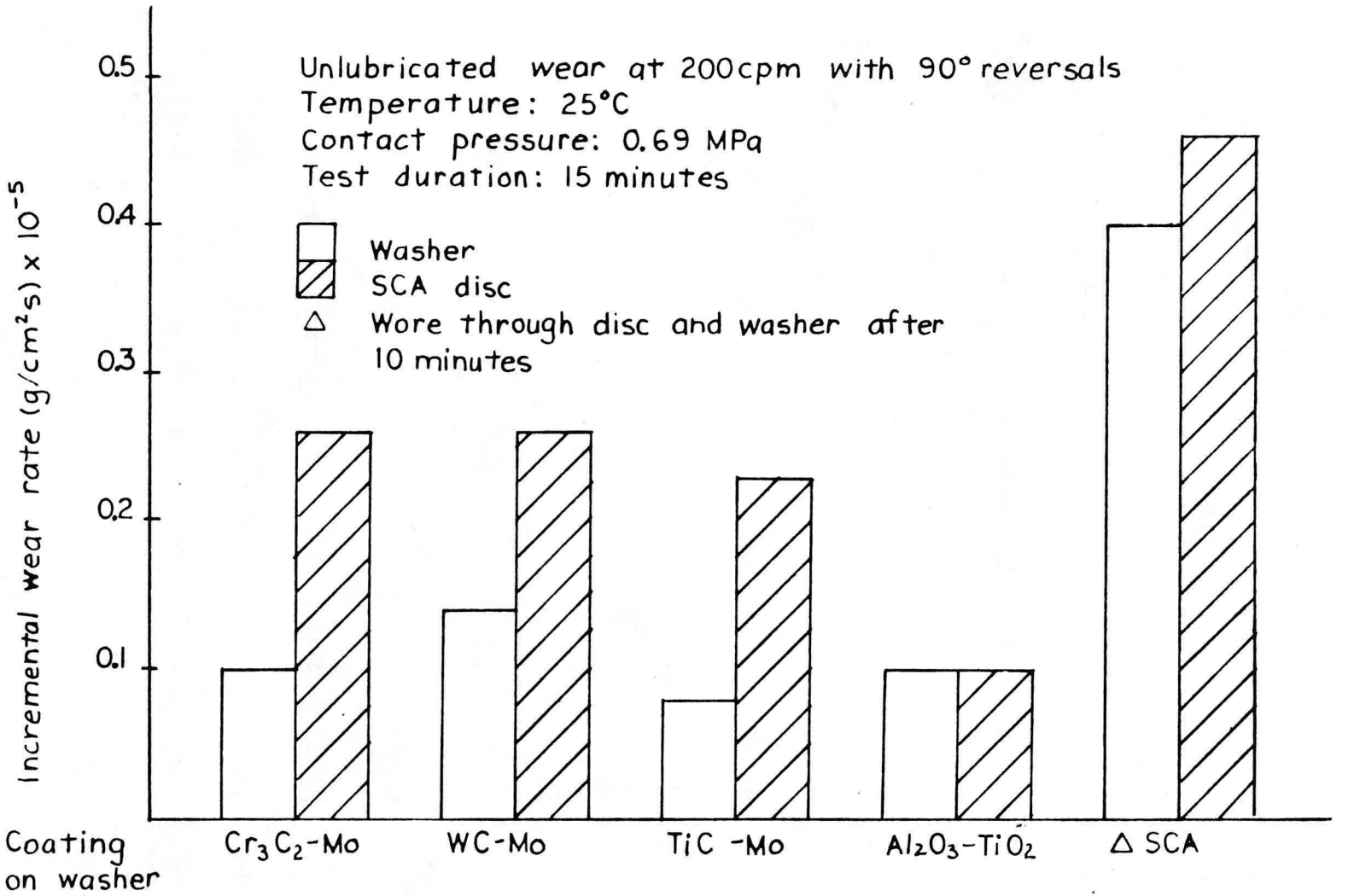

Figure 5. Comparison of the wear rates of Cr_3C_2, WC-Mo, TiC-Mo, Al_2O_3-TiO_2 washer on SCA discs at 25°C and 0.69 MPa.

XBL 8510-4162

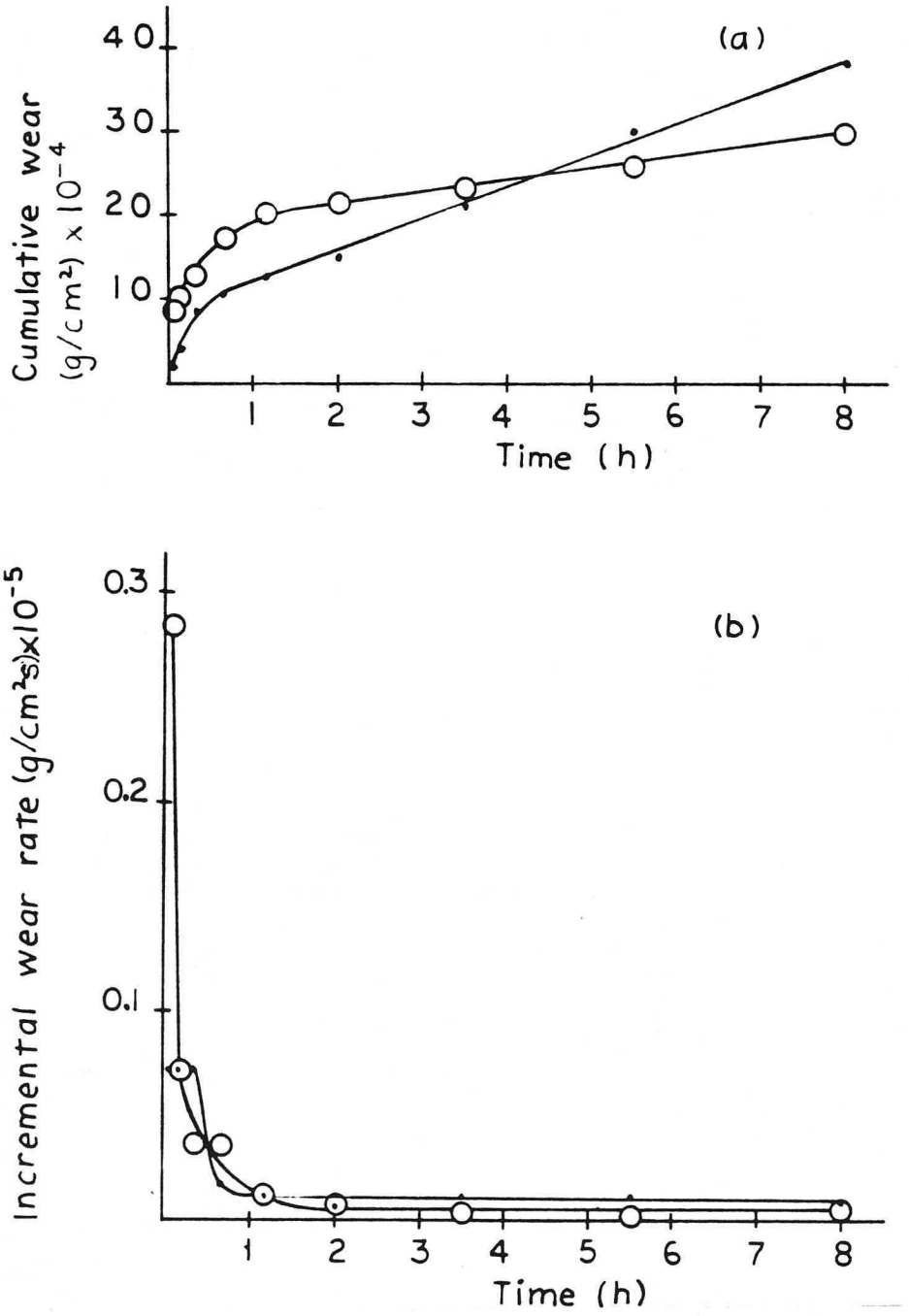

Figure 6. Wear curves of Cr_3C_2-Mo washer on SCA disc at 25°C and 0.17 MPa for 8 hours.

XBL 8510-4161

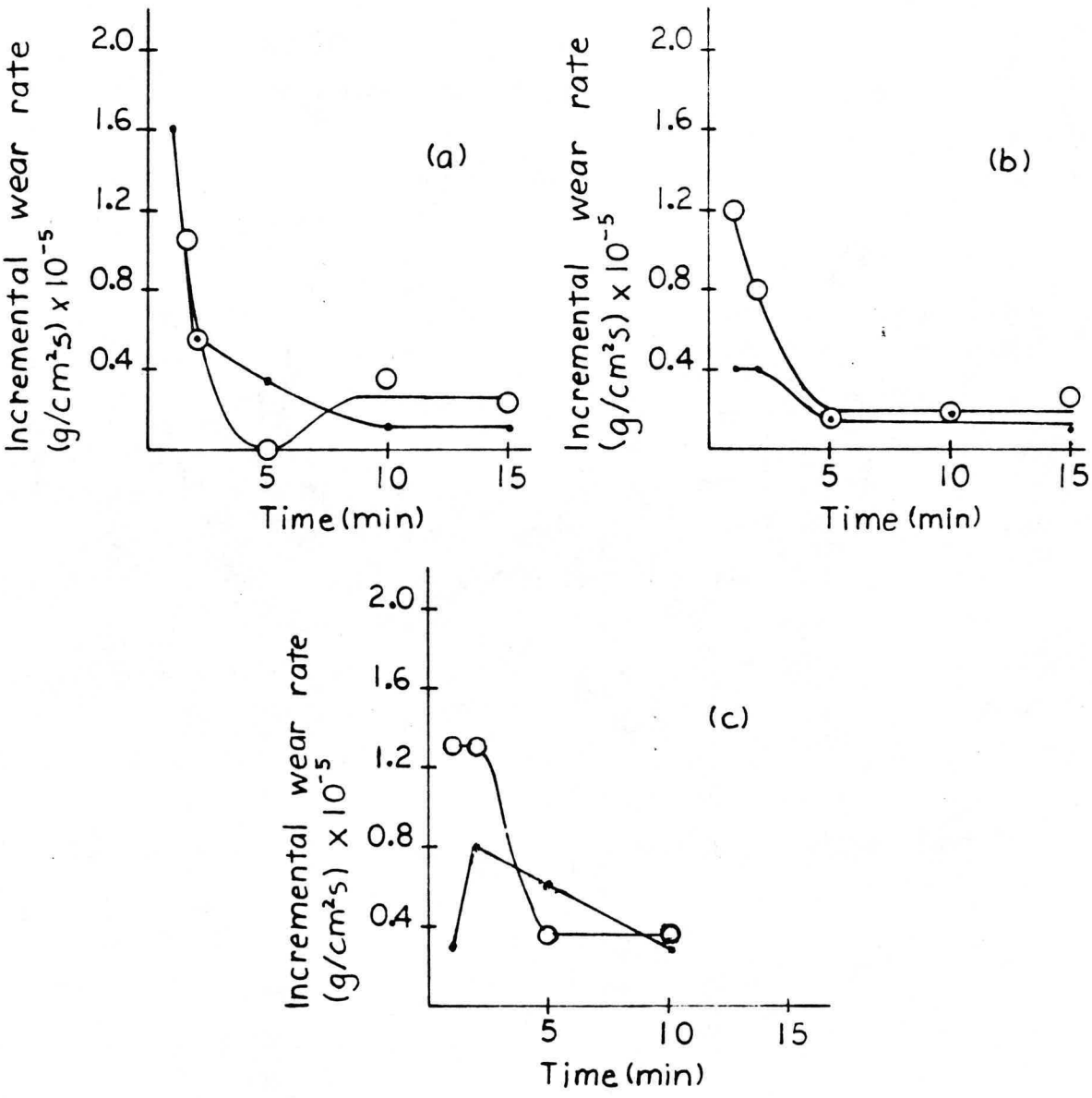

Figure 7. Wear Curves of Cr_3C_2-Mo washer on SCA disc at 25°C and 0.69 MPa, 6.9MPa and 14MPa.

XBL 8510-4160

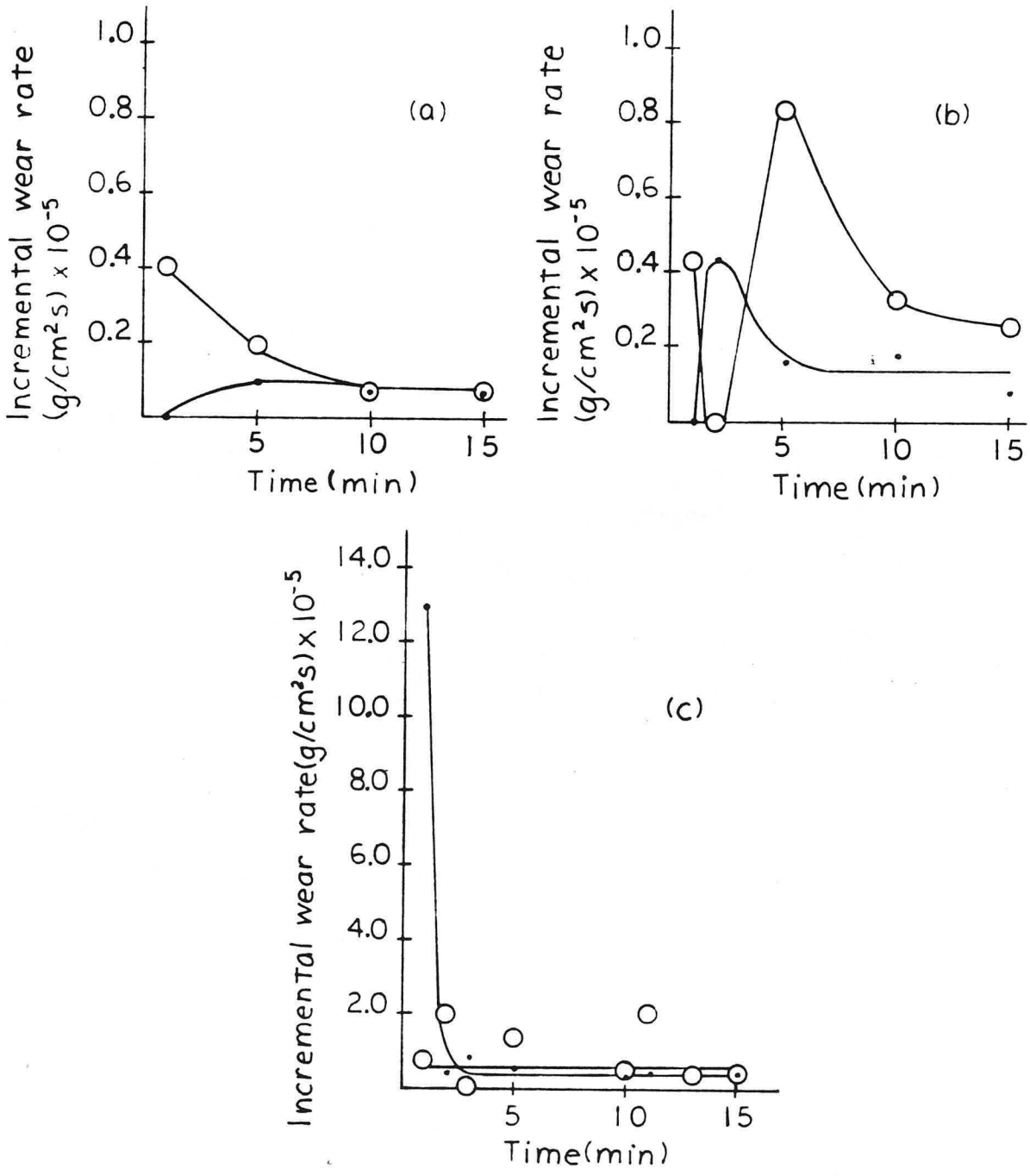

Figure 8. Wear curves of WC-Mo washer on SCA disc at 25°C and 425°C.

XBL 8510-4159

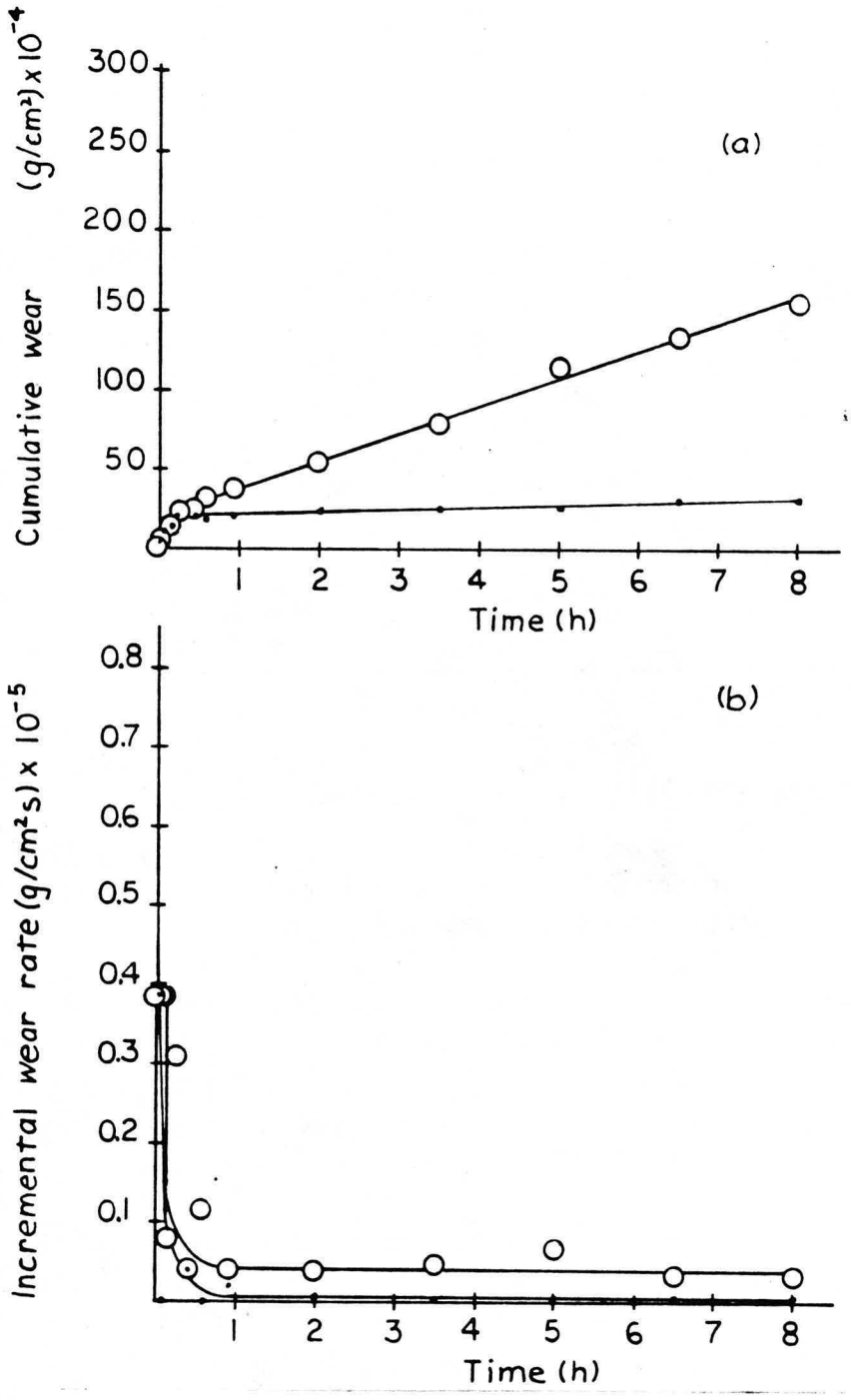

Figure 9. Wear curves of WC-Mo washer on SCA disc at 25°C and 0.69MPa for 8 hours.

XBL 8510-4158

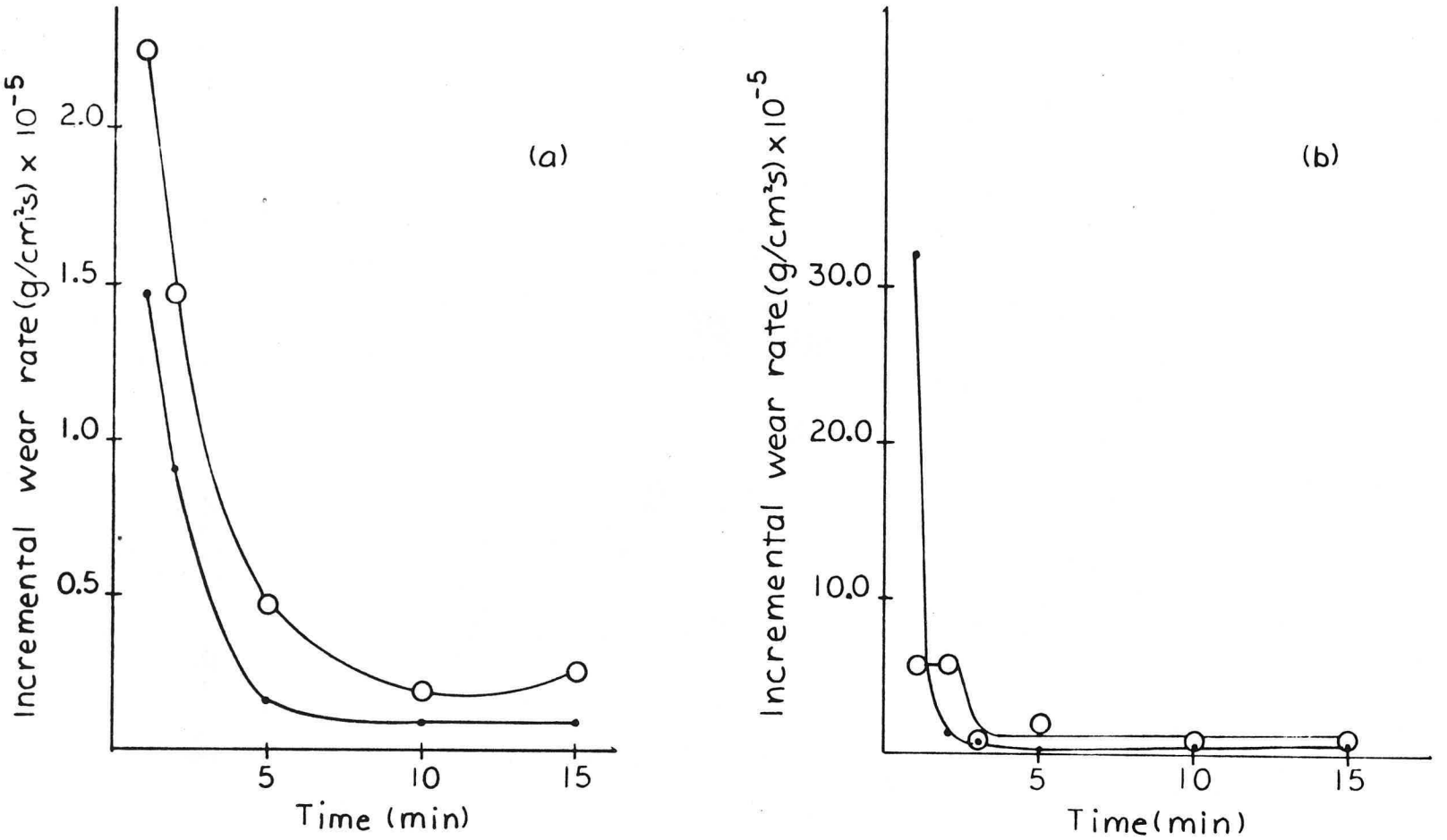

Figure 10. Wear curves of TiC-Mo washer on SCA disc at 25°C and 425°C.

XBL 8510-4157

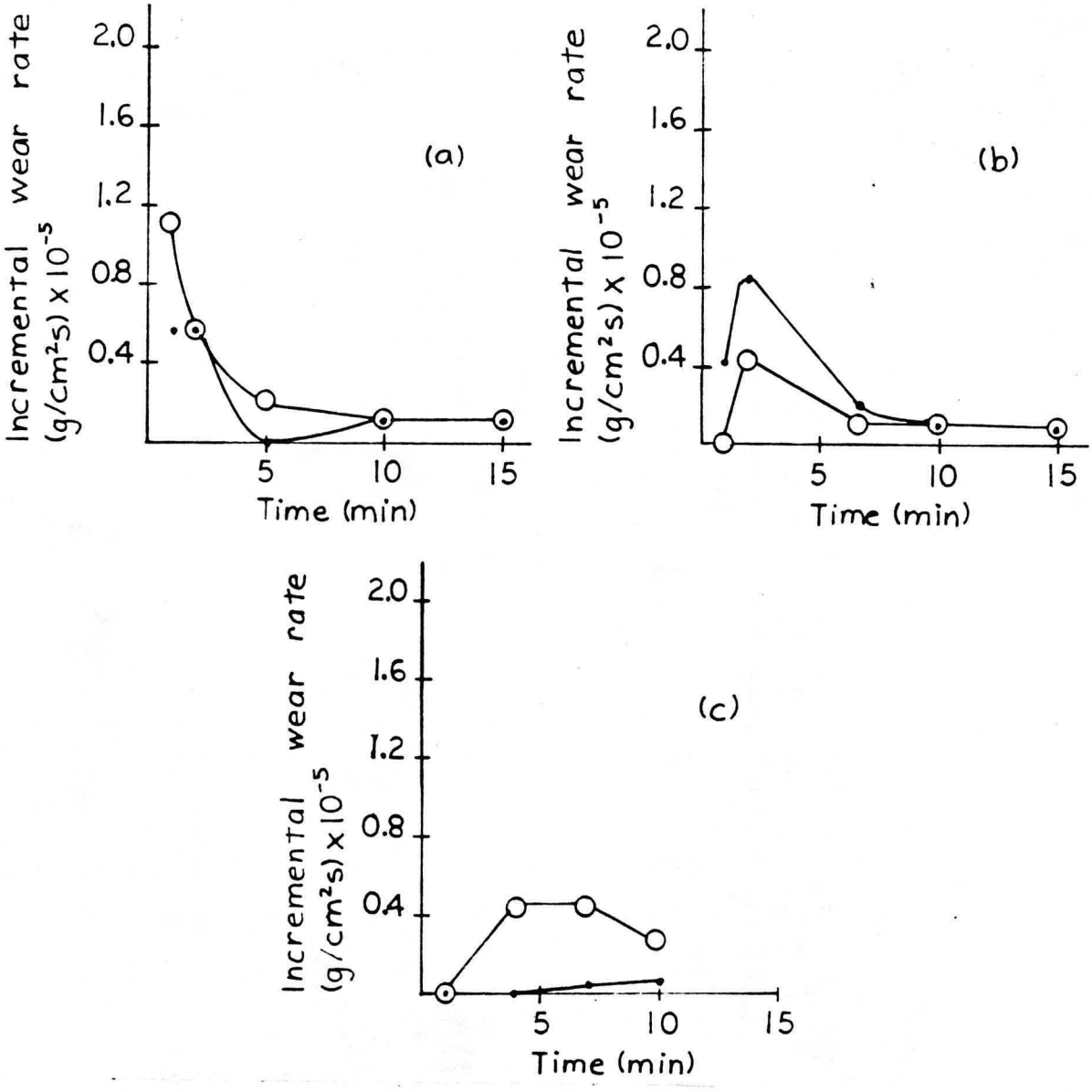

Figure 11. Wear curves of Al_2O_3-TiO_2 washer on SCA disc at 25°C.

XBL 8510-4156

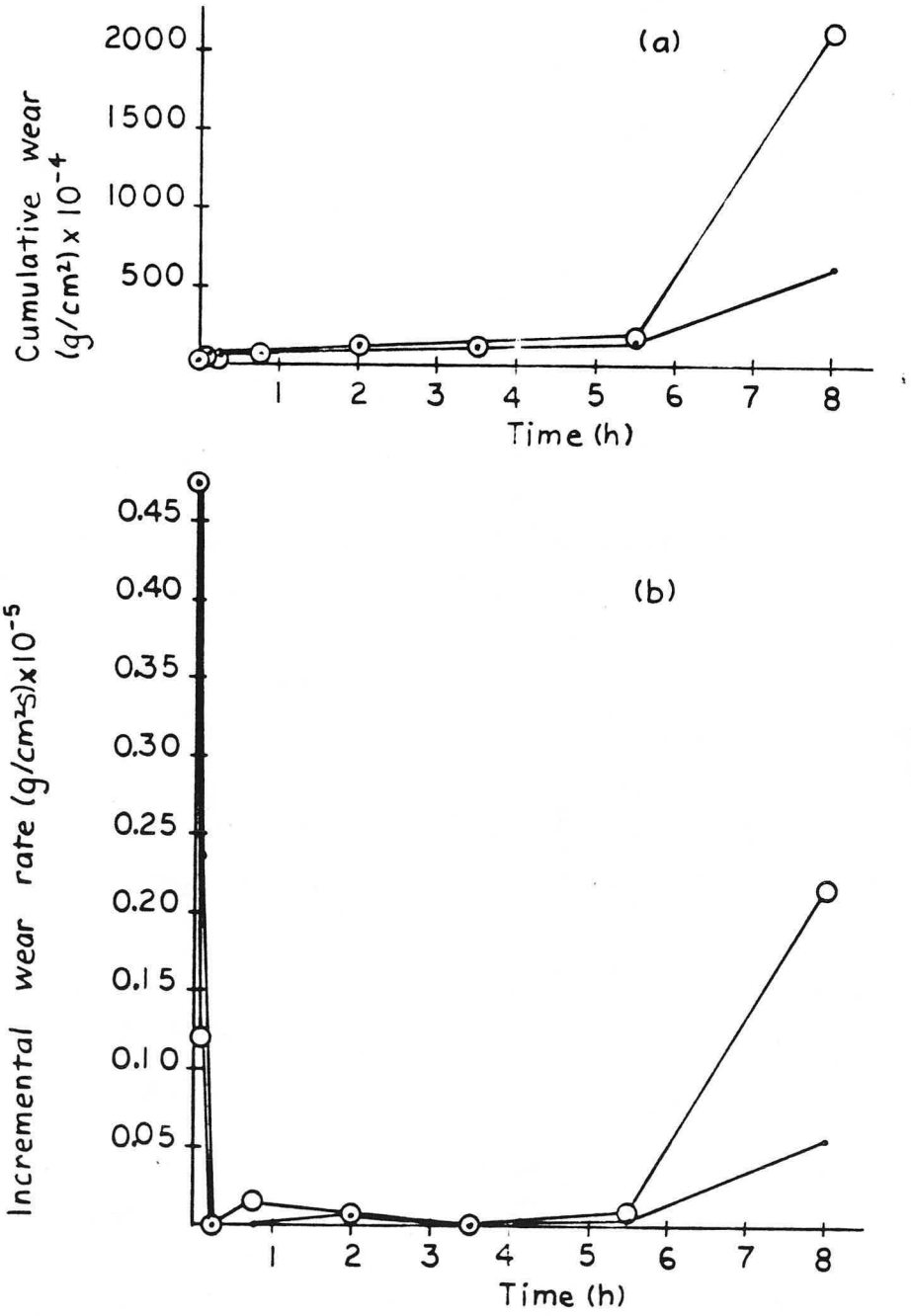

Figure 12. Wear curves of Al_2O_3-TiO_2 washer on SCA disc at 25°C and 0.69MPa for 8 hours.

XBL 8510-4164

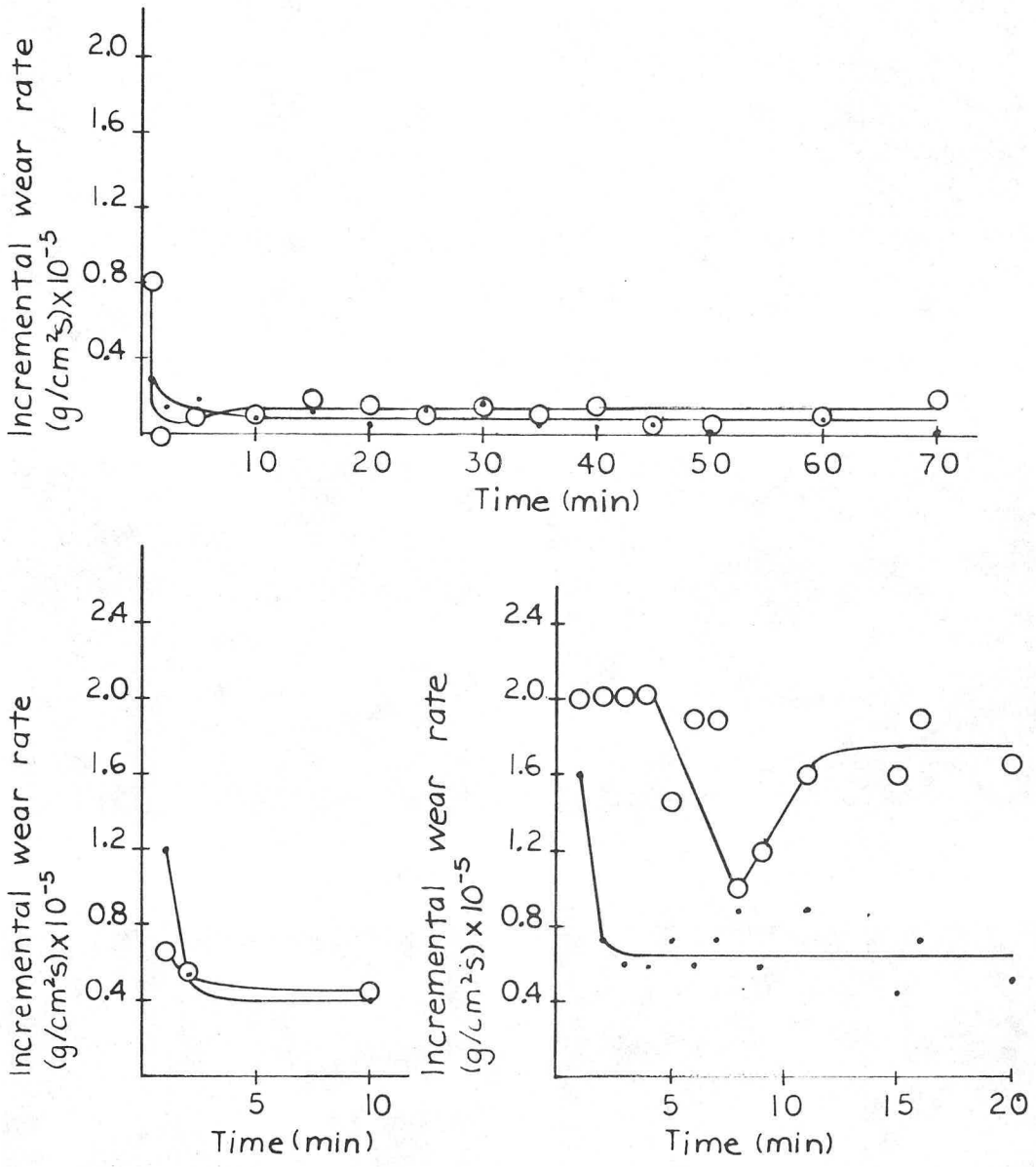

Figure 13. Wear curves of SCA washer on SCA disc at 25°C and 425°C.

XBL 8510-4165

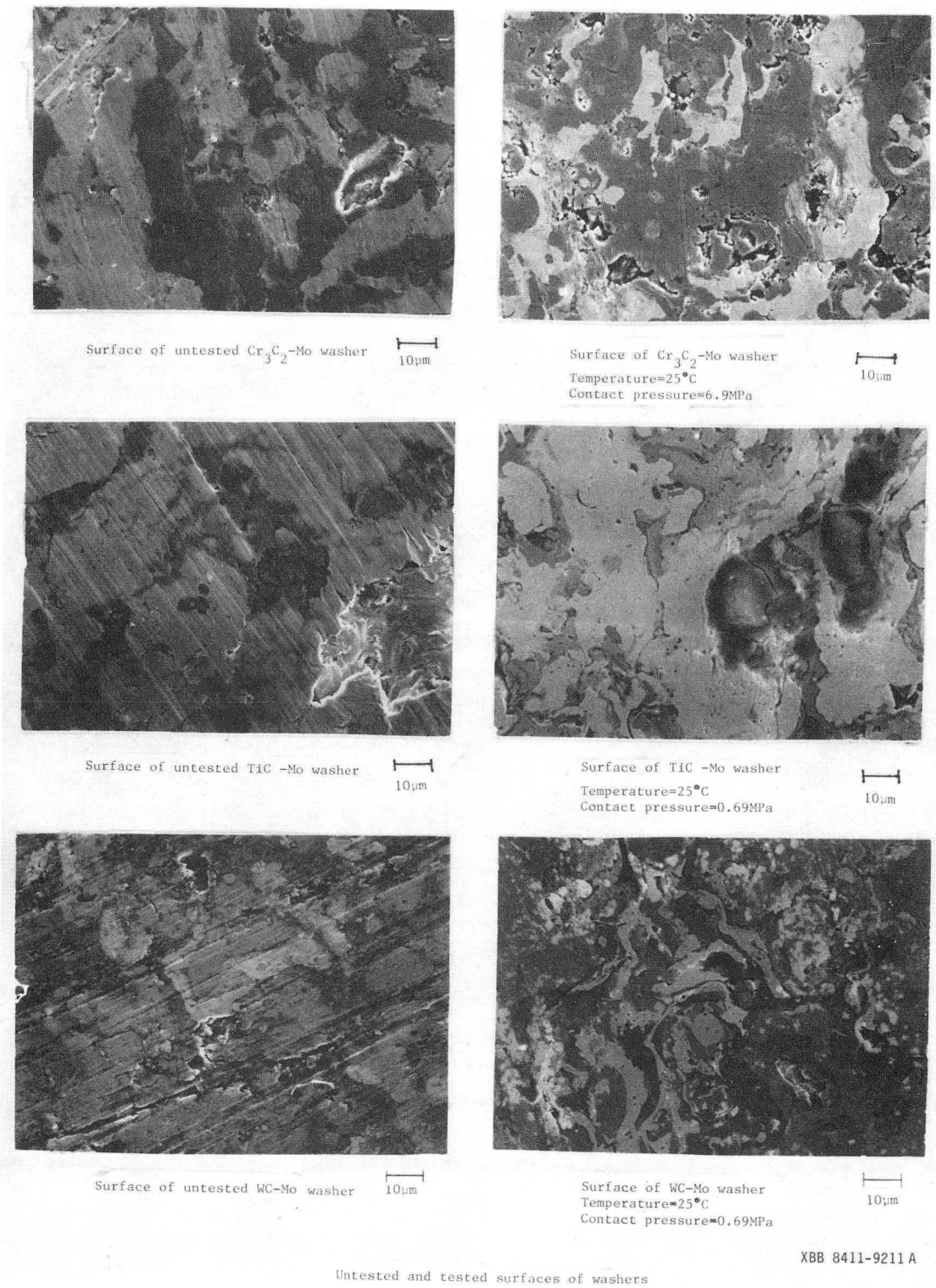

Figure 14. Untested and tested surfaces of Cr_3C_2-Mo, TiC-Mo and WC-Mo washers.

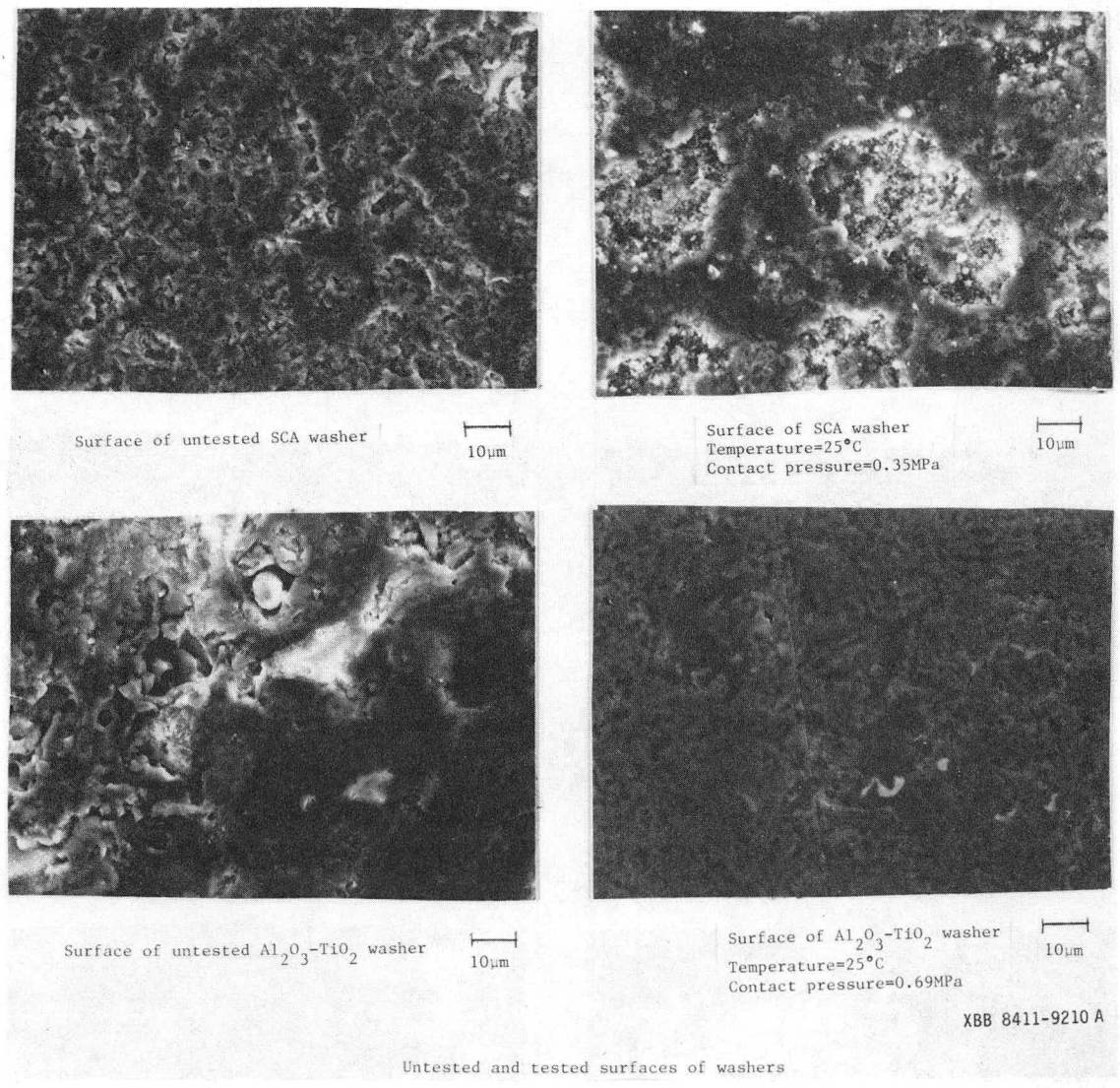

Figure 15. Untested and tested surfaces of Al_2O_3-TiO_2 and SCA washers.

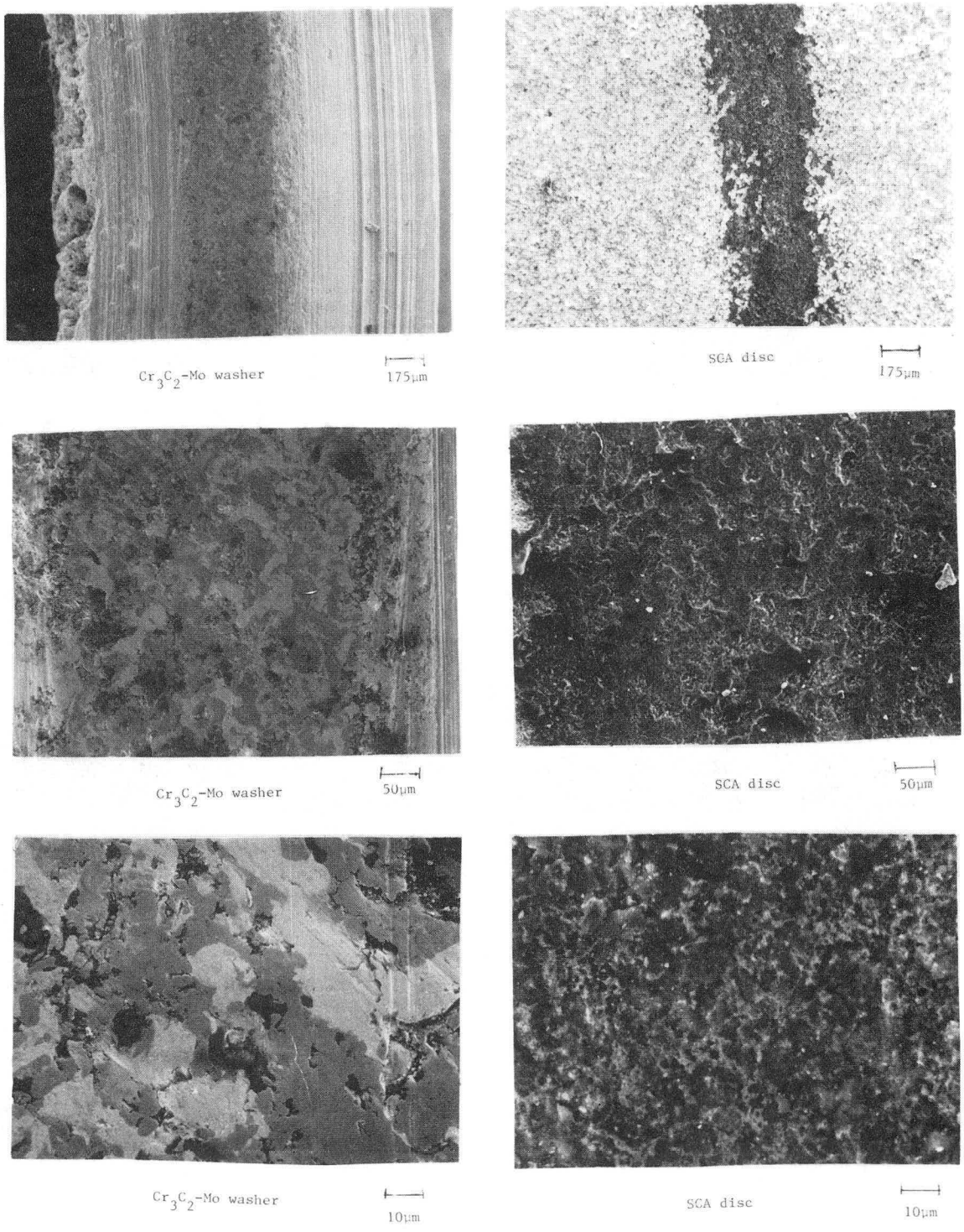

Figure 16. Surface of Cr_3C_2-Mo washer and SCA disc at 25°C and 0.69MPa.

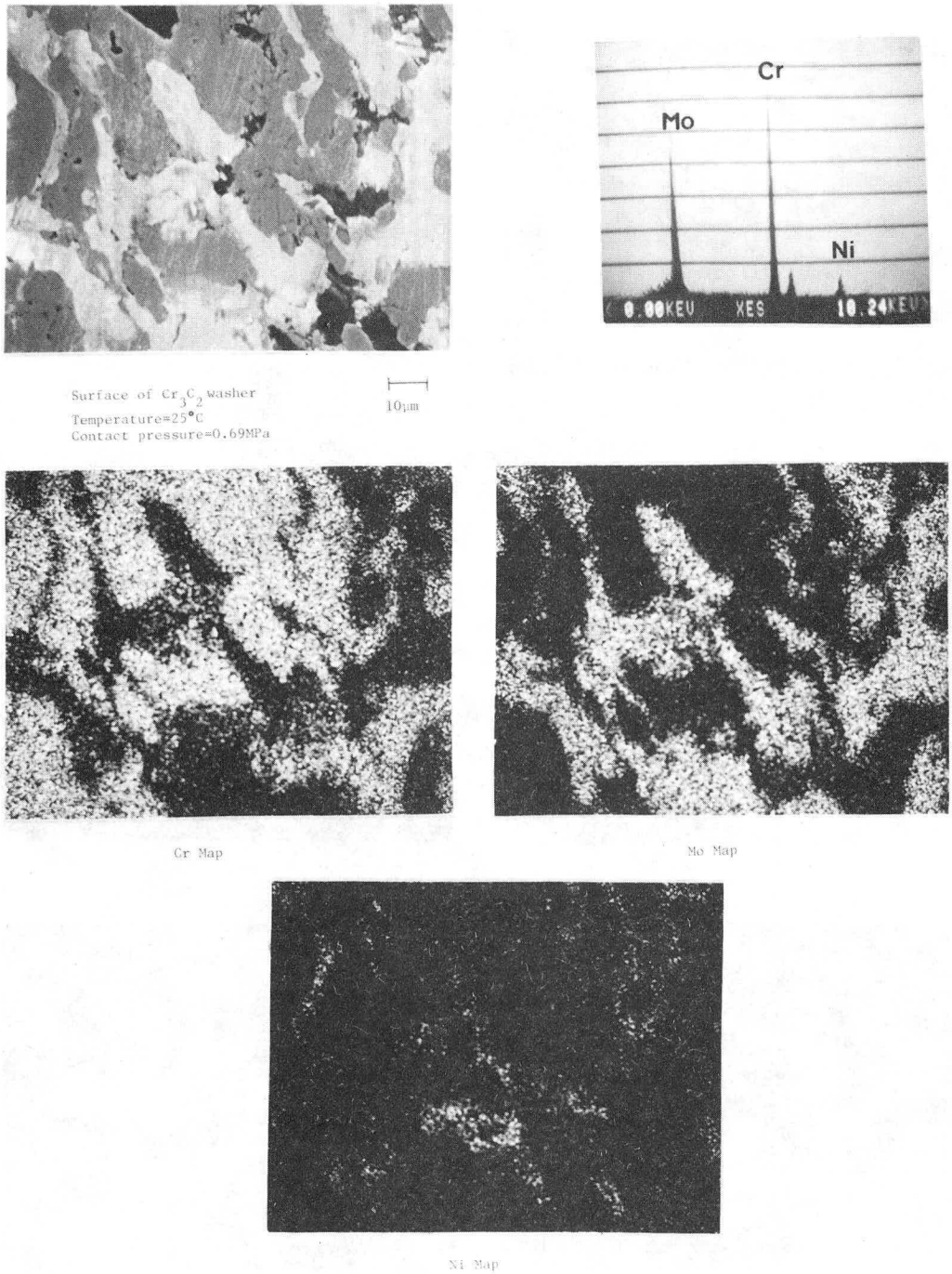

Figure 17. X-ray maps of the surface of Cr_3C_2-Mo washer at 25°C and 0.69MPa.

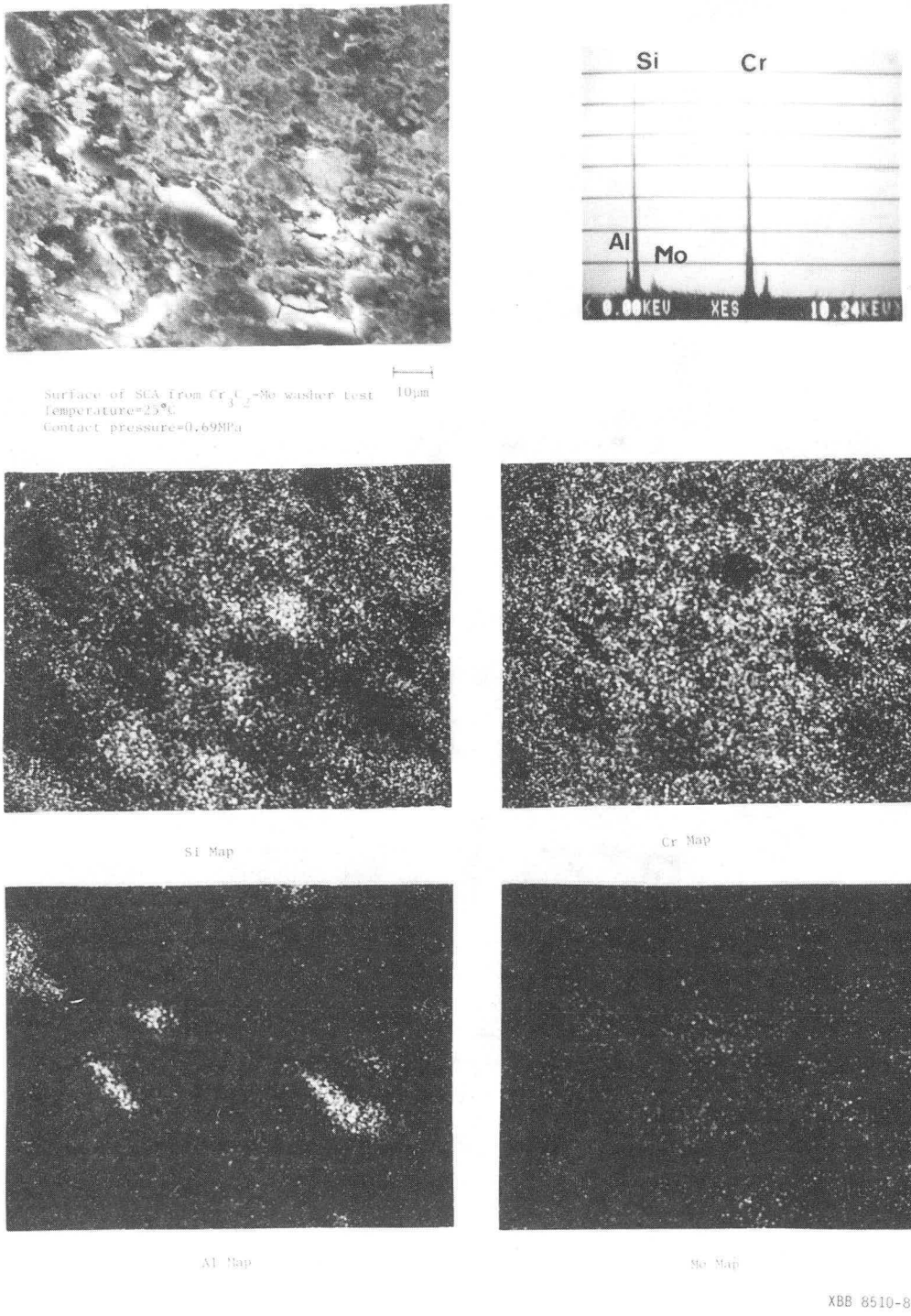

Figure 18. X-ray maps of the surface of SCA disc from Cr_3C_2-Mo washer test at 25°C and 0.69MPa.

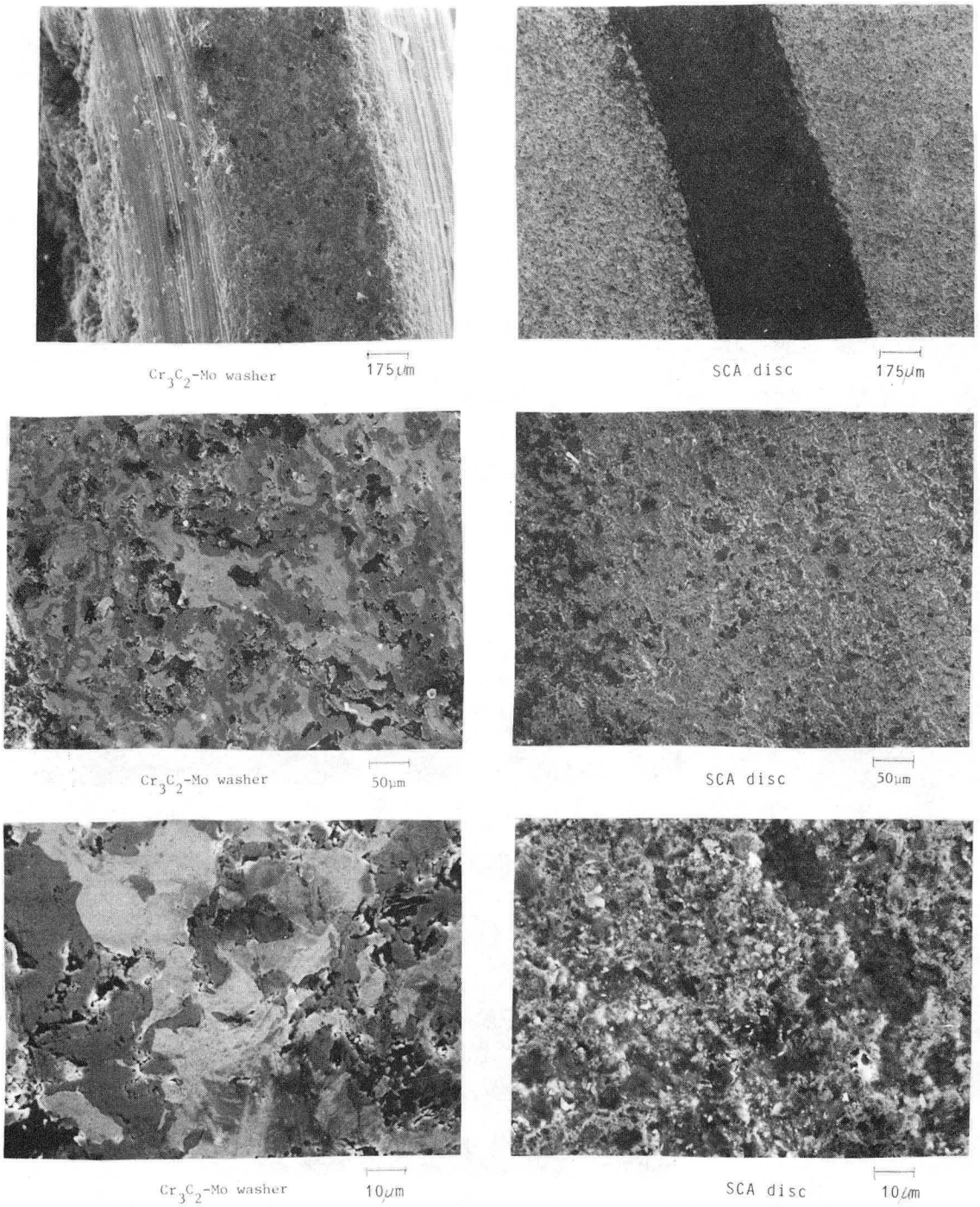

Figure 19. Surface of Cr_3C_2-Mo washer and SCA disc at 25°C and 6.9MPa.

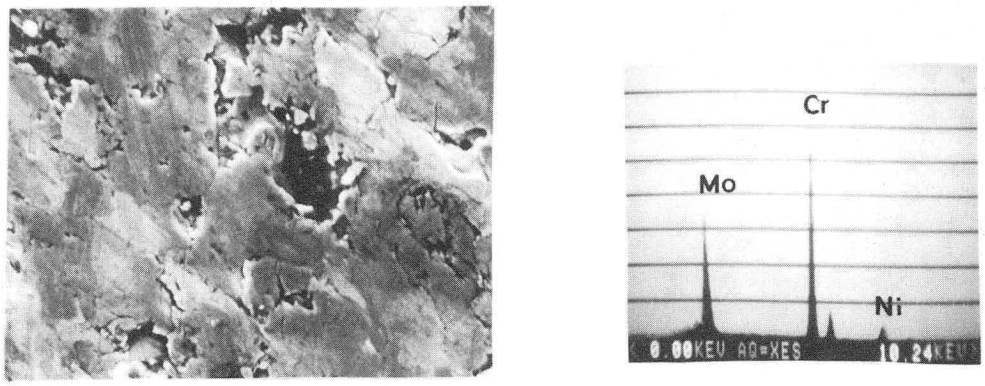

Surface of Cr_3C_2-Mo washer
Temperature=25°C
Contact pressure=6.9MPa

10μm

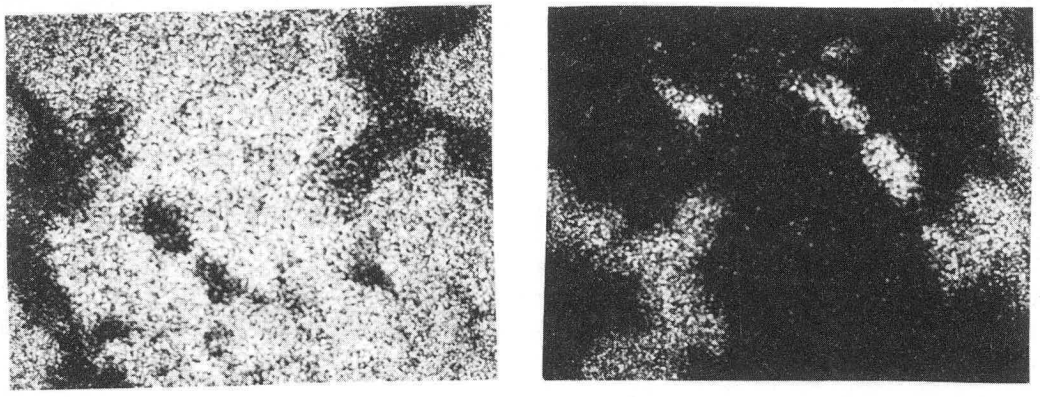

Cr Map

Mo Map

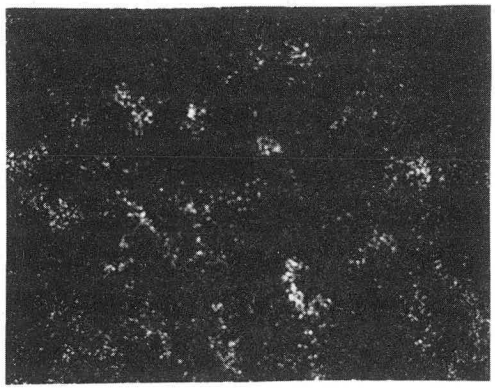

Ni Map

XBB 8510-8087

X-ray maps of the surface of Cr_3C_2-Mo washer at 25°C.

Figure 20. X-ray maps of the surfaces of Cr_3C_2-Mo washer at 25°C and 6.9MPa.

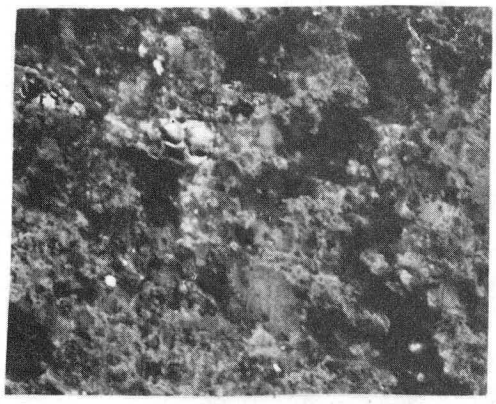

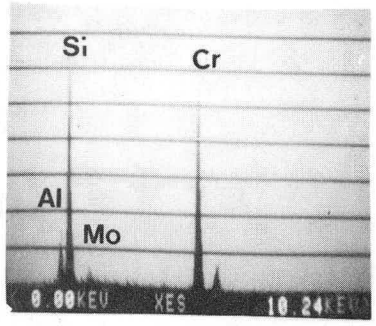

Surface of SCA disc from Cr_3C_2-Mo washer test.
Temperature=25°C
Contact pressure=6.9MPa

10μm

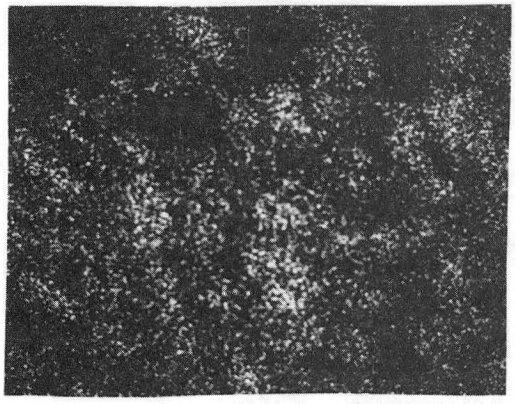

Si Map

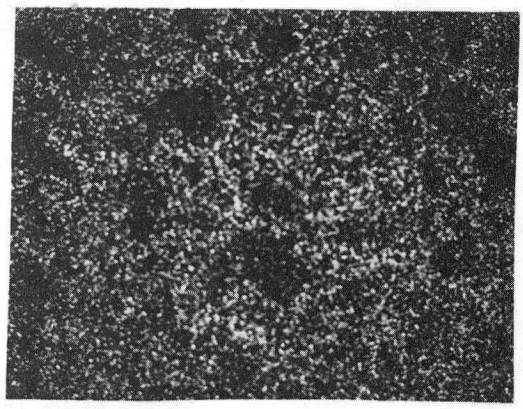

Cr Map

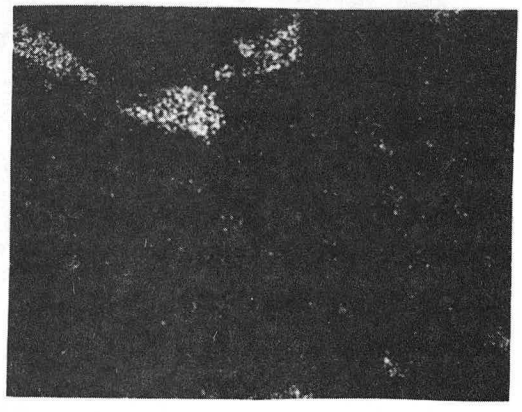

Al Map

X-ray maps of the surface of SCA disc at 25°C.

XBB 8510-8088

Figure 21. X-ray maps of the surface of SCA disc from Cr_3C_2-Mo washer test at 25°C and 6.9MPa.

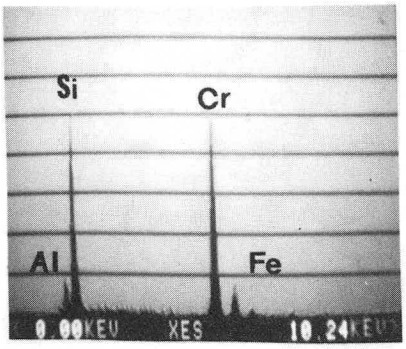

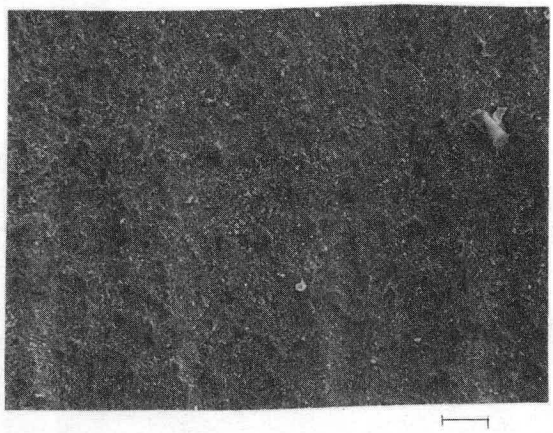

SCA disc 50μm

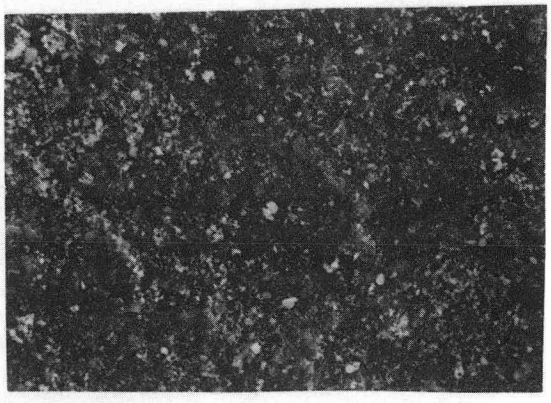

SCA disc 10μm

XBB 8411-9220

SCA disc from Cr_3C_2-Mo washer test
Temperature=425°C
Contact pressure=0.17MPa

Figure 22. Surface of SCA disc worn on Cr_3C_2-Mo washer at 425°C and 0.17MPa.

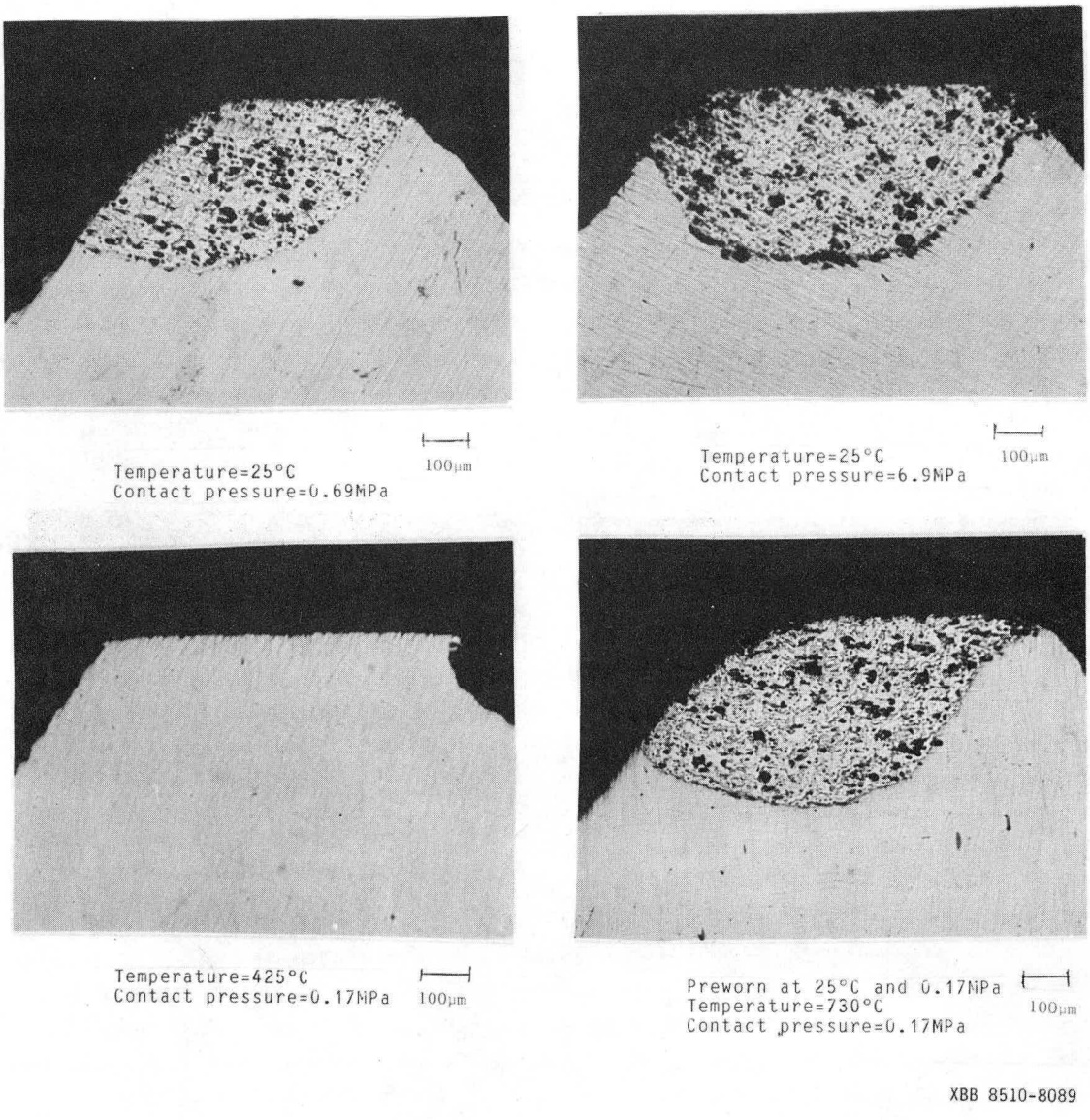

Cross section of Cr_3C_2-Mo washers.

Figure 23. Cross section of Cr_3C_2-Mo washer at 25°C, 425°C and 730°C.

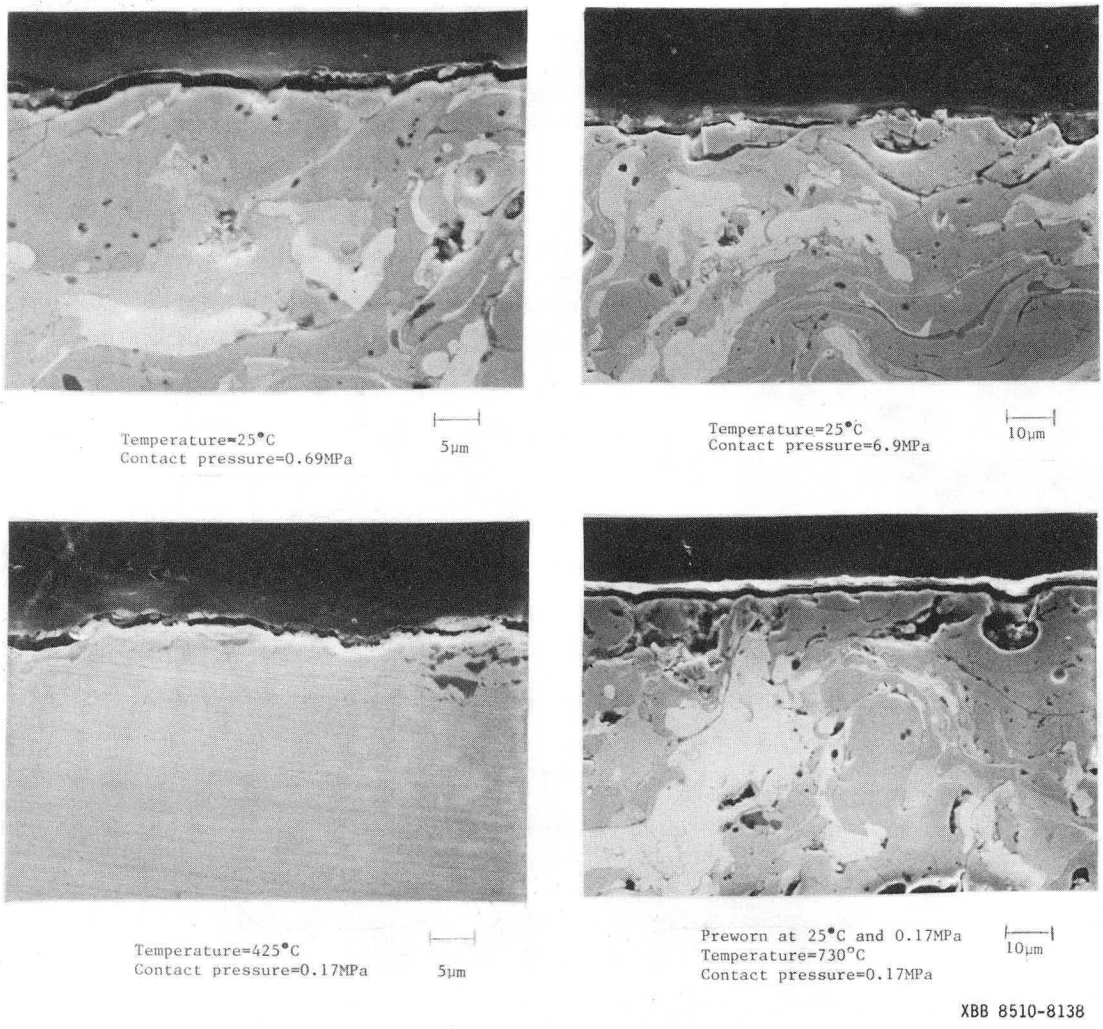

Cross section of Cr_3C_2-Mo washers.

Figure 24. High magnification cross section of Cr_3C_2-Mo washer at 25°C, 425°C and 730°C.

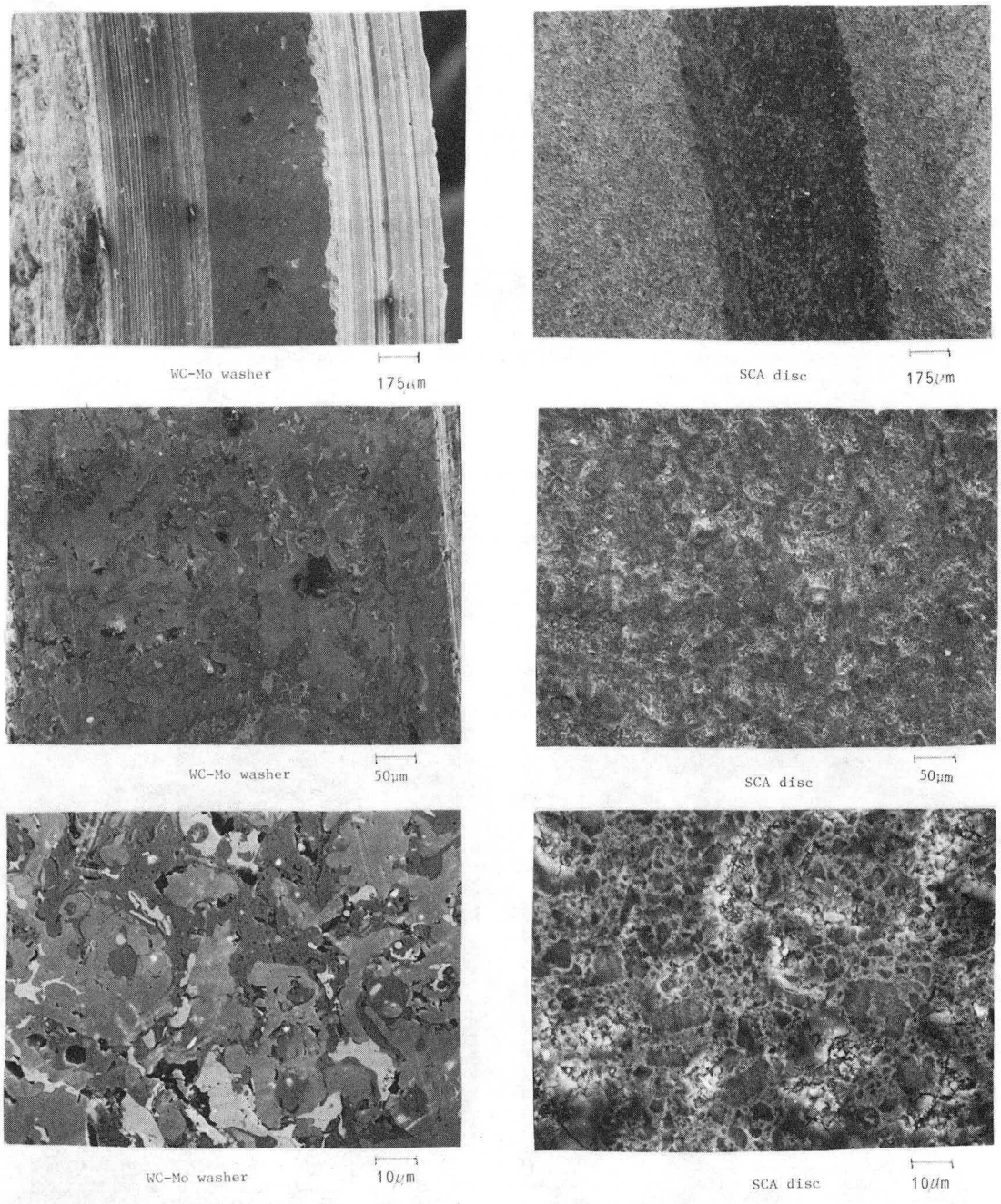

Figure 25. Surface of WC-Mo washer and SCA disc at 25°C and 0.69MPa.

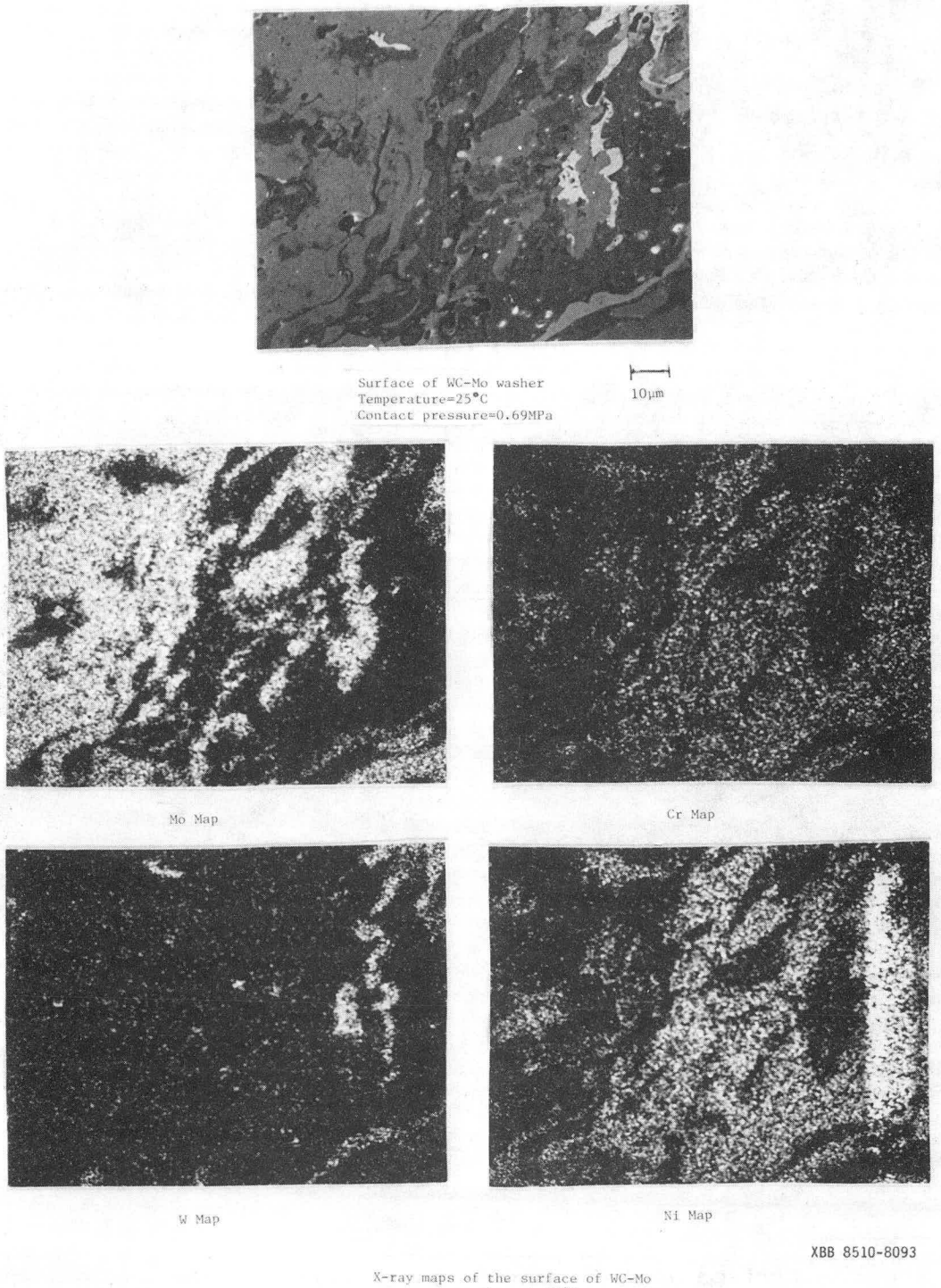

Figure 26. X-ray maps of the surface of WC-Mo washer at 25°C and 0.69MPa.

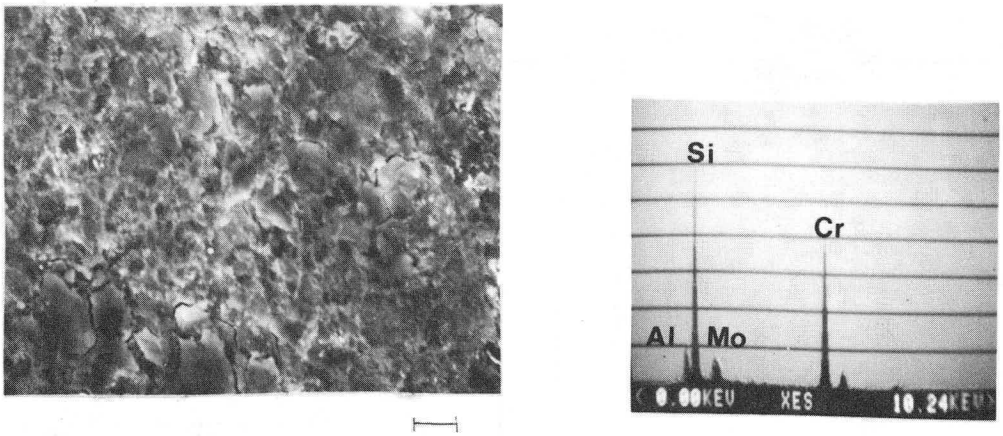

Surface of SCA disc from WC-Mo washer test. 10μm
Temperature=25°C
Contact pressure=0.69MPa

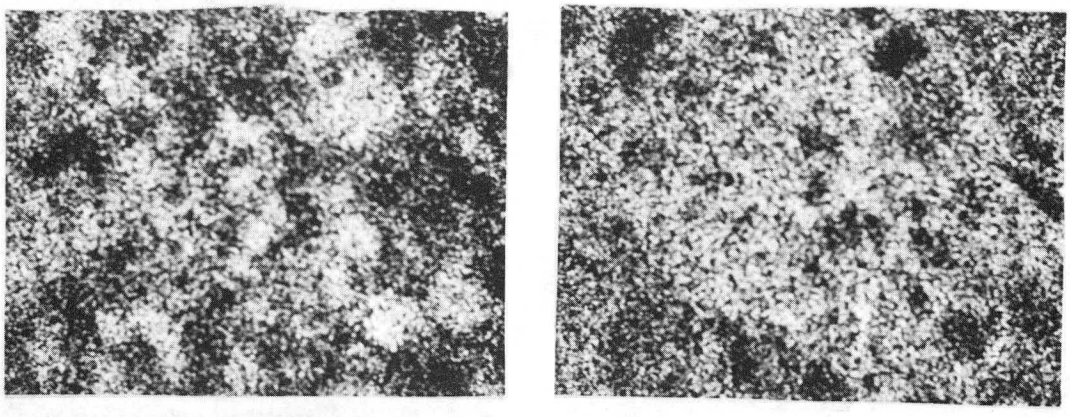

Si Map

Cr map

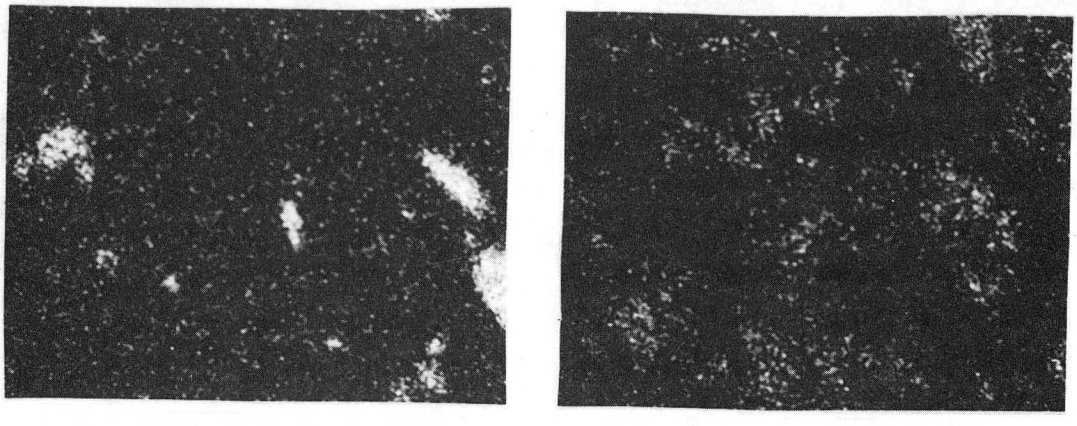

Al map

Mo Map

XBB 8411-9195

X-ray maps of the surface of SCA disc at 25°C.

Figure 27. X-ray maps of the surface of SCA disc from WC-Mo washer test at 25°C and 0.69MPa.

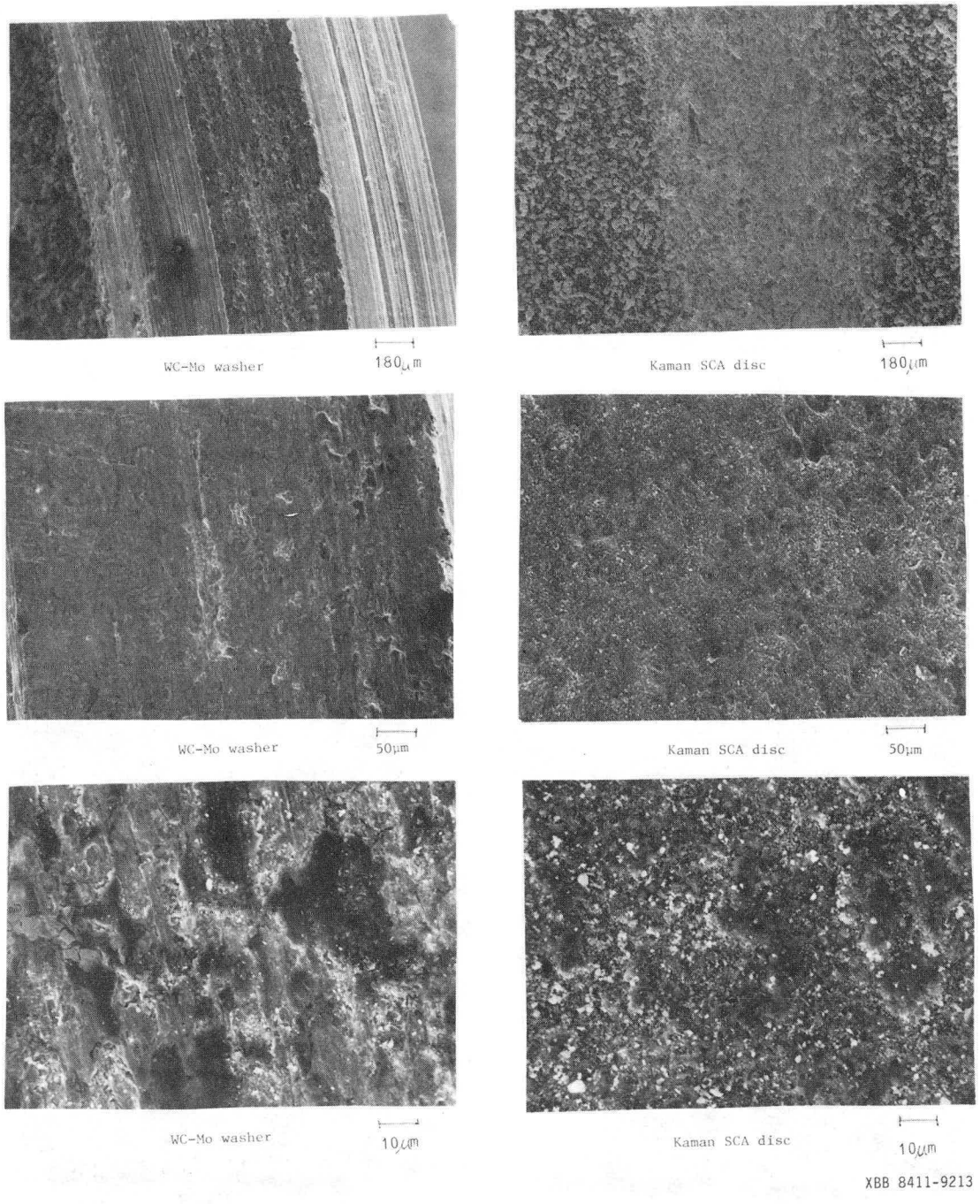

Figure 28. Surface of WC-Mo washer and SCA disc at 425°C and 0.17MPa.

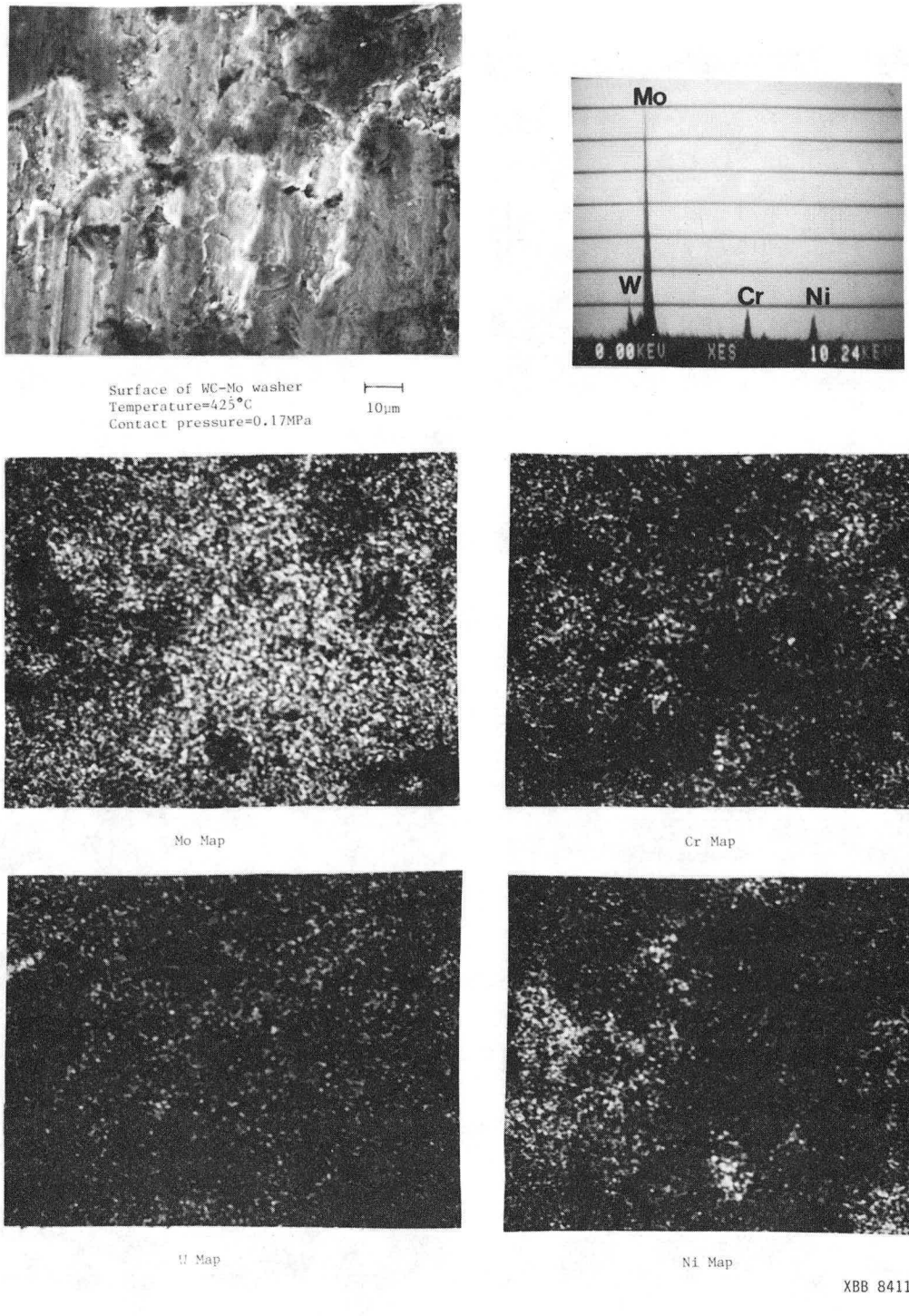

Figure 29. X-ray maps of the surface of WC-Mo washer at 425°C and 0.17MPa.

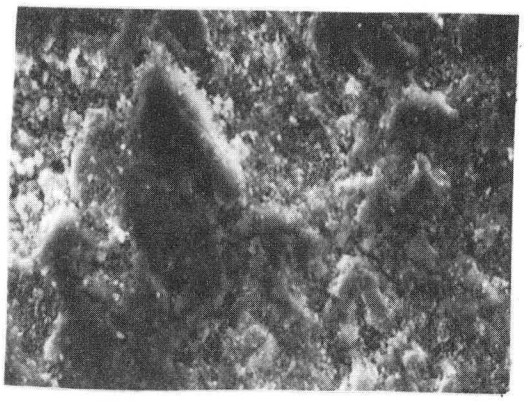

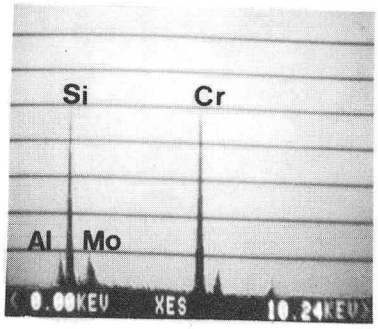

Surface of SCA disc from WC-Mo washer test
Temperature=425°C
Contact pressure=0.17MPa

10μm

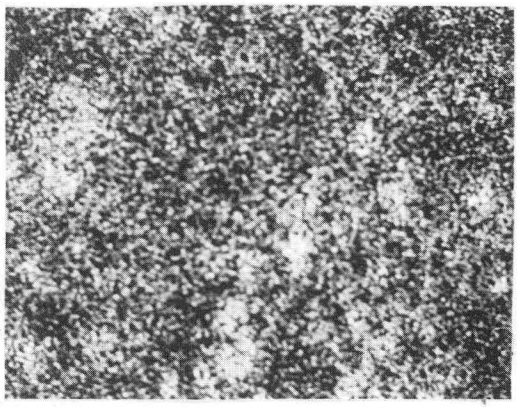

Si Map

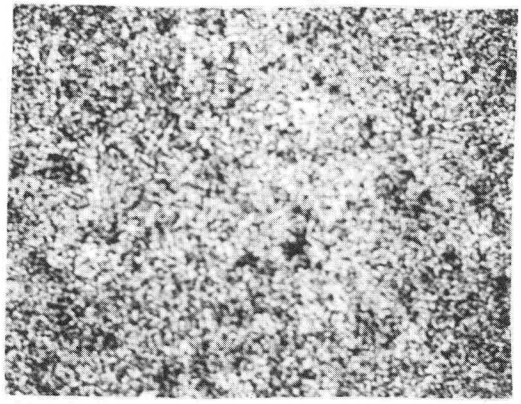

Cr Map

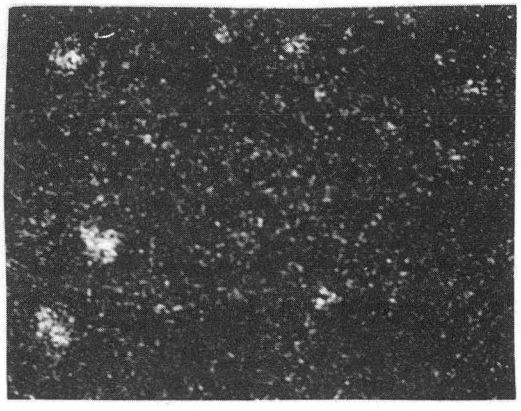

Al Map

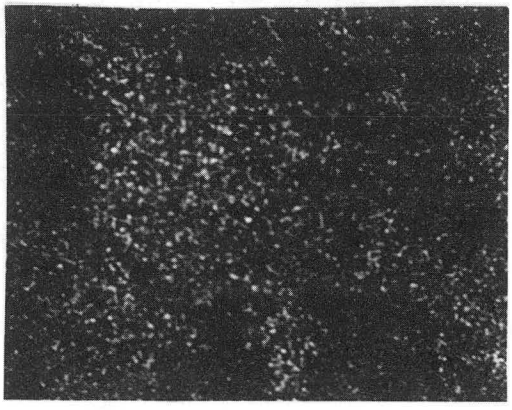

Mo Map

XBB 8411-9196

Figure 30. X-ray maps of the surface of SCA disc from WC-Mo washer test at 425°C and 0.17MPa.

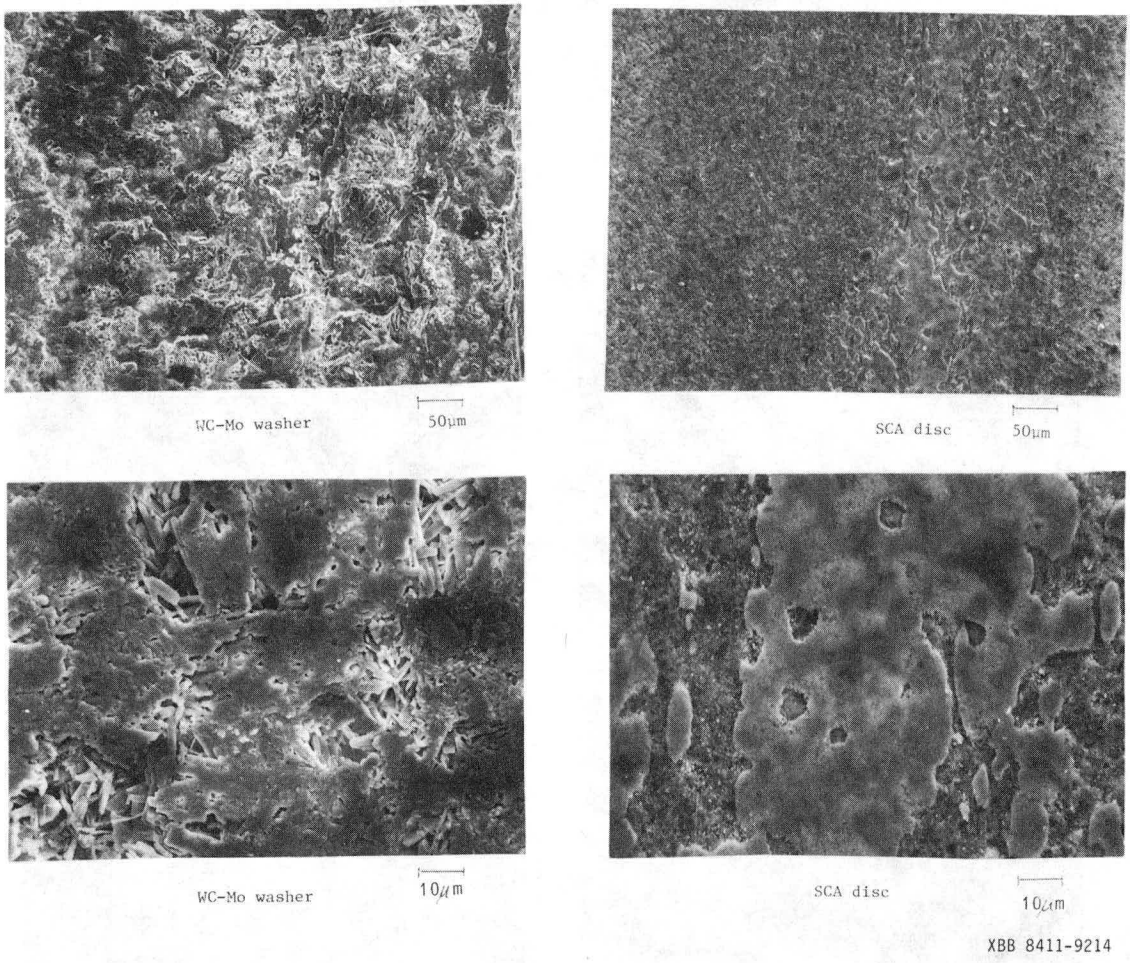

Surface of washer and disc
Temperature=730°C
Contact pressure=0.17MPa

Figure 31. Surface of WC-Mo washer and SCA disc at 730°C and 0.17MPa.

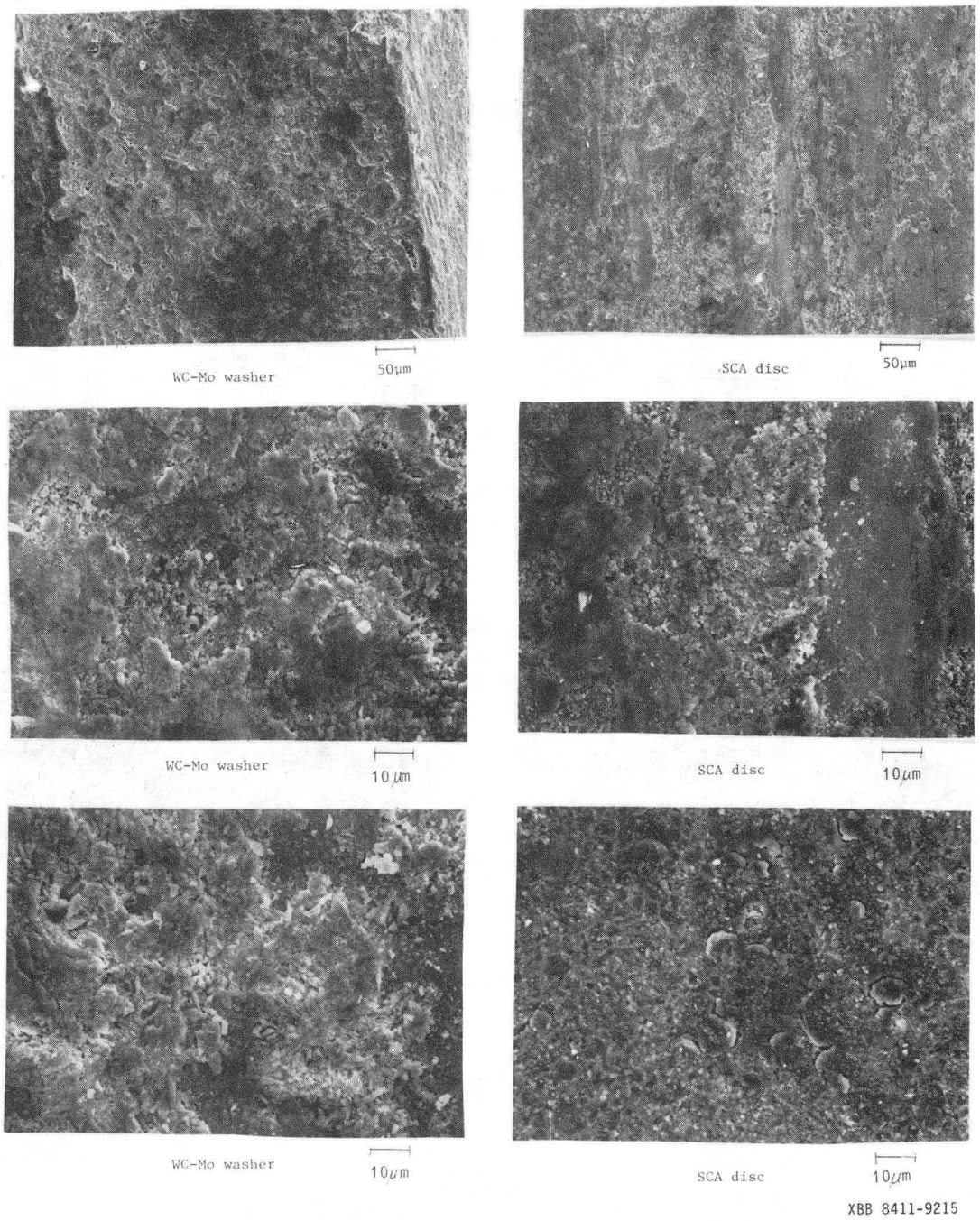

Figure 32. Surface of preworn WC-Mo washer and SCA disc at 730°C and 0.17MPa.

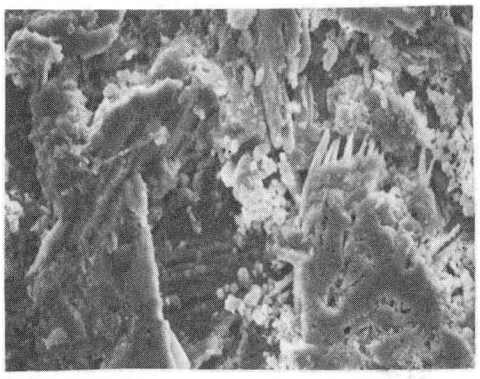

Surface of WC-Mo washer
Temperature=730°C
Contact pressure=0.17MPa

10 μm

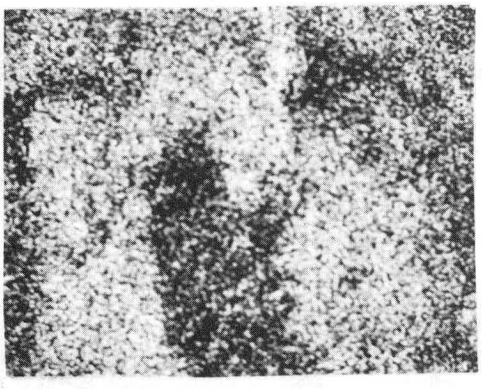

Mo Map

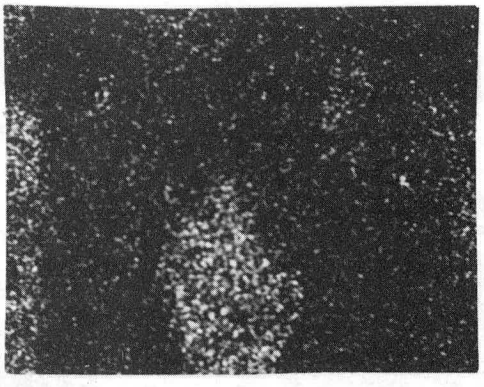

Cr Map

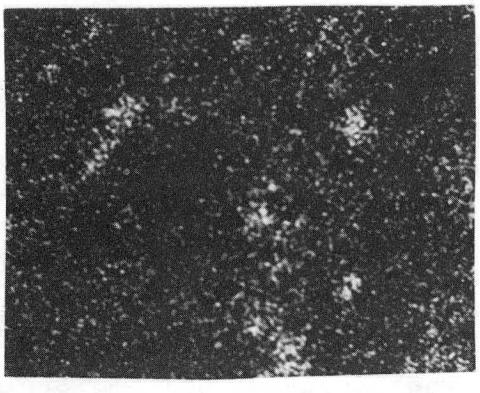

W Map

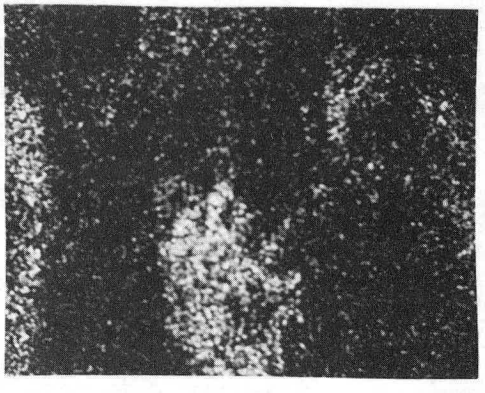

Ni Map

XBB 8411-9199

X-ray maps of the surface of WC-Mo washer at 730°C.

Figure 33. X-ray maps of the surface of WC-Mo washer at 730°C and 0.17MPa.

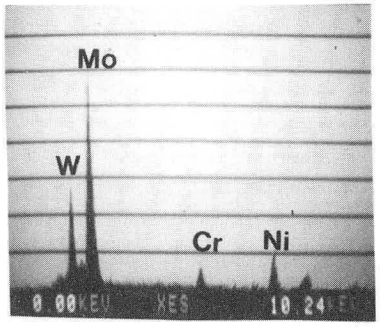

Surface of WC-Mo washer preworn at 25°C
Temperature=730°C
Contact pressure=0.17MPa

10μm

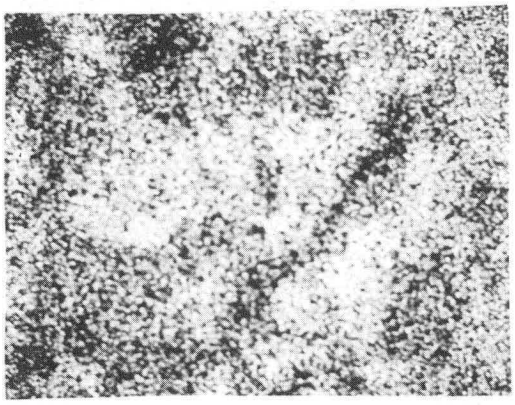

Mo Map

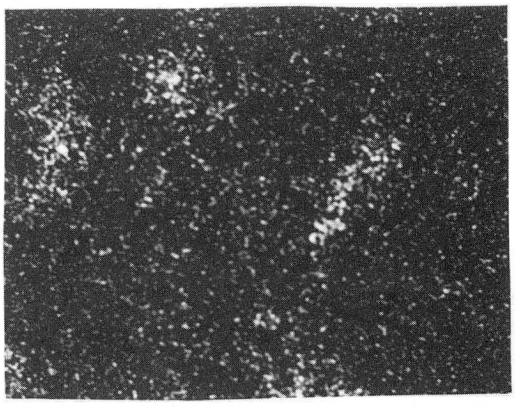

Cr Map

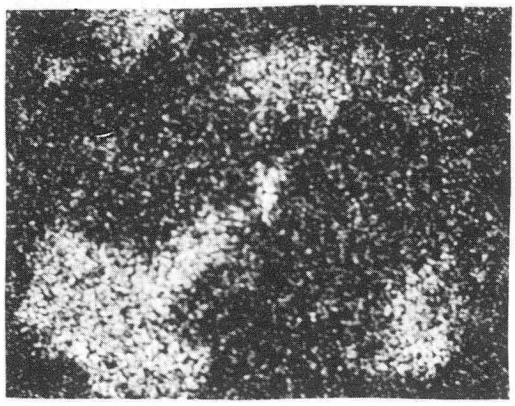

W Map

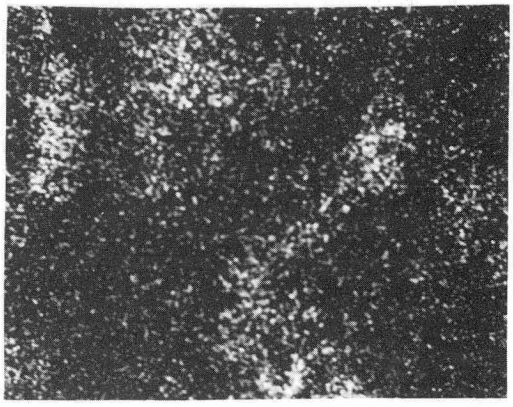

Ni Map

XBB 8411-9200

X-ray maps of the surface of WC-Mo washer preworn at 25°C.

Figure 34. X-ray maps of the surface of preworn WC-Mo at 730°C and 0.17MPa.

Surface of SCA disc from WC-Mo washer test 10μm
Temperature=730°C
Contact pressure=0.17MPa

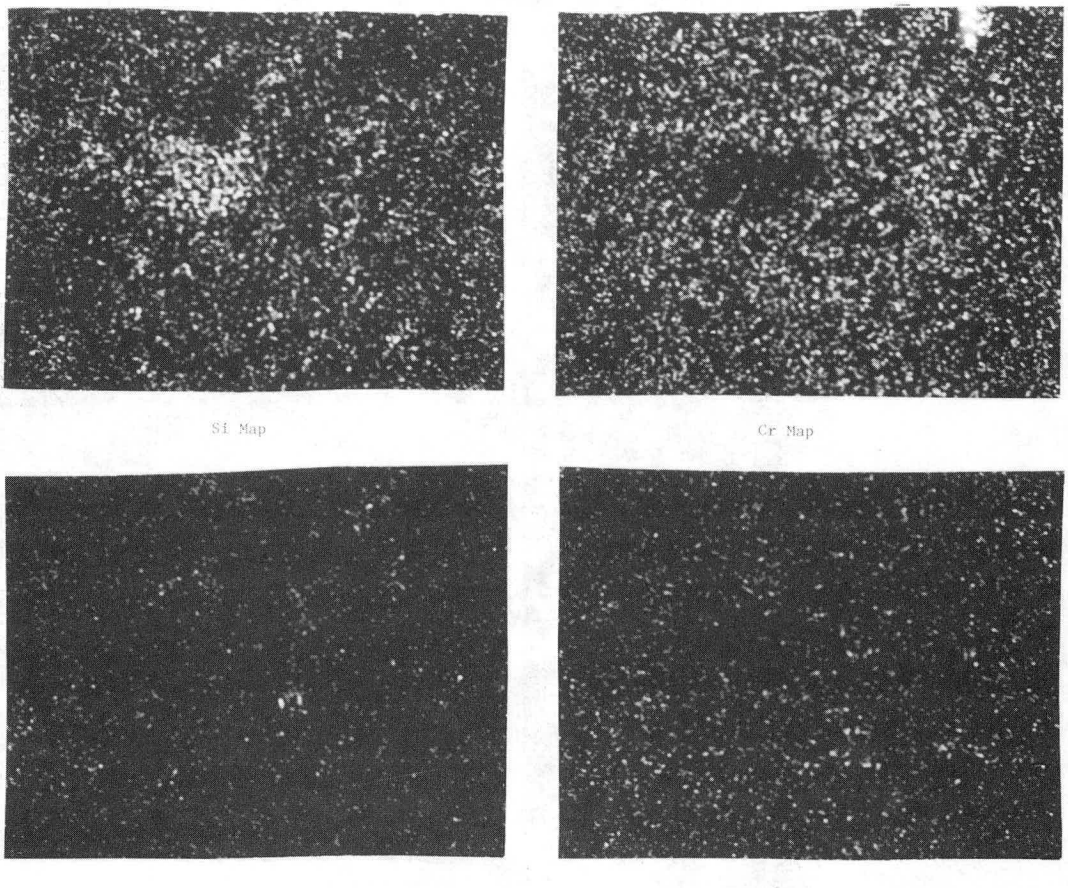

X-ray maps of the surface of Kaman SCA disc at 730°C.

Figure 35. X-ray maps of the surface of the SCA disc from the WC-Mo washer test at 730°C and 0.17MPa.

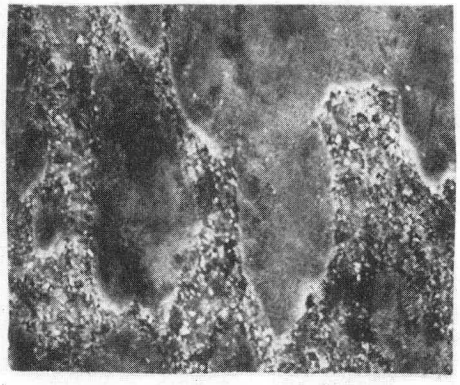

Surface of SCA disc from WC-Mo washer test preworn at 25°C and 0.17MPa
Temperature=730°C
Contact pressure=0.17MPa

10μm

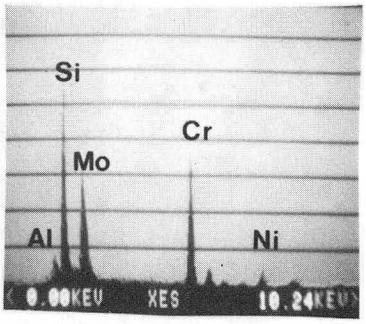

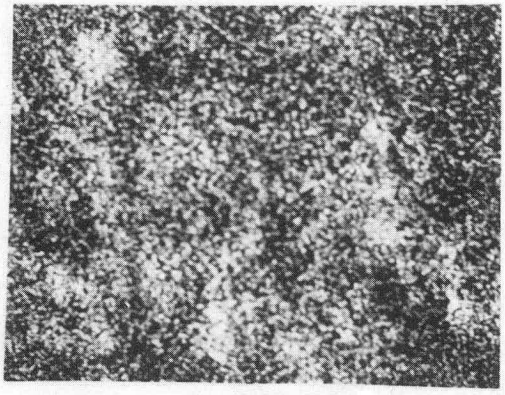

Si Map

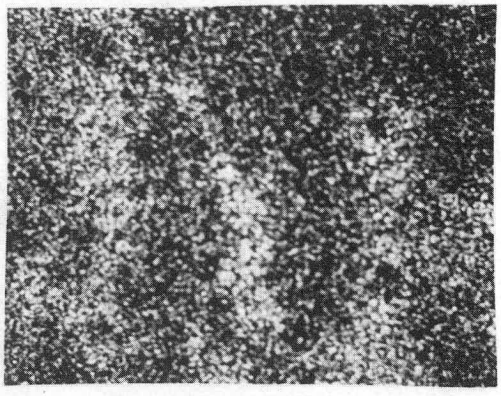

Cr Map

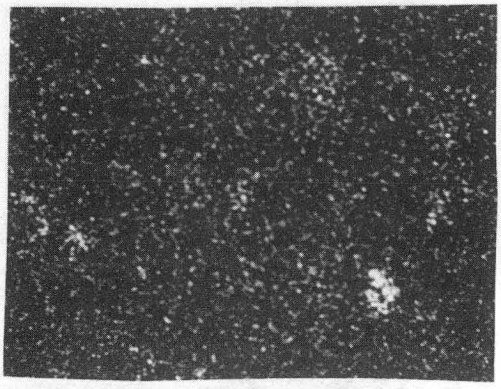

Al Map

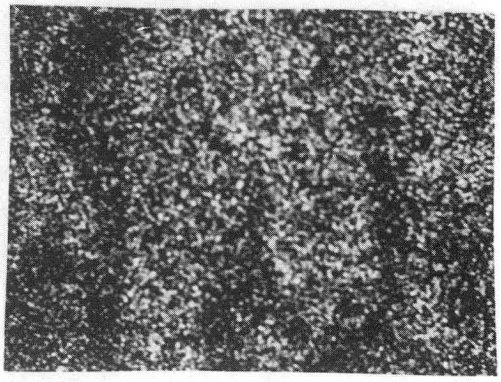

Mo Map

XBB 8411-9198

X-ray maps of the surface of SCA disc preworn at 25°C and 0.17MPa.

Figure 36. X-ray maps of the surface of the preworn SCA disc from the WC-Mo washer test at 730°C and 0.17MPa.

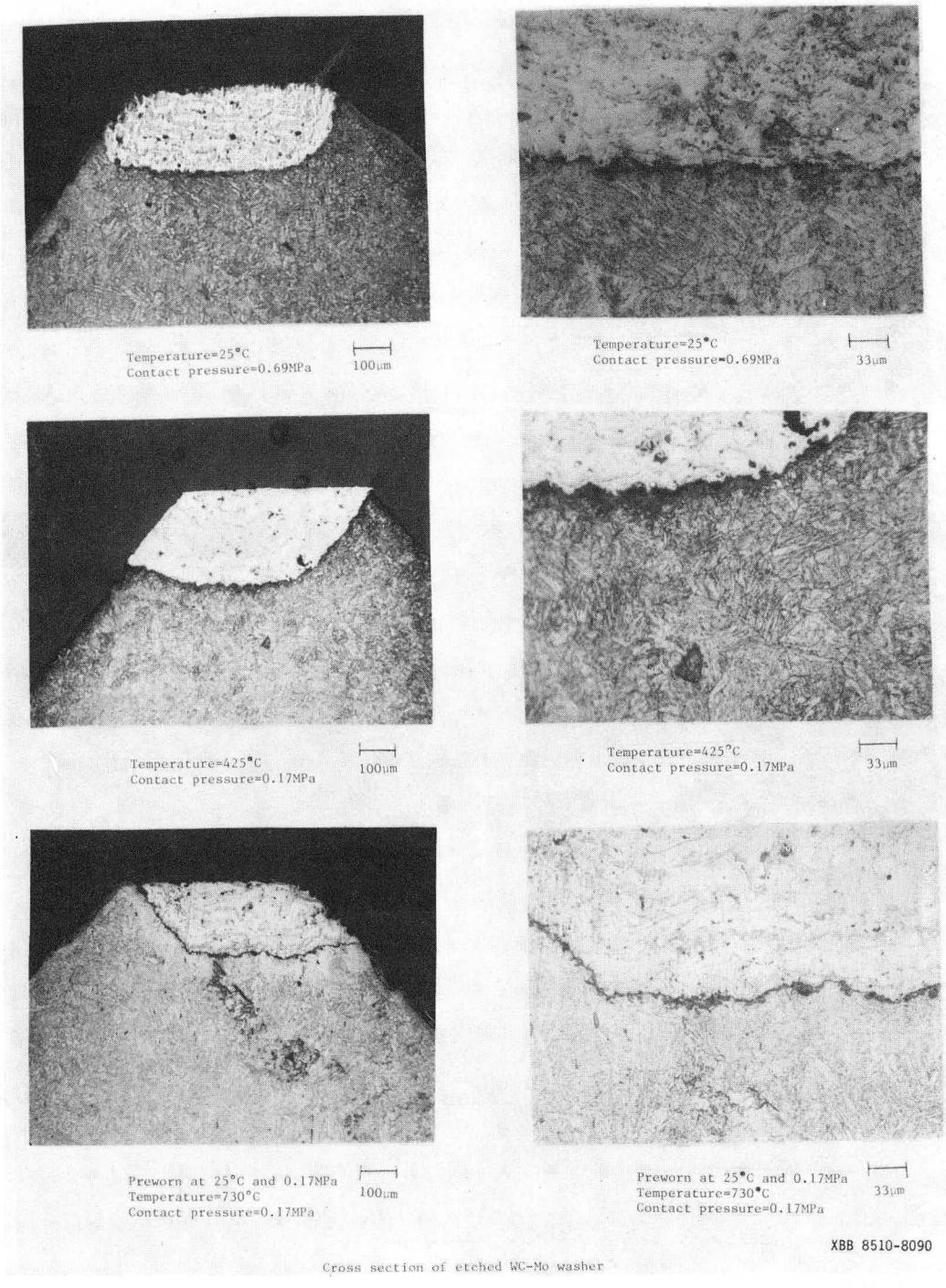

Figure 37. Cross section of WC-Mo washer at 25°C, 425°C and 730°C.

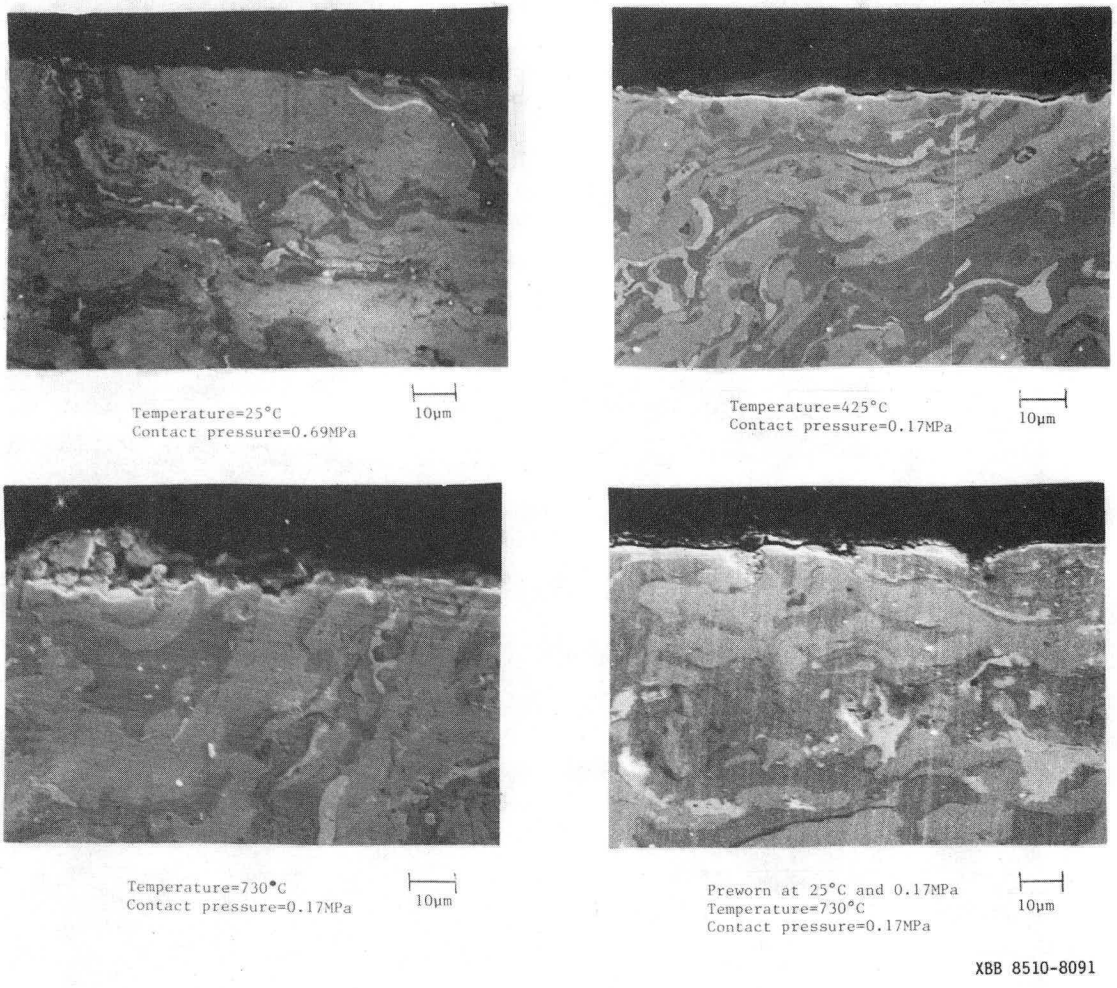

Cross section of WC-Mo washers.

Figure 38. High magnification cross section of WC-Mo washer at 25°C, 425°C and 730°C.

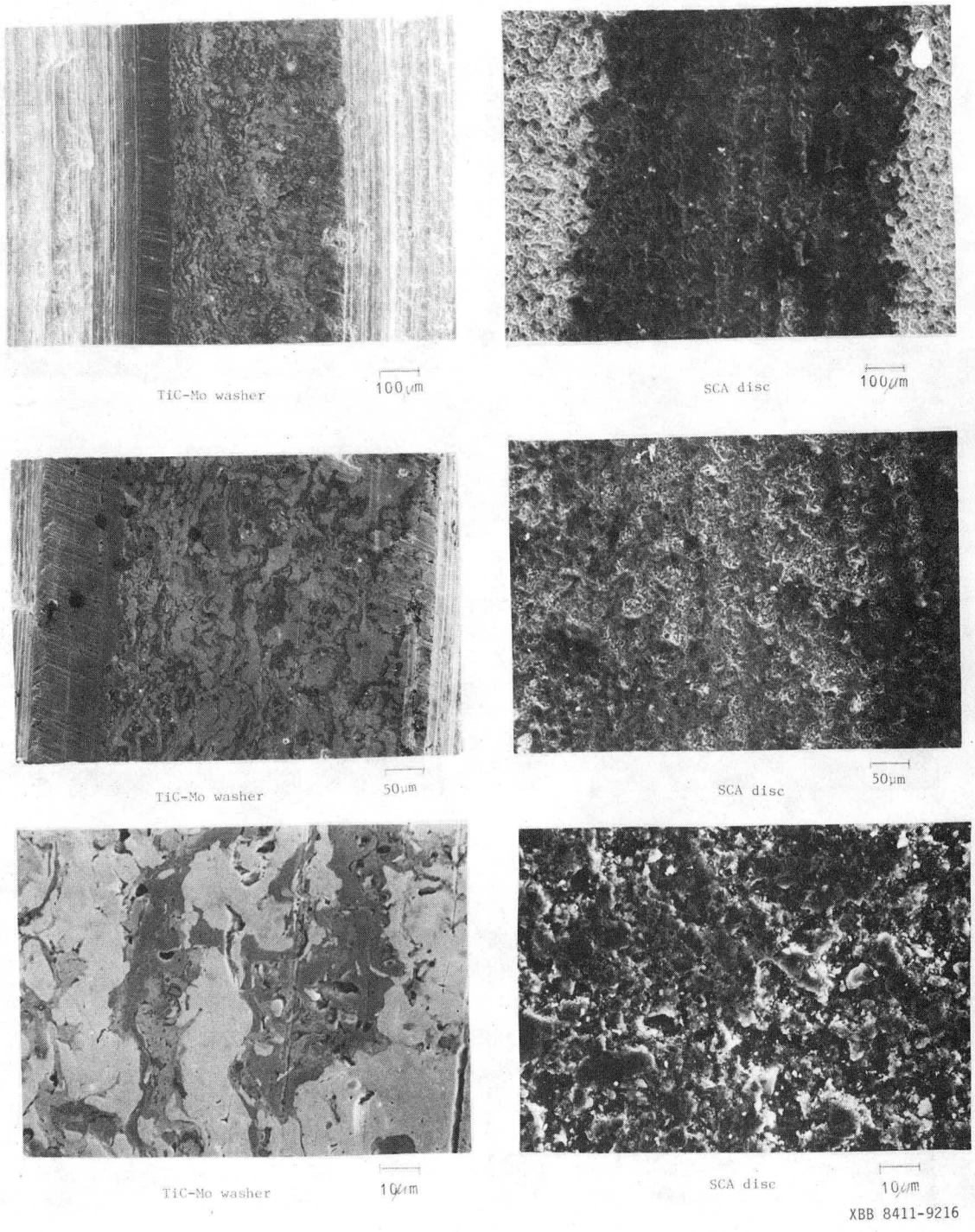

Figure 39. Surface of TiC-Mo washer and SCA disc at 25°C and 0.69MPa.

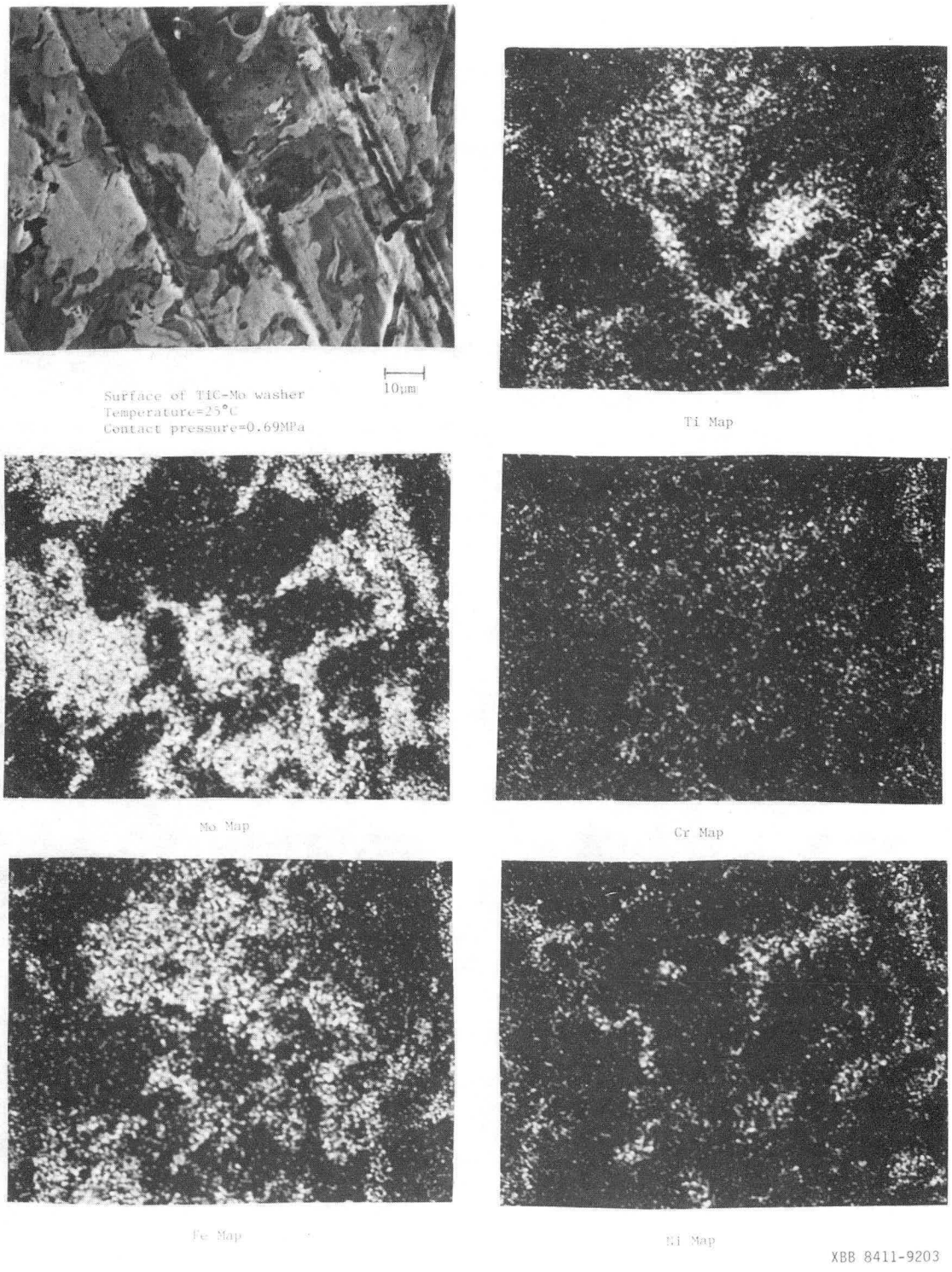

Figure 40. X-ray maps of the surface of TiC-Mo washer at 25°C and 0.69MPa.

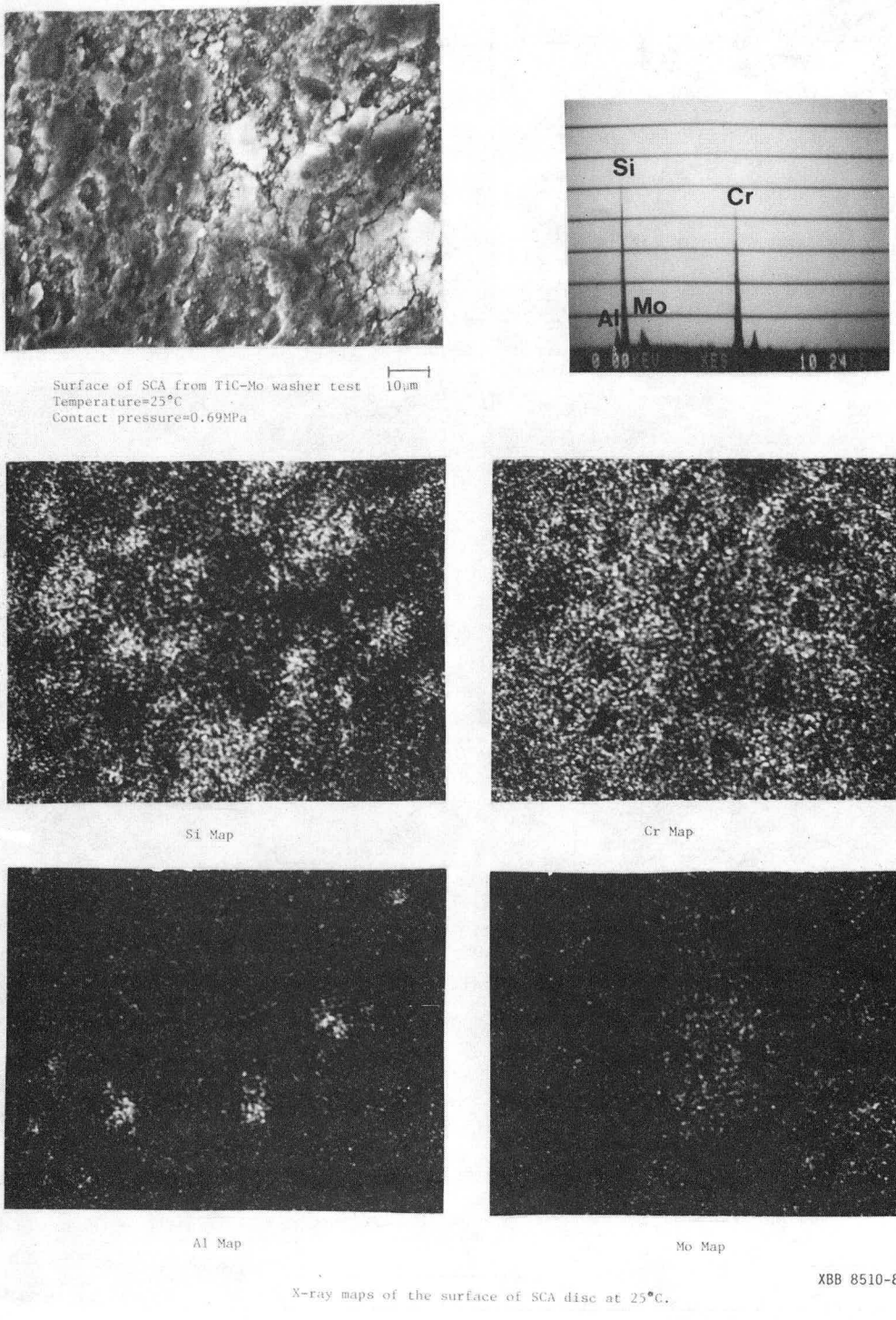

Figure 41. X-ray maps of the surface of SCA disc from the TiC-Mo washer at 25°C and 0.69MPa.

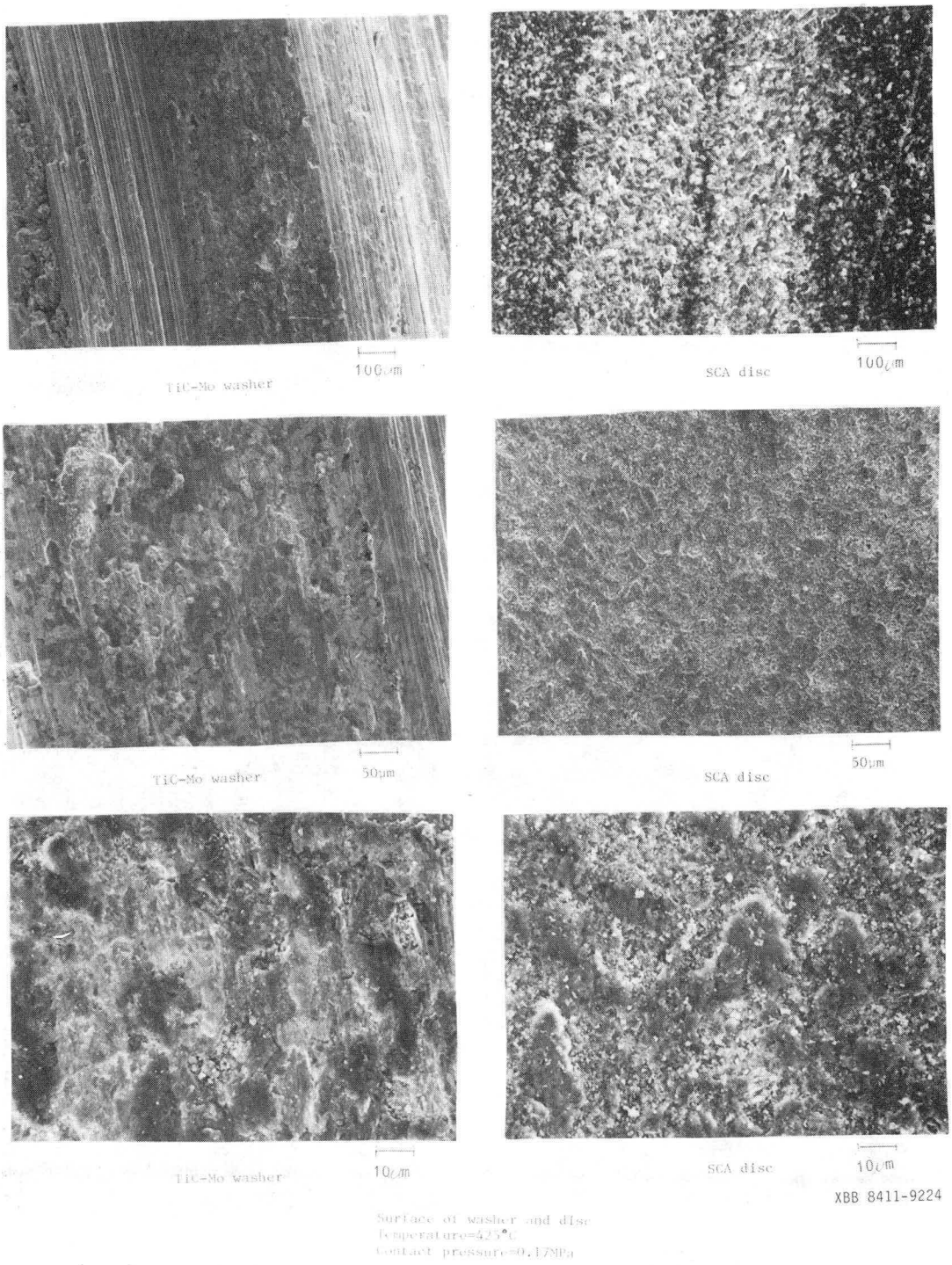

Figure 42. Surface of the TiC-Mo washer and SCA disc at 425°C and 0.17MPa.

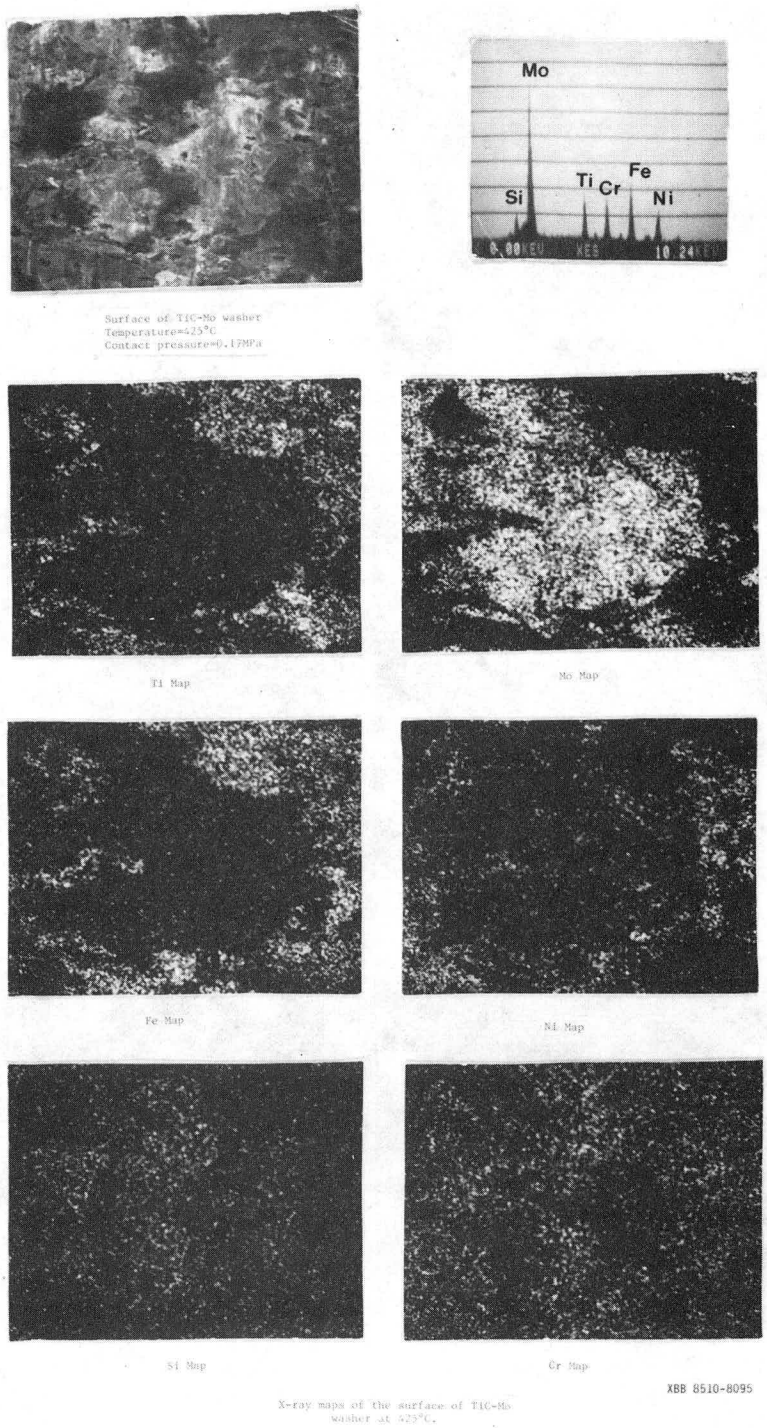

Figure 43. X-ray maps of the surface of TiC-Mo washer at 425°C and 0.17MPa.

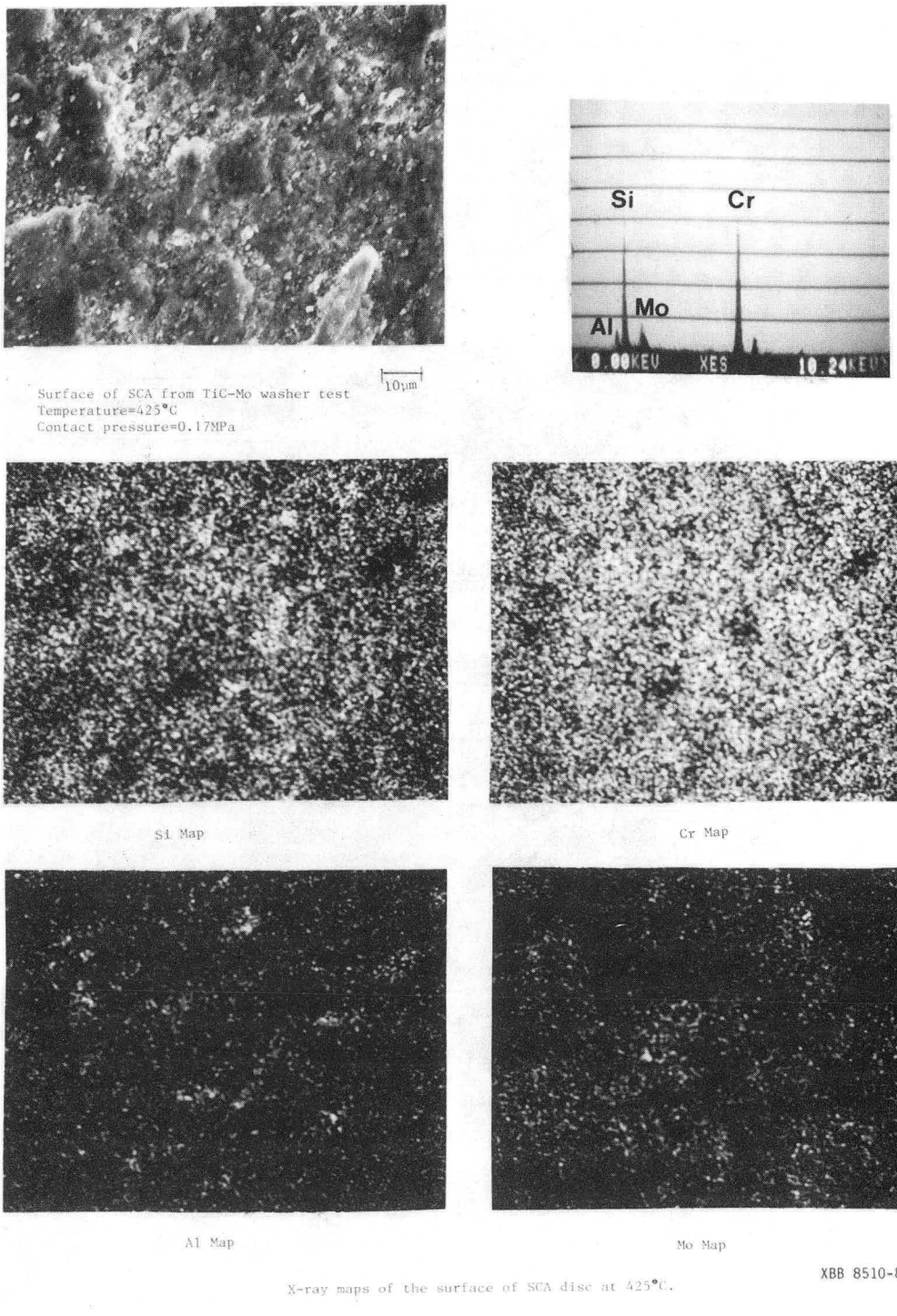

Figure 44. X-ray maps of the surface of SCA disc from TiC-Mo washer test at 425°C and 0.17MPa.

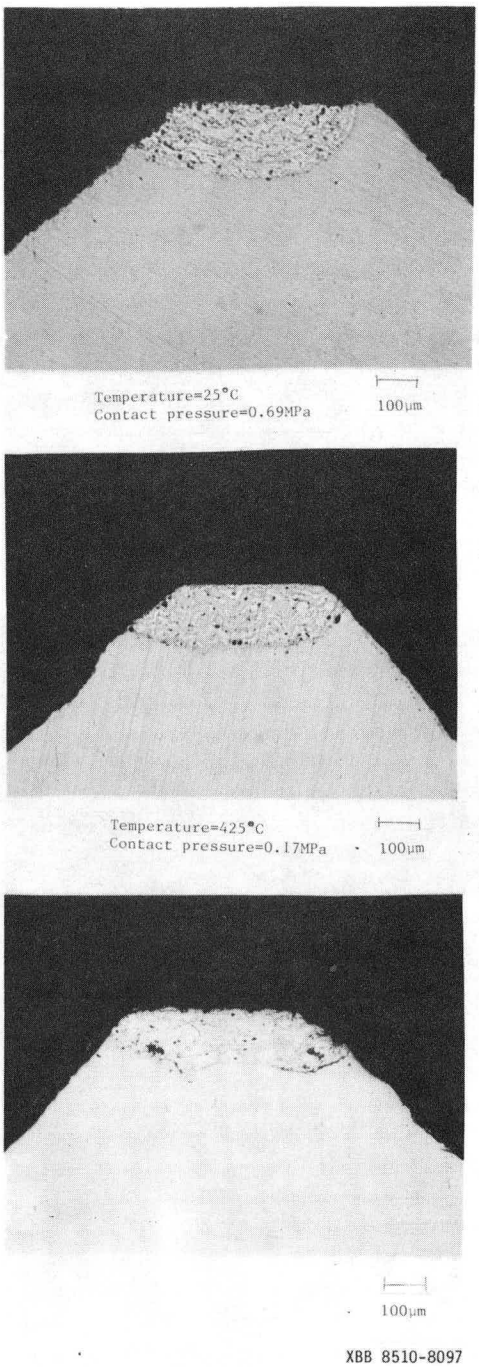

Figure 45. Cross section of TiC-Mo washer at 25°C, 425°C and 730°C.

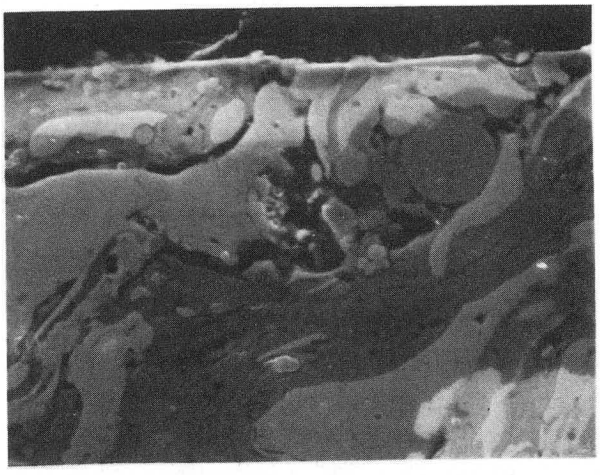

Temperature=25°C
Contact pressure=0.69MPa

5μm

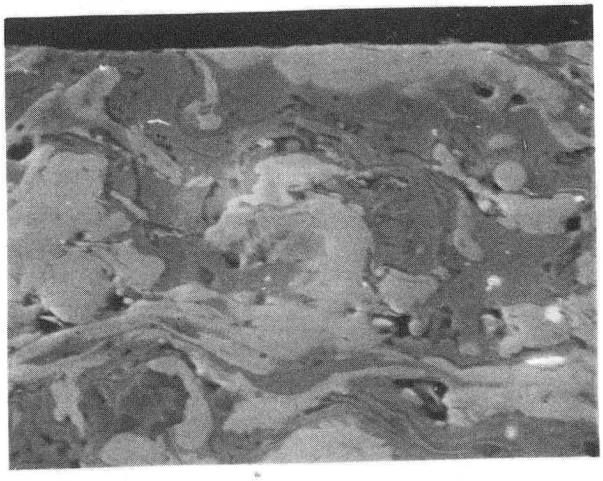

Temperature=425°C
Contact pressure=0.17MPa

5μm

XBB 8510-8098

Cross section of TiC-Mo washers.

Figure 46. High magnification cross section of TiC-Mo washer at 25°C and 425°C.

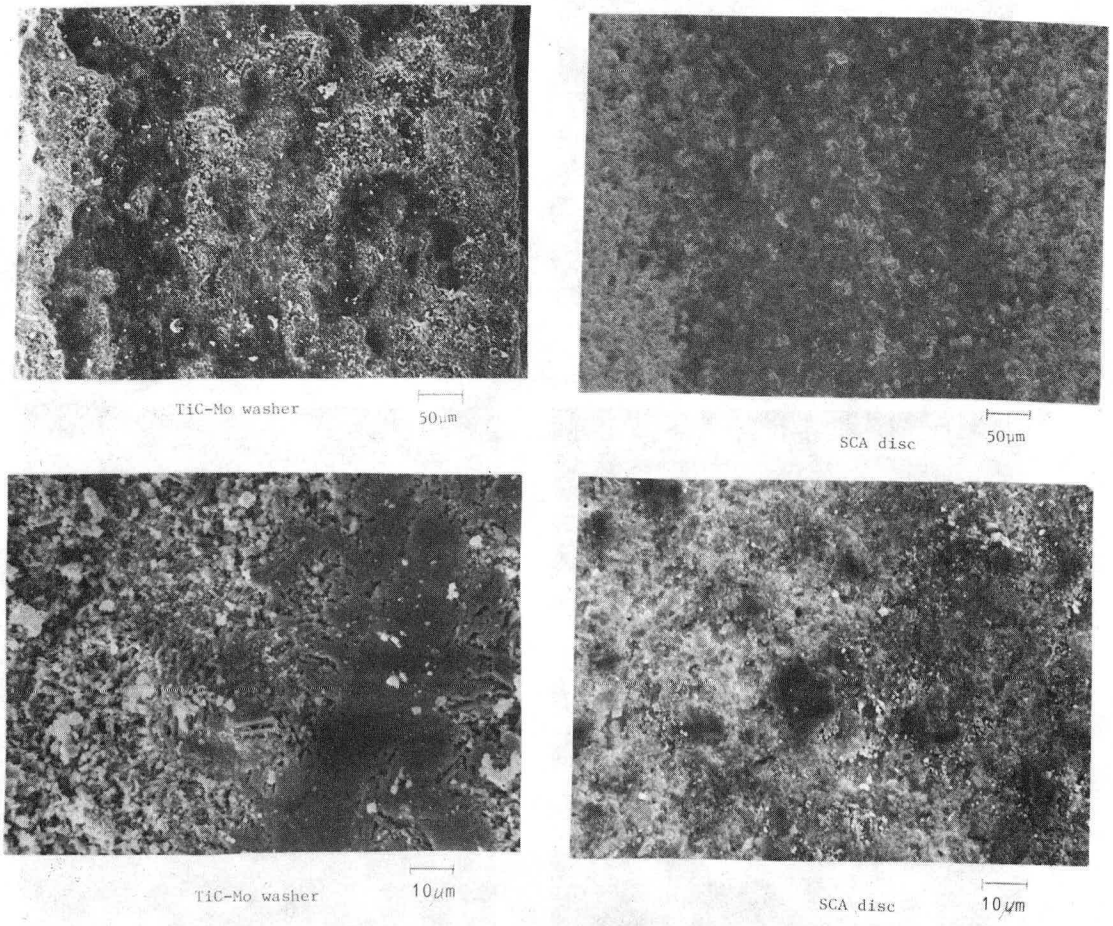

Figure 47. Surface of TiC-Mo washer and SCA disc at 730°C and 0.17MPa.

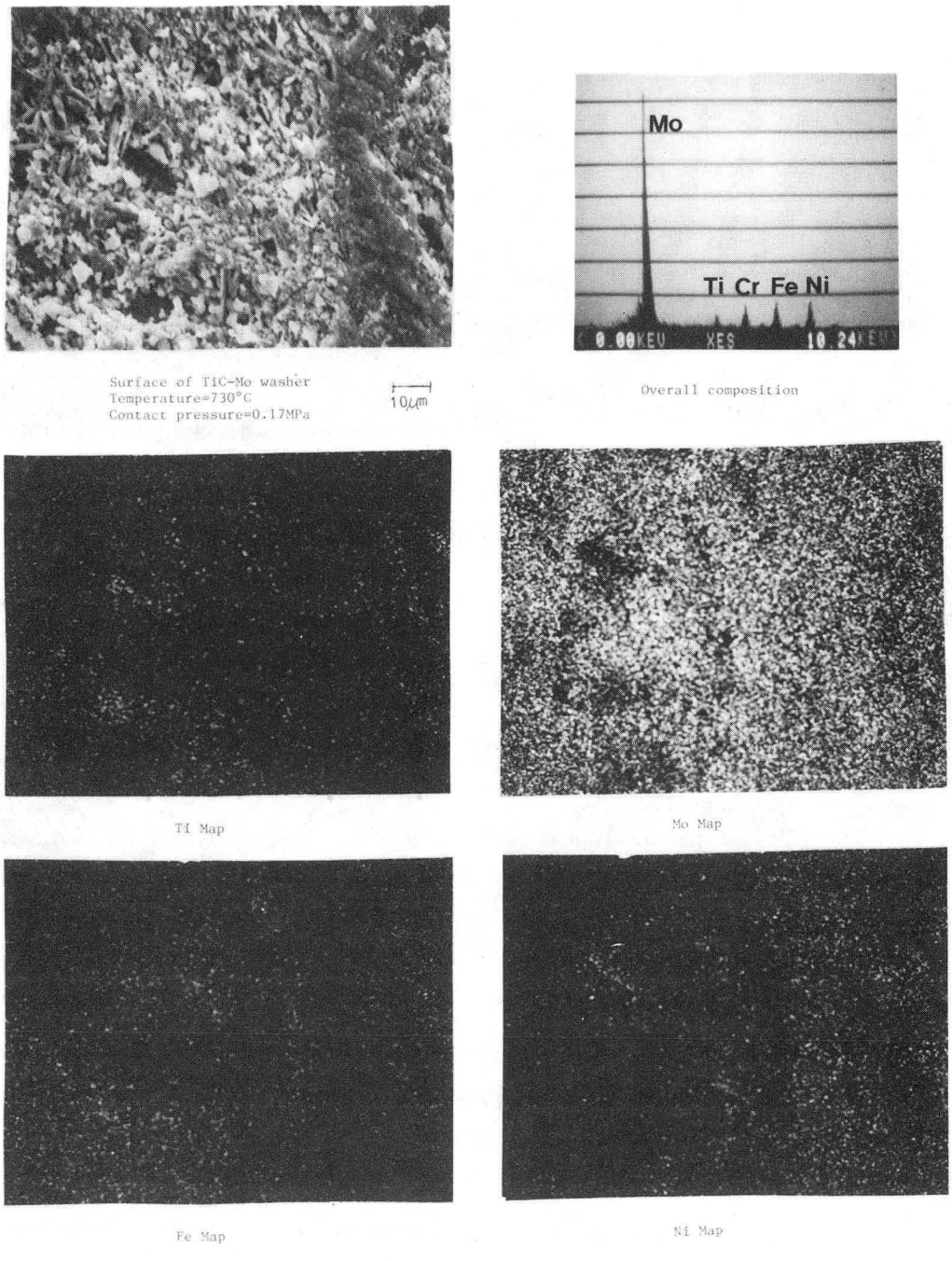

X-ray maps of the surface of TiC-Mo washer at 730°C.

Figure 48. X-ray maps of the surface of TiC-Mo washer at 730°C and 0.17MPa.

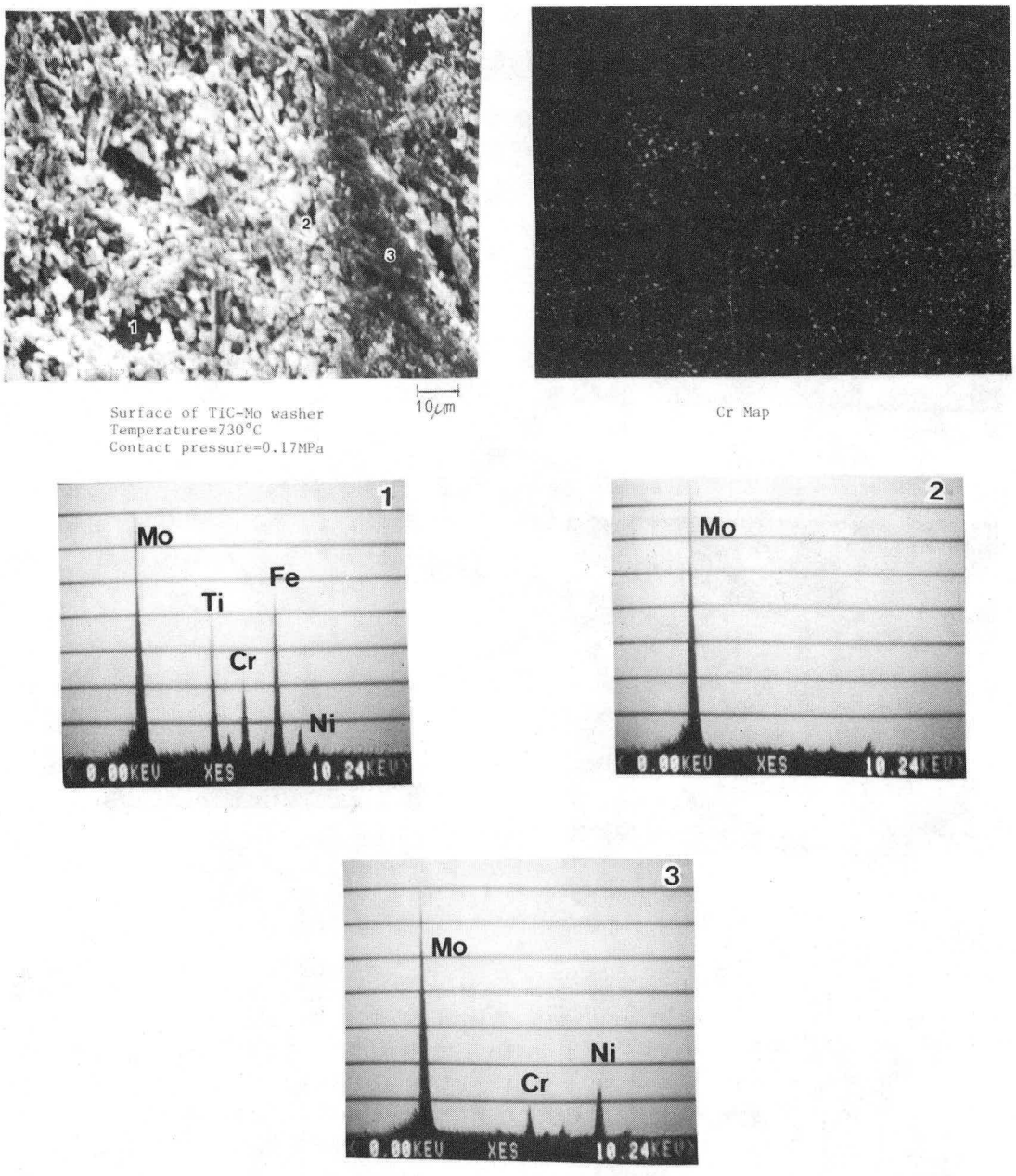

Figure 49. X-ray analysis of the surface of TiC-Mo washer at 730°C and 0.17MPa.

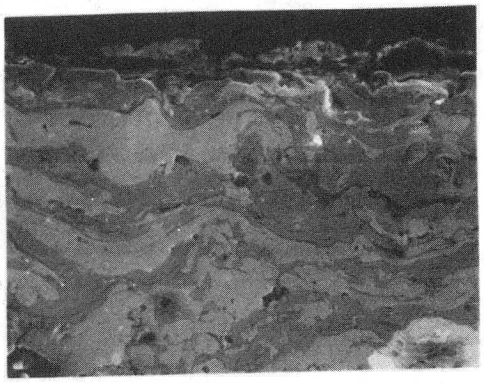

10μm

Cross section of TiC washer
Temperature=730°C
Contact pressure=0.17MPa

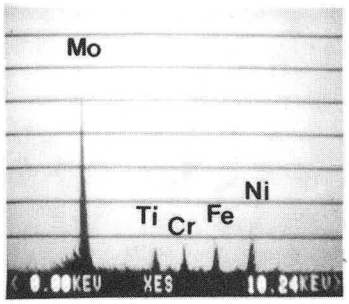

Overall composition

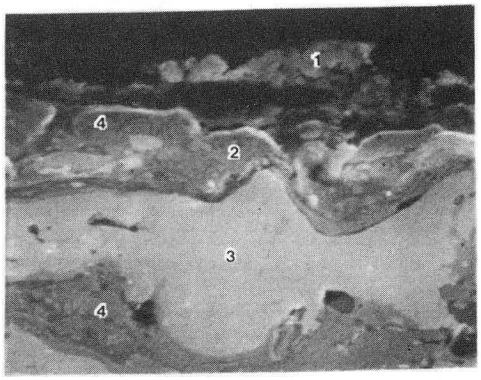

5μm

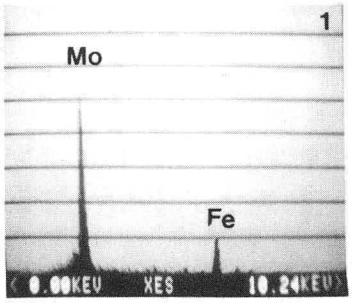

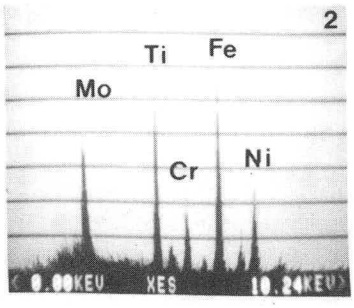

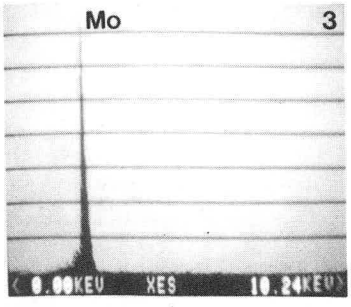

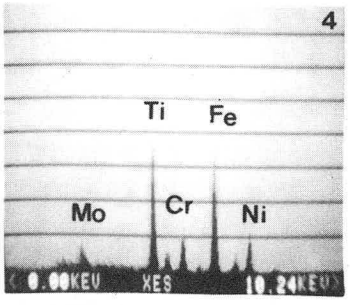

XBB 8510-8102

X-ray analysis of a cross section
of a TiC washer at 730°C and
0.17MPa.

Figure 50. X-ray analysis of the cross section of TiC-Mo washer at 730°C and 0.17MPa.

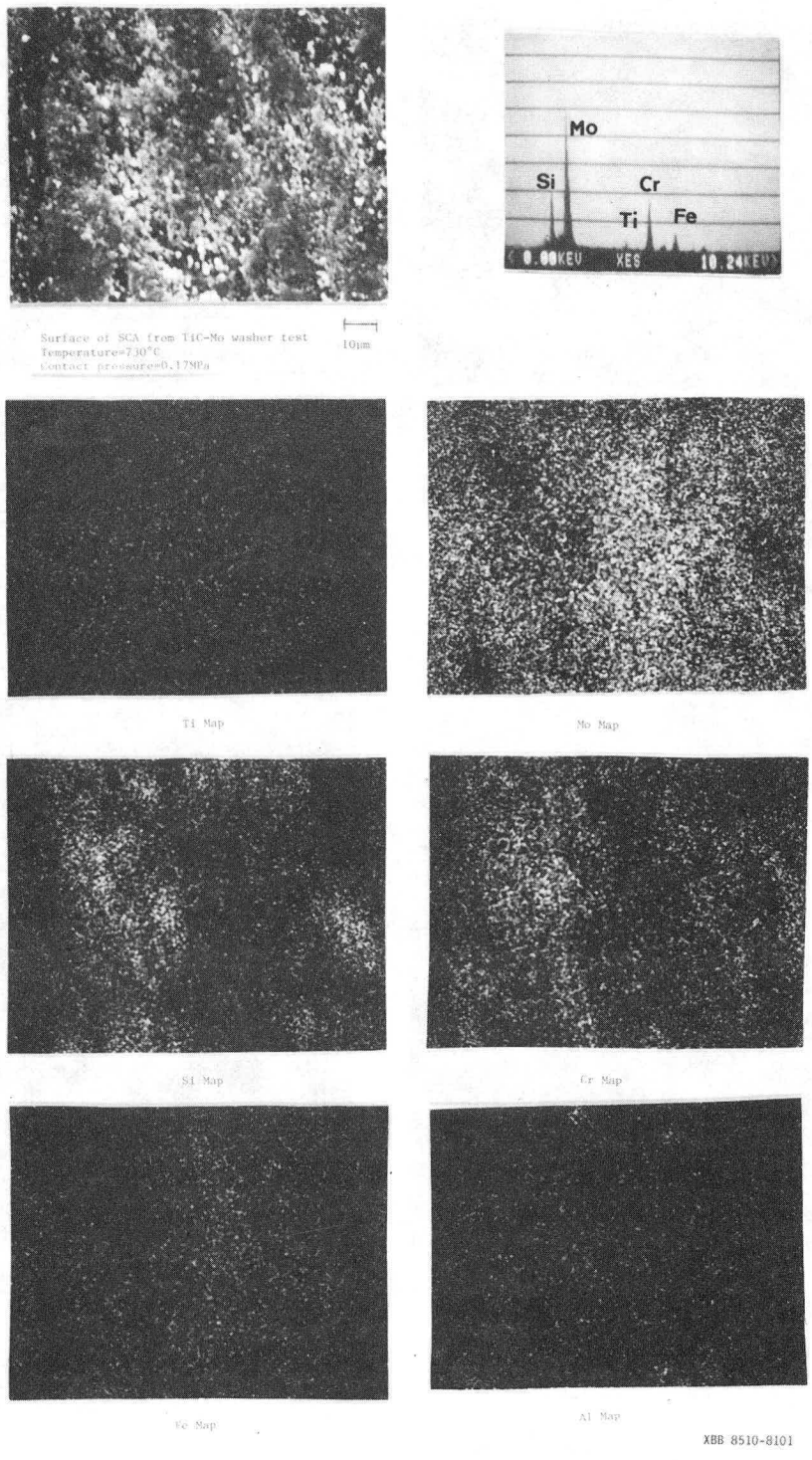

Figure 51. X-ray maps of the surface of SCA disc from TiC-Mo washer test at 730°C and 0.17MPa.

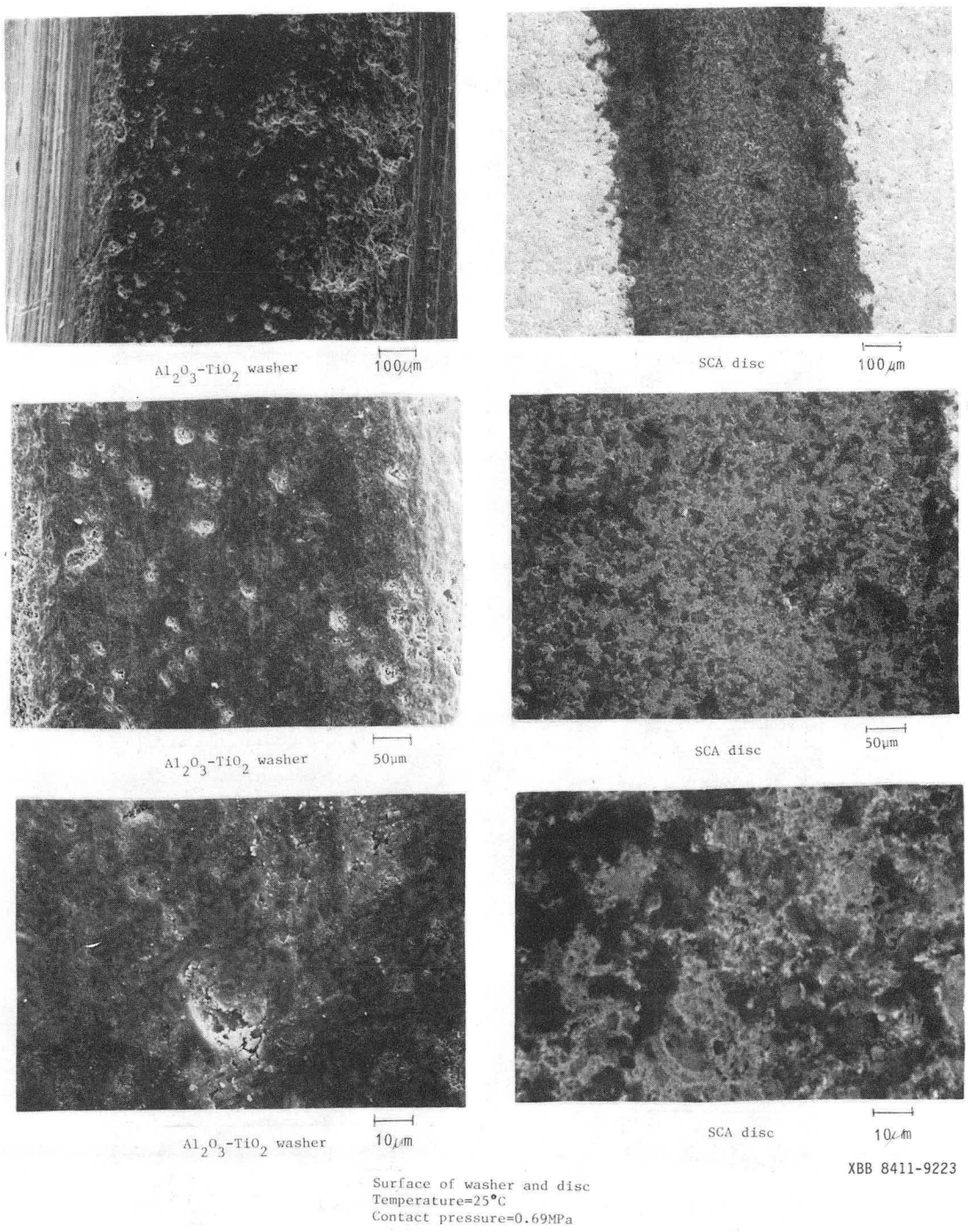

Figure 52. Surface of Al_2O_3-TiO_2 washer and SCA disc at 25°C and 0.69MPa.

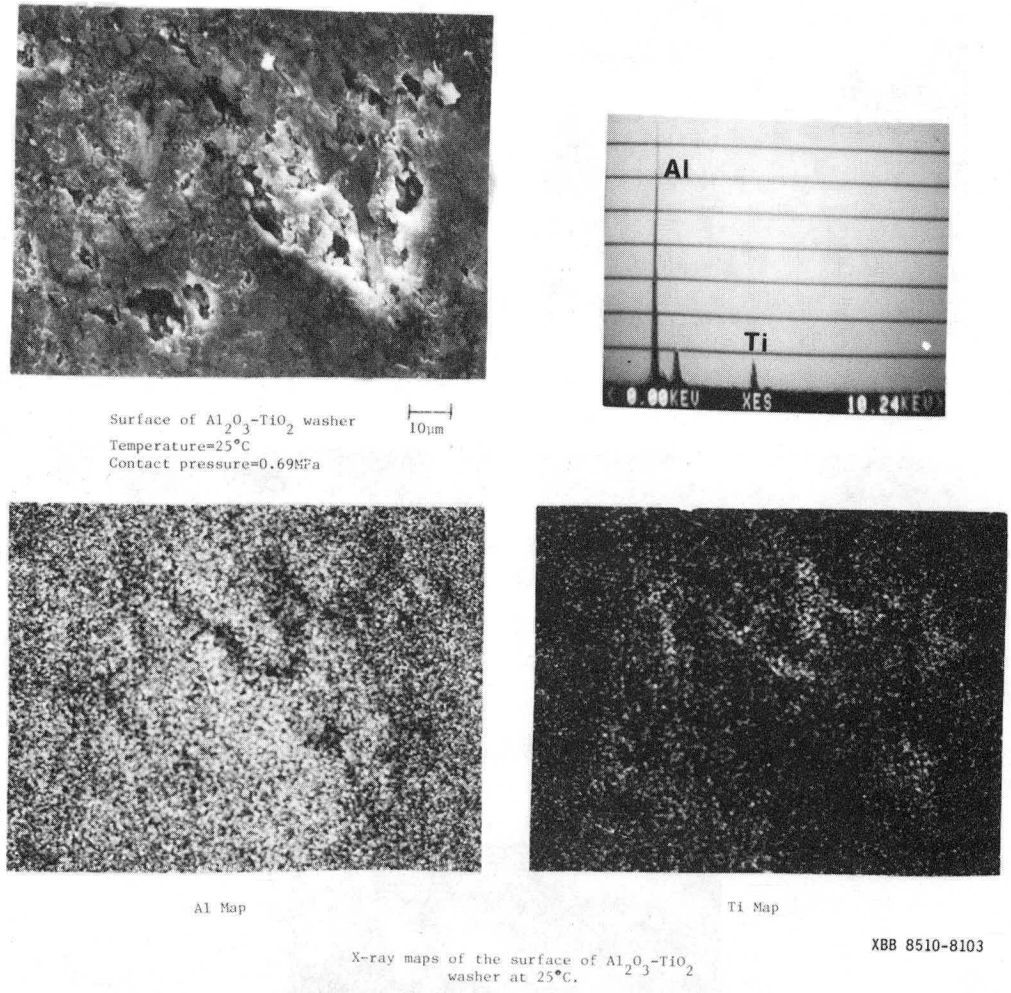

Figure 53. X-ray maps of the surface of Al_2O_3-TiO_2 washer at 25°C and 0.69MPa.

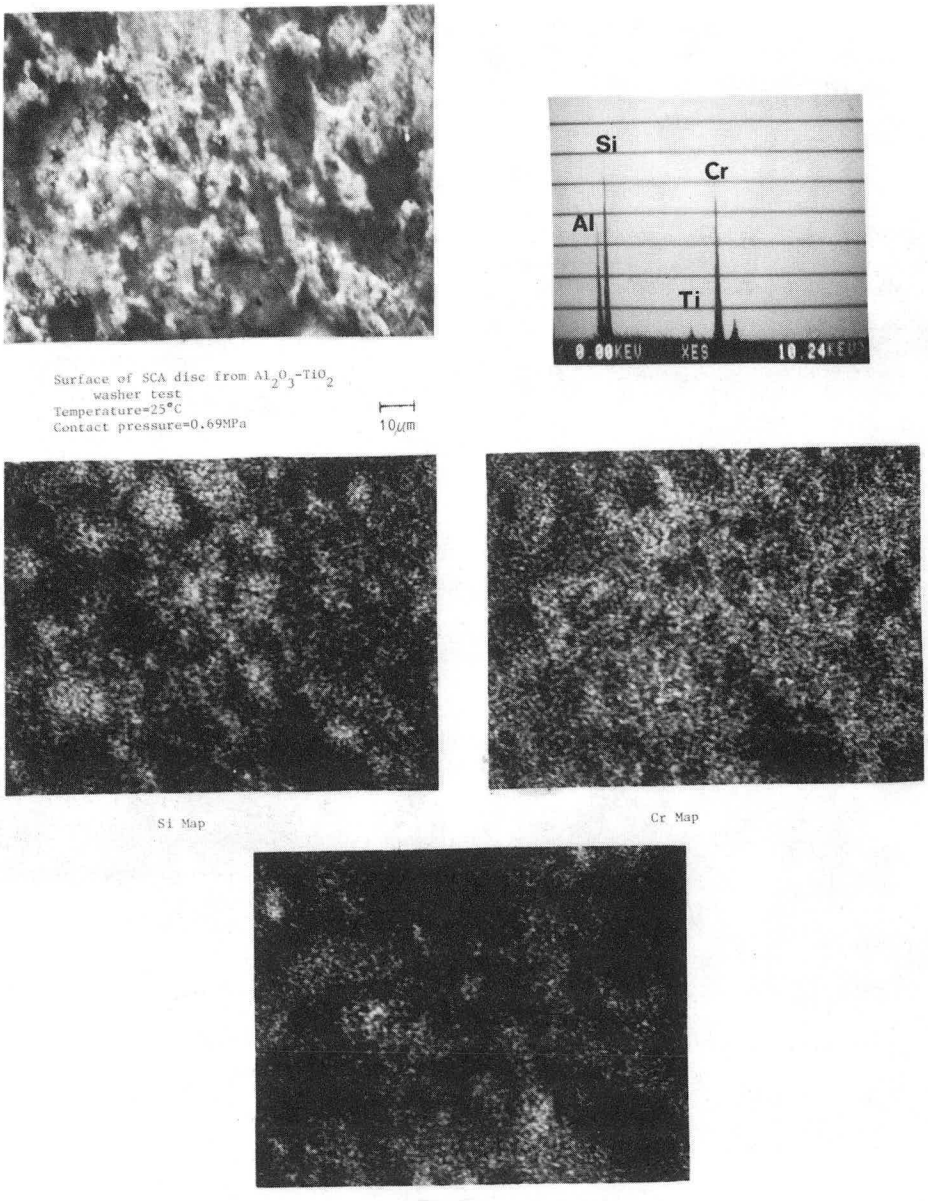

X-ray maps of the surface of SCA disc at 25°C.

Figure 54. X-ray maps of the surface of SCA disc from Al_2O_3-TiO_2 washer test at 25°C and 0.69MPa.

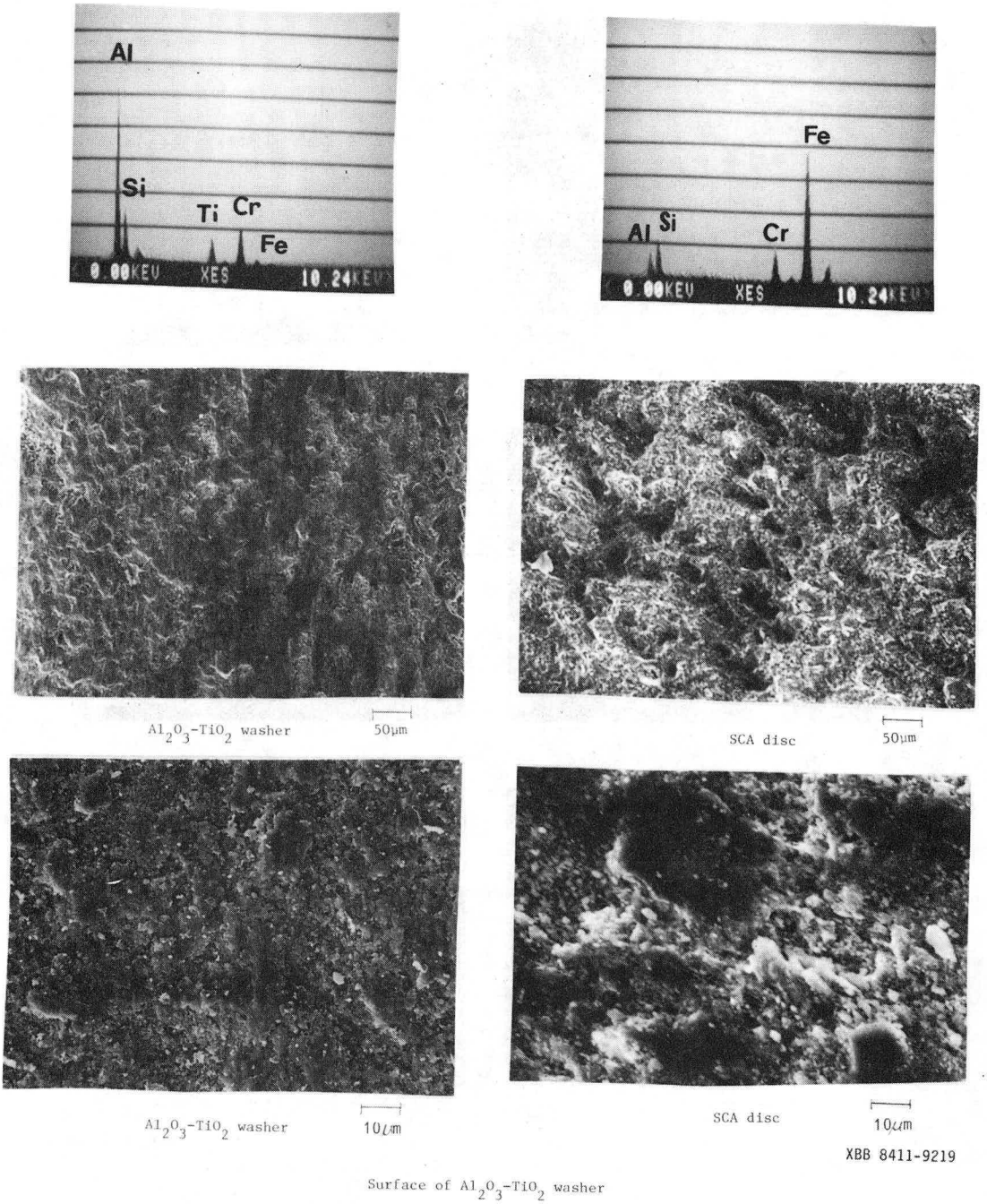

Surface of Al_2O_3-TiO_2 washer
Temperature=425°C
Contact pressure=0.17MPa

Figure 55. Surface of Al_2O_3-TiO_2 washer and SCA disc at 425°C and 0.17MPa.

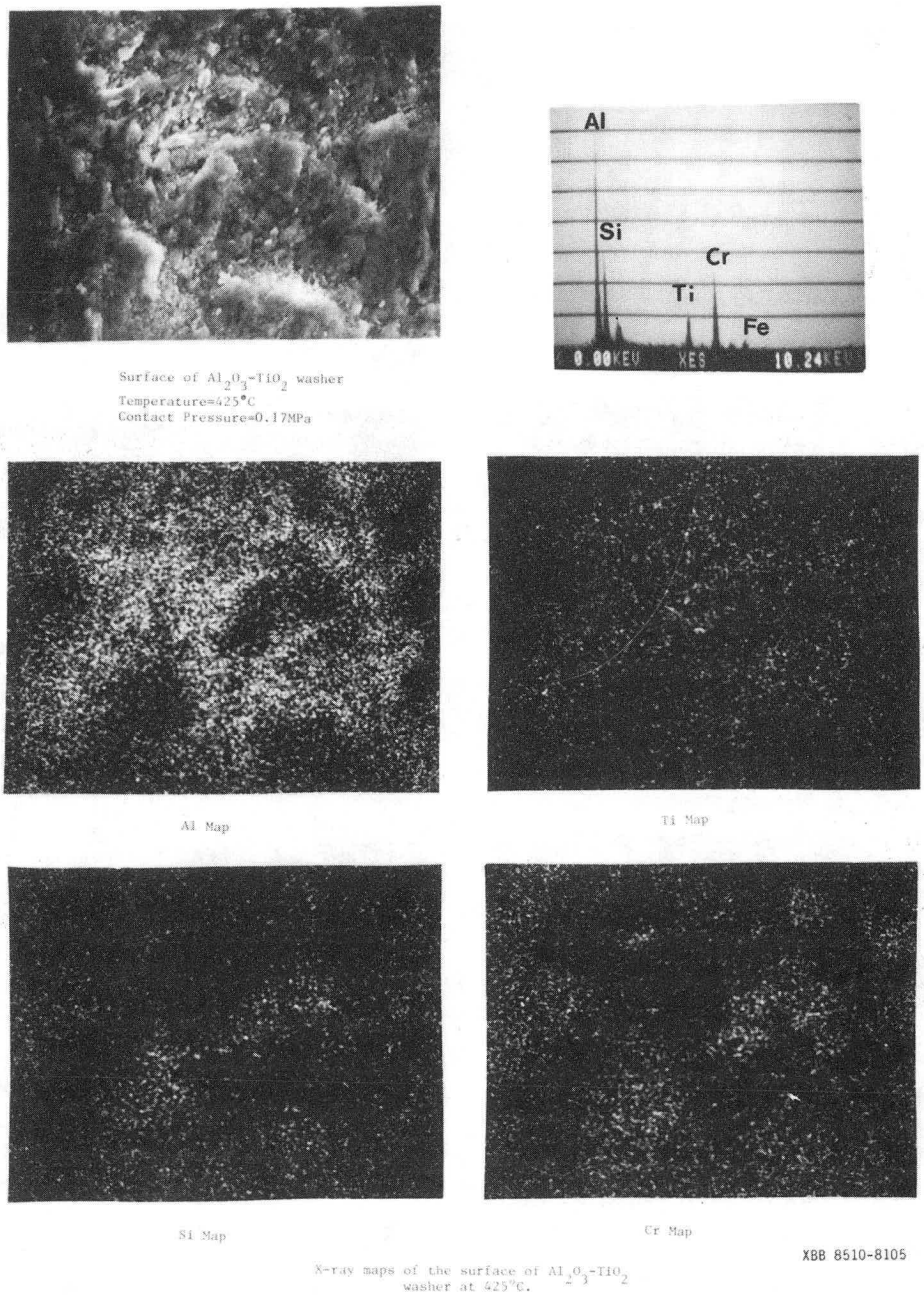

Figure 56. X-ray maps of the surface of Al_2O_3-TiO_2 washer at 425°C and 0.17 MPa.

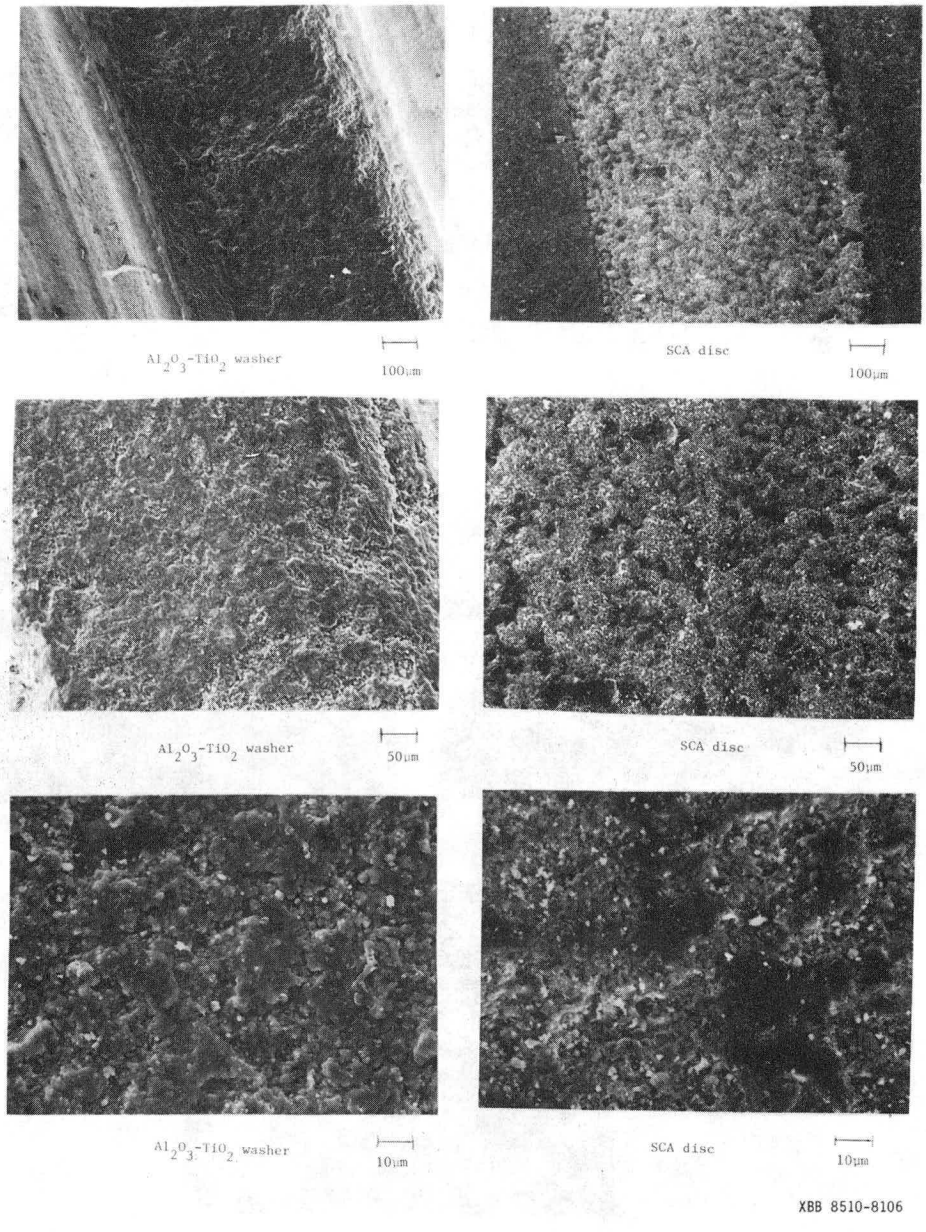

Figure 57. Surface of Al_2O_3-TiO_2 washer and SCA disc at 730°C and 0.17MPa.

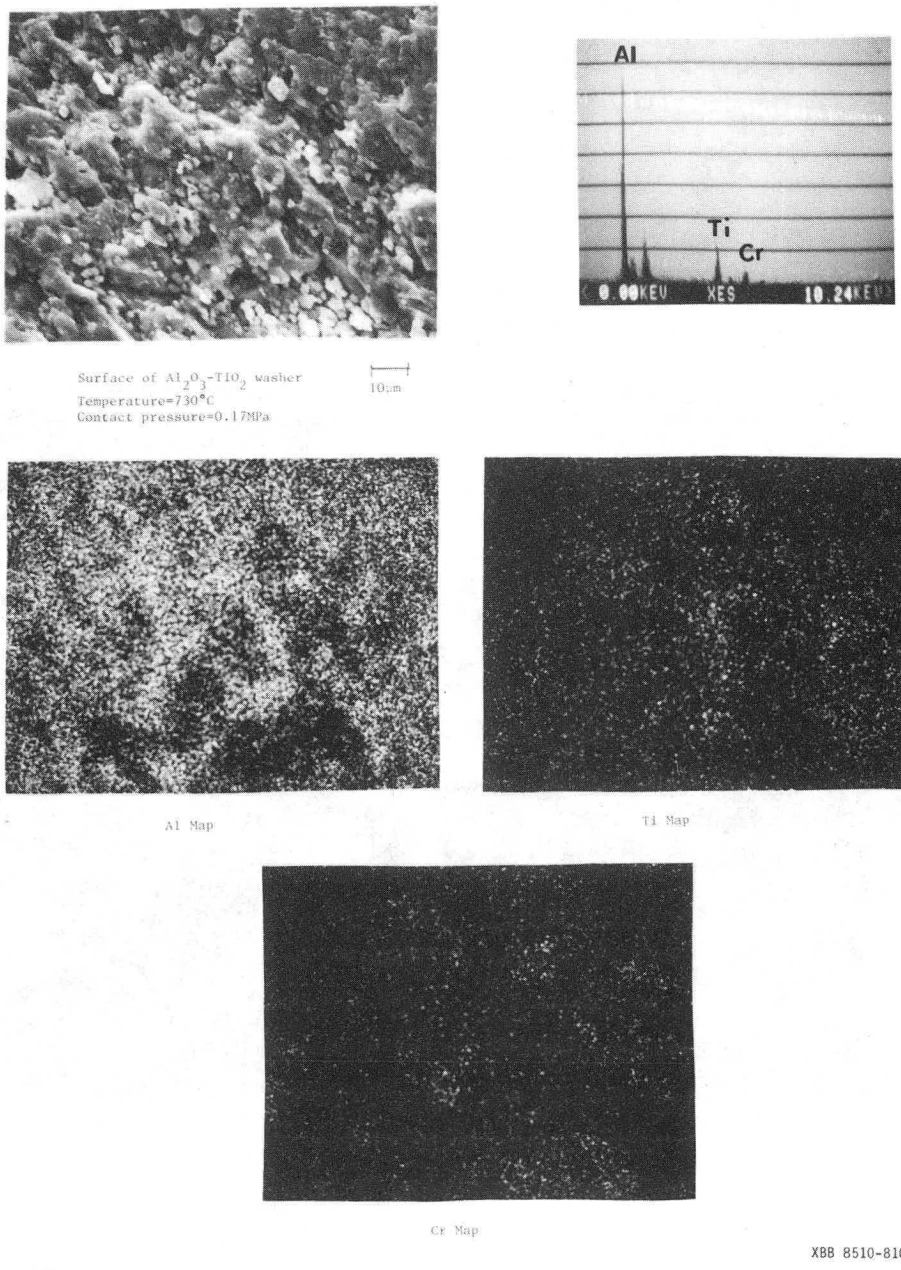

Figure 58. X-ray maps of the surface of Al_2O_3-TiO_2 washer at 730°C and 0.17MPa.

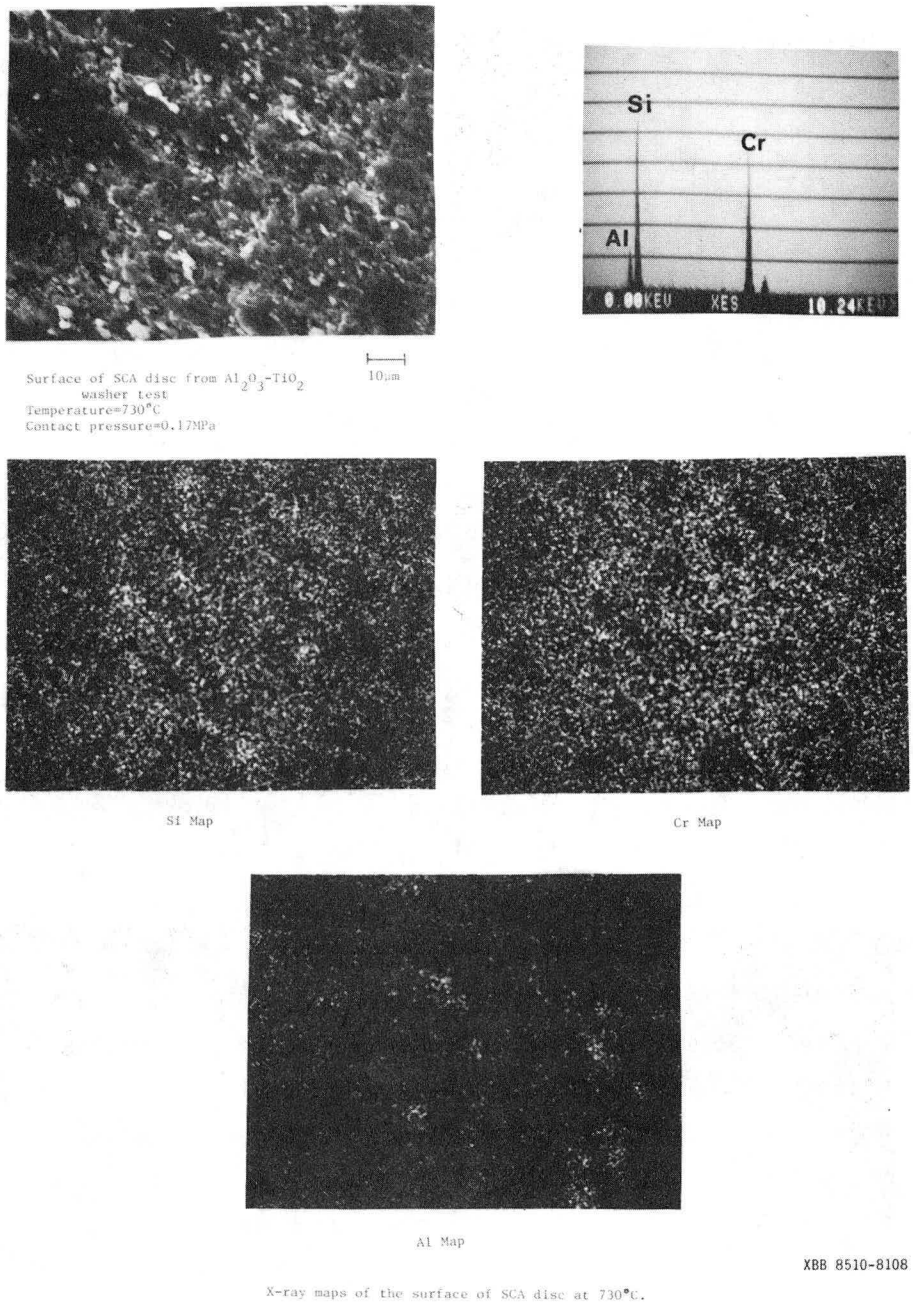

Figure 59. X-ray maps of the surface of SCA disc from Al_2O_3-TiO_2 washer test at 730°C and 0.17MPa.

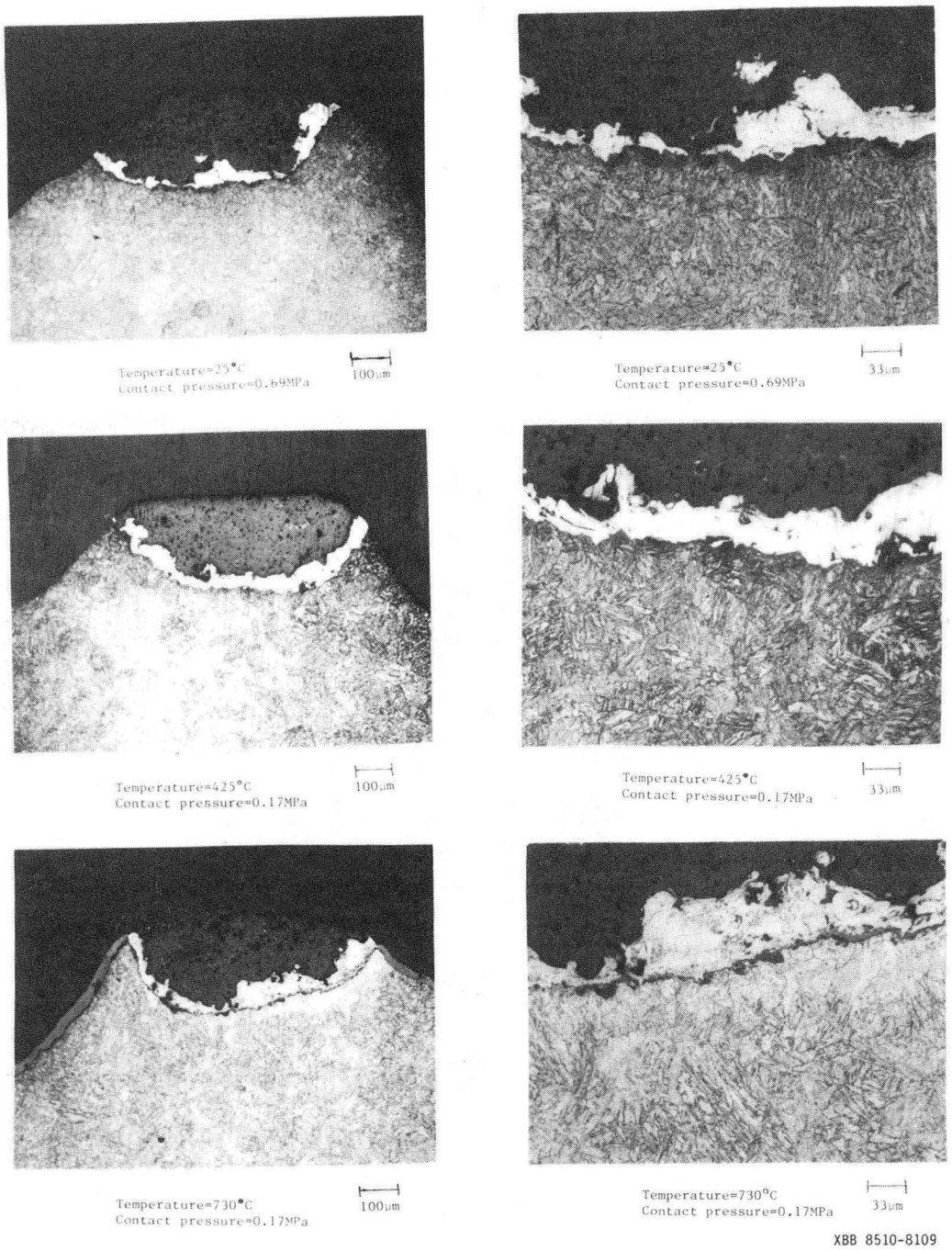

Figure 60. Cross section of Al_2O_3-TiO_2 washer at 25°C, 425°C and 730°C.

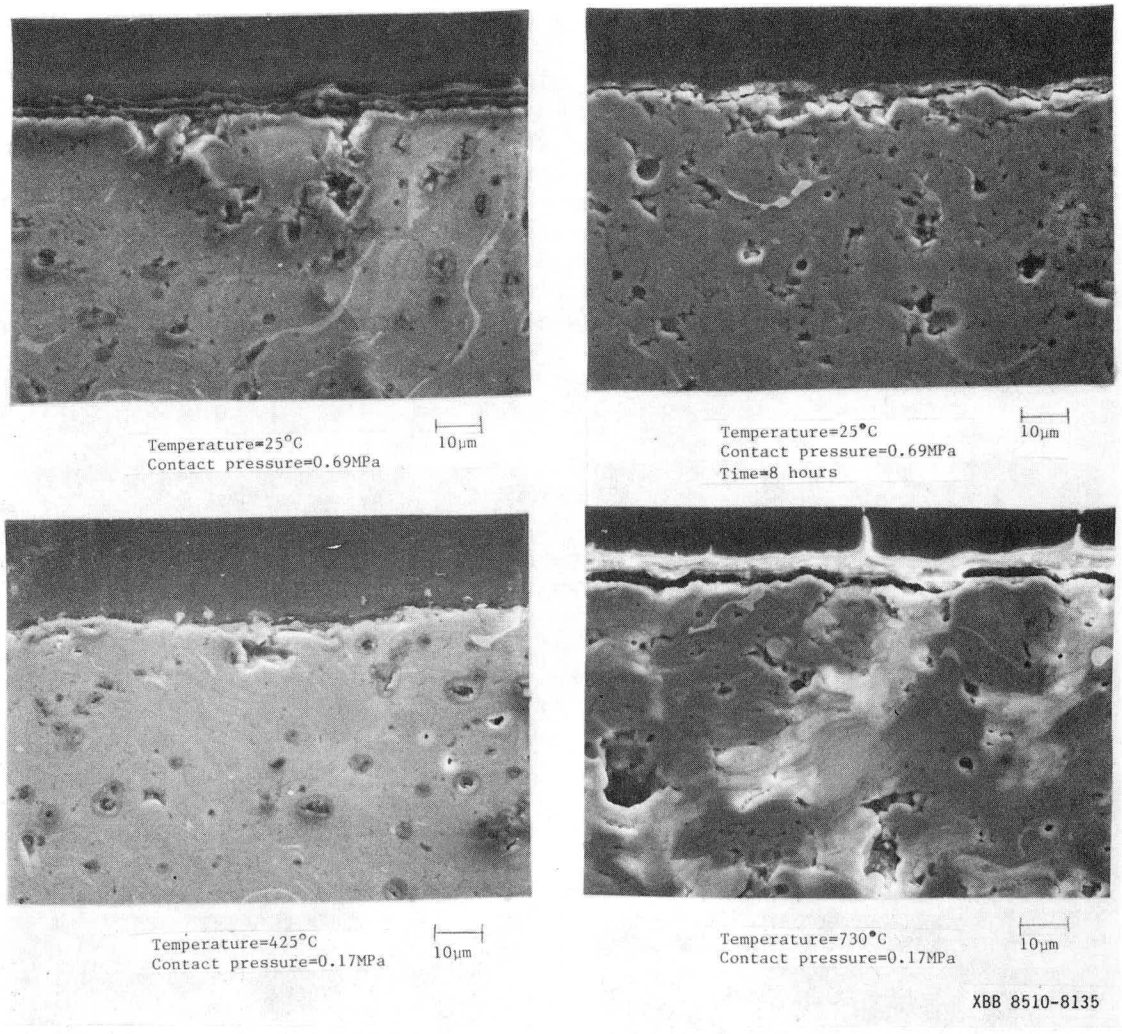

Figure 61. High magnification cross section of Al_2O_3-TiO_2 washer at 25°C, 425°C and 730°C.

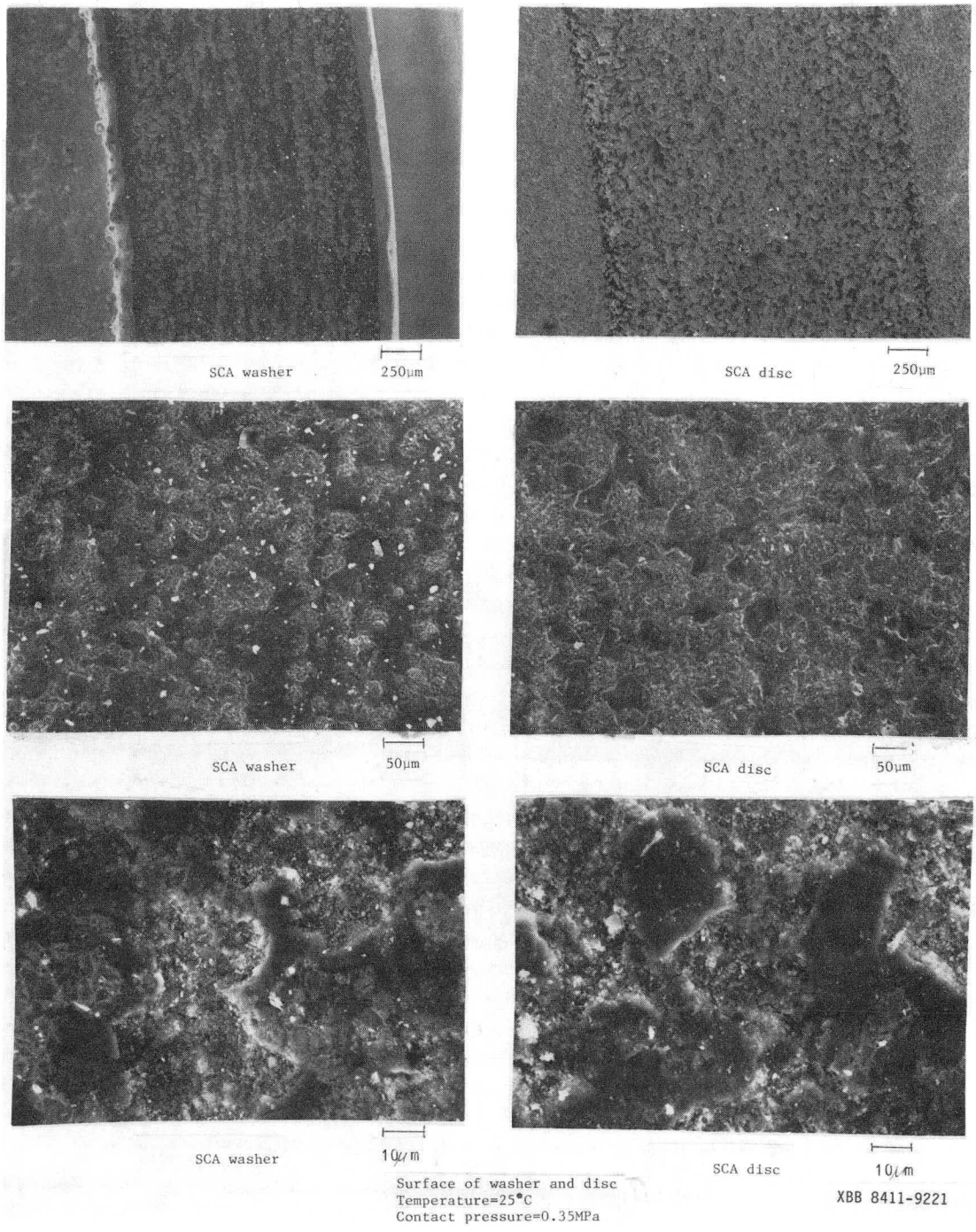

Figure 62. Surface of SCA washer and disc at 25°C and 0.35MPa.

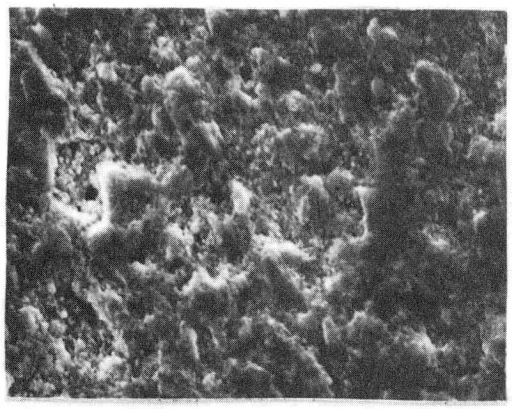

Surface of untested SCA disc
Temperature=25°C

10μm

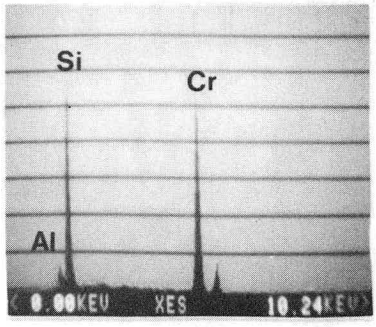

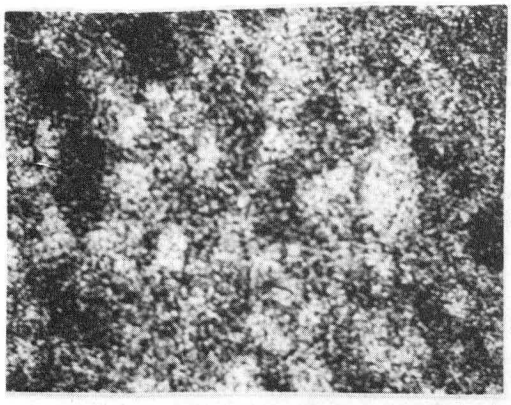

Si Map

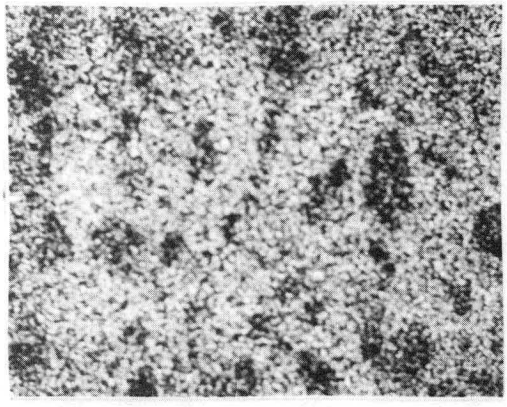

Cr Map

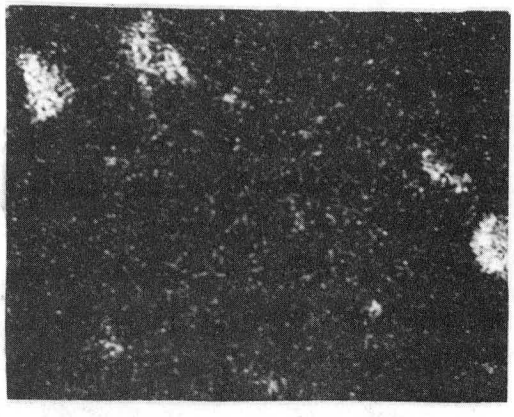

Al Map

XBB 8411-9204 A

Figure 63. X-ray maps of surface of untested SCA disc.

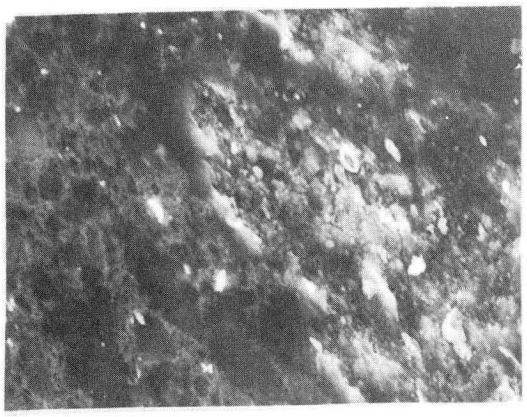

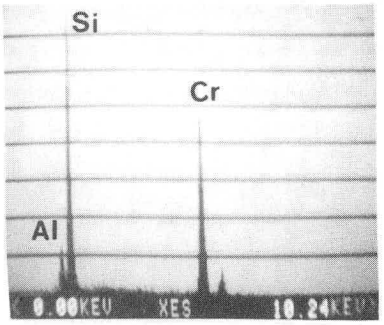

Surface of SCA washer
Temperature=25°C
Contact pressure=0.35MPa

10μm

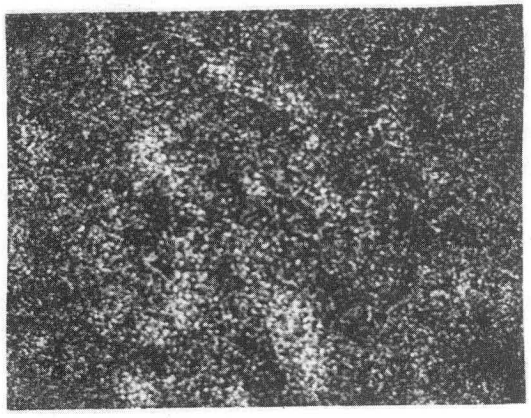

Si Map

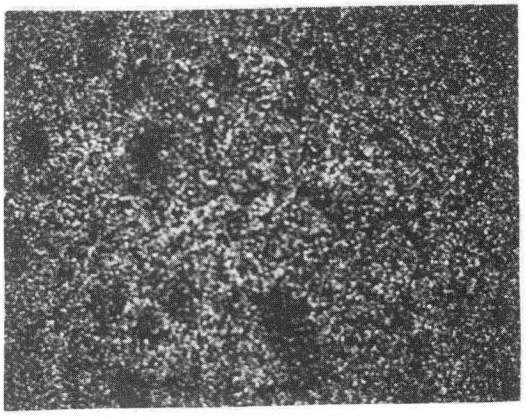

Cr Map

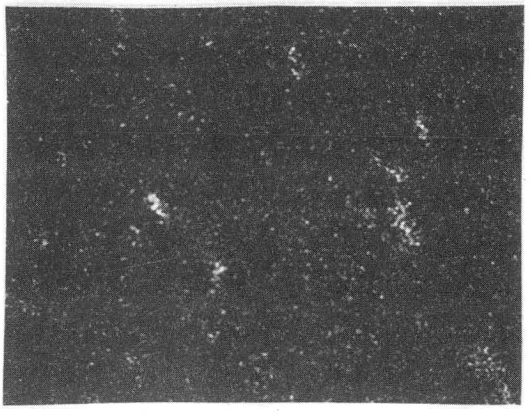

Al Map

XBB 8510-8110

Figure 64. X-ray maps of surface of SCA washer at 25°C and 0.35MPa.

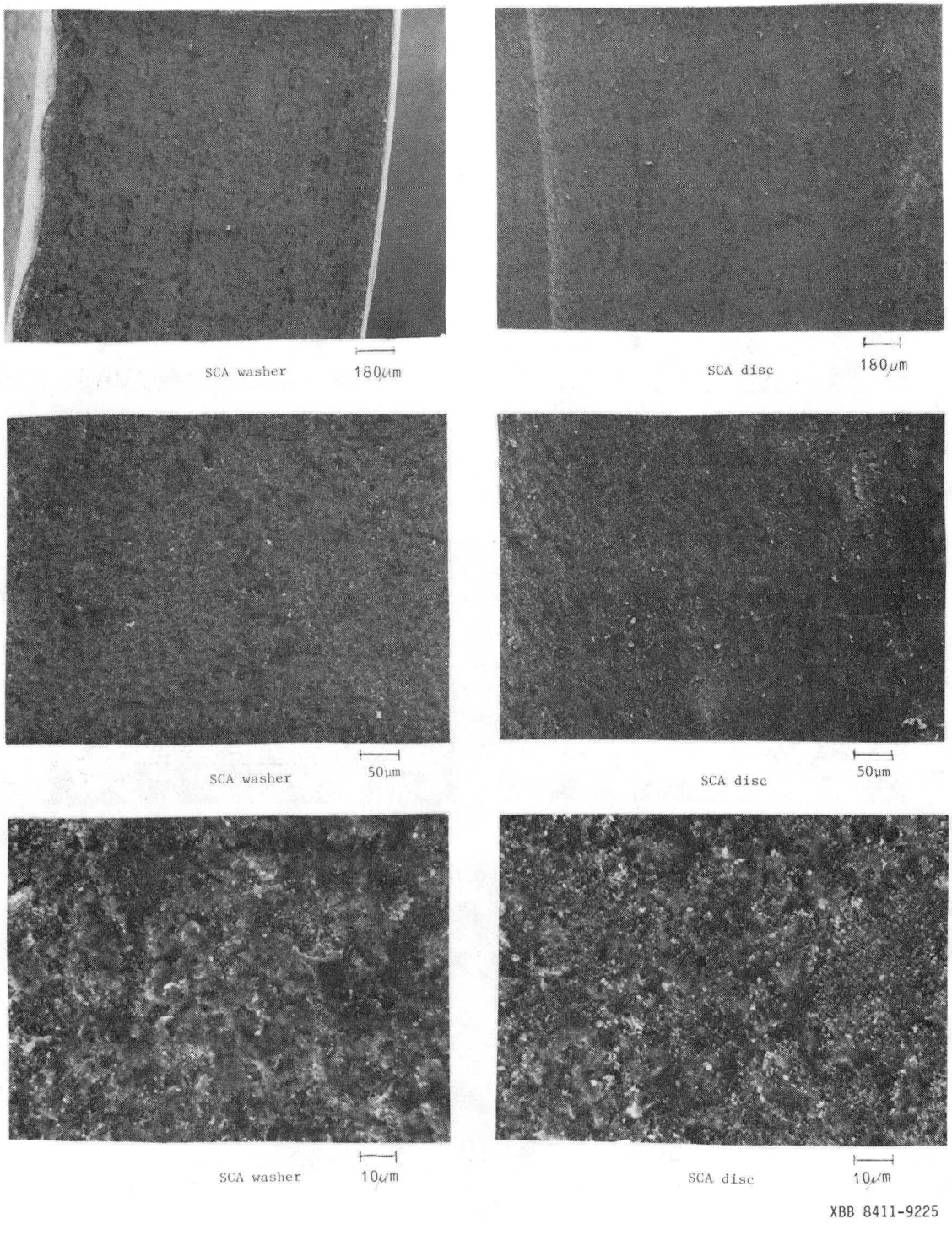

Figure 65. Surface of SCA washer and disc at 425°C and 0.17MPa.

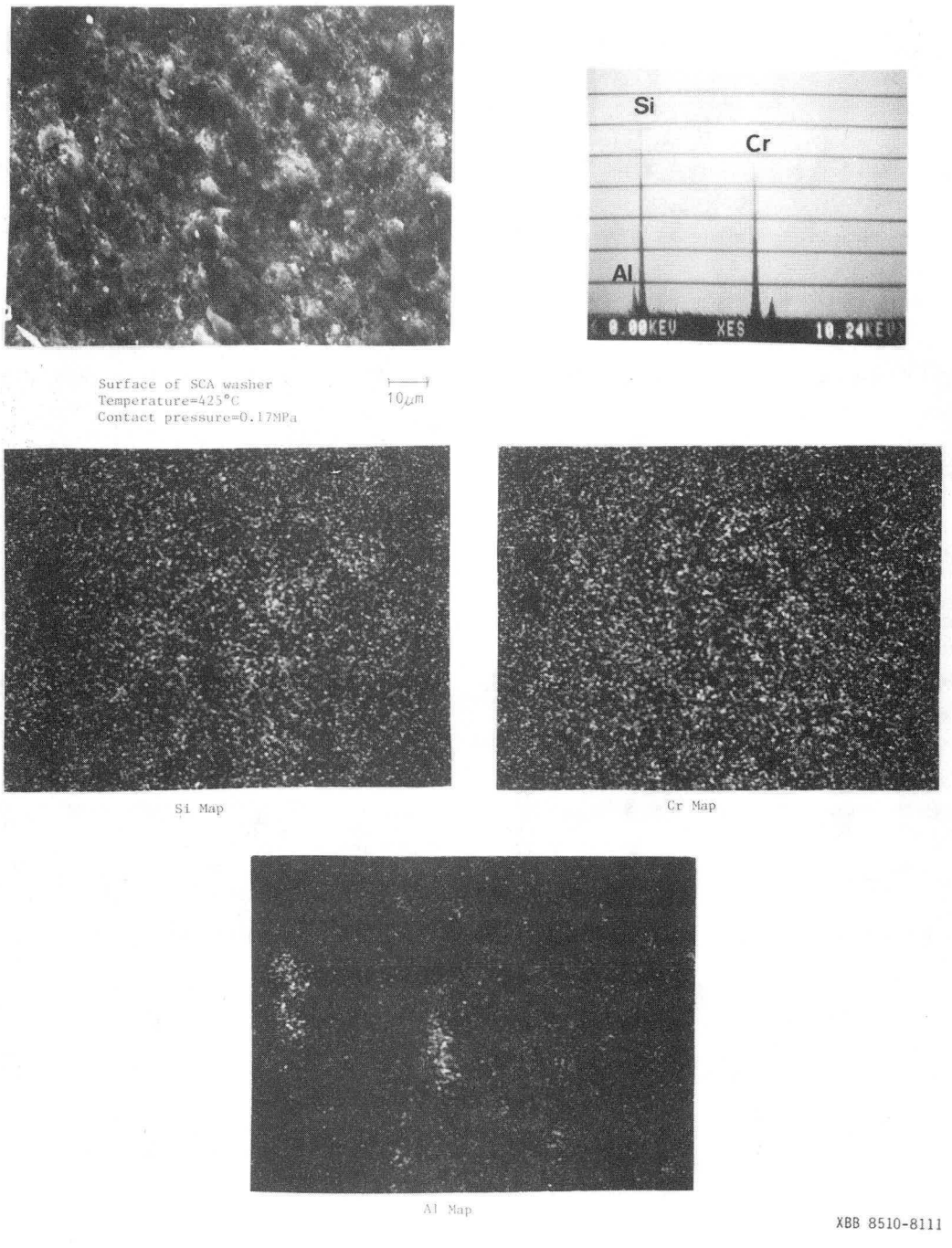

Figure 66. X-ray maps of the surface of SCA washer at 425°C and 0.17MPa.

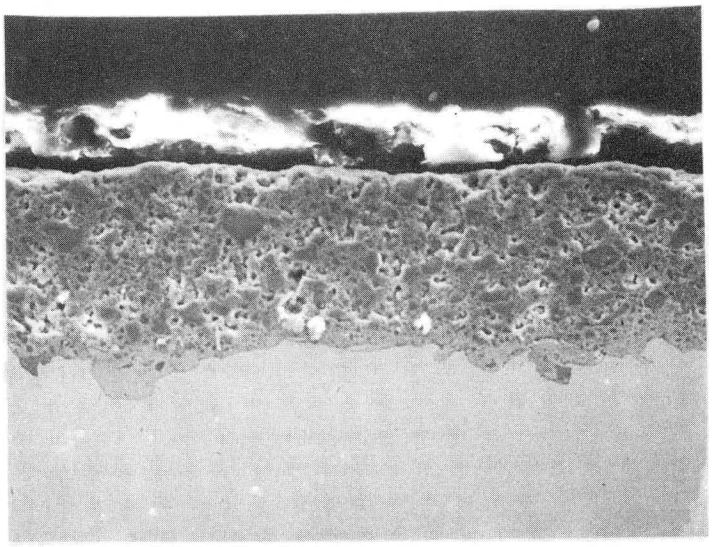

Temperature=25°C
Contact pressure=0.35MPa

20μm

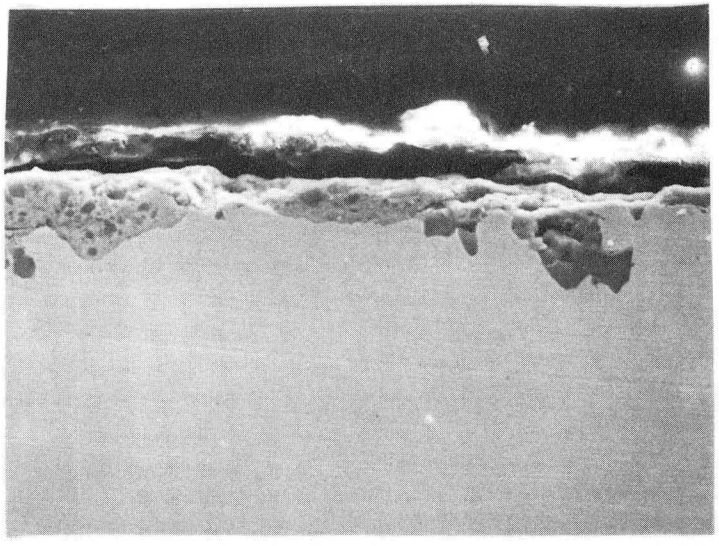

Temperature=425°C
Contact pressure=0.17MPa

10μm

XBB 8510-8133

Cross section of SCA washer

Figure 67. Cross section of SCA washer at 25°C and 425°C.

LAWRENCE BERKELEY LABORATORY
TECHNICAL INFORMATION DEPARTMENT
UNIVERSITY OF CALIFORNIA
BERKELEY, CALIFORNIA 94720